Advanced Equalization Techniques for Digital Coherent Optical Receivers

Arlunno, Valeria; Tafur Monroy, Idelfonso ; Larsen, Knud J.; Zibar, Darko

Publication date:
2013

Document Version
Publisher's PDF, also known as Version of record

Advanced Equalization Techniques for Digital Coherent Optical Receivers

Valeria Arlunno

Supervisors:
Professor Idelfonso Tafur Monroy,
Professor Knud J. Larsen and
Associate Professor Darko Zibar

Delivery Date: 30$^{\text{th}}$ June 2013

DTU Fotonik
Department of Photonics Engineering
Technical University of Denmark
Building 343
2800 Kgs. Lyngby
DENMARK

DTU Fotonik
Institut for Fotonik

Abstract

This PhD thesis addresses the design and performance evaluation of advanced Digital Signal Processing (DSP) algorithms for coherent optical fiber transmission systems. The research results presented in this thesis report on transmission of highly spectrally efficient optical communication systems employing multiplexing techniques with polarization multiplexing and multi-level modulations format. Advanced digital signal processing techniques offer robustness and flexibility for next generation high capacity optical fibre networks and are therefore considered as key building blocks in next generation digital coherent receivers.

The research results presented in this thesis are pioneering in two areas: first the use of feedback equalization structures and second the use of digital signal processing for receiver structure supporting Orthogonal Frequency Division Multiplexing (OFDM) and reconfigurable format detection.

Feedback equalization structure have been investigated in high order modulation formats transmission, when combined with coding techniques, and for closed spaced multiplexing scenario. Highlight results presented in this PhD thesis include evaluation and implementation of a novel approach based on joint encoding and equalization technique, known as Turbo Equalization (TE). This scheme is demonstrated to be powerful in transmission impairments mitigation for high order modulations formats, such as 16 Quadrature Amplitude Modulation (QAM), considered a key technology for high speed high capacity optical links thanks to their increased spectral efficiency. The proposed TE algorithm is successfully applied in dispersion managed link transmission. Then, an extension of the TE algorithm is applied to uncompensated link transmission scenario. Moreover the new proposed approach uses a lower complexity convolutional code compared to state of the art reports.

Furthermore, in order to fulfill the strict constrains of spectral efficiency, this thesis shows the application of digital adaptive equalizer for recon-

figurable and Ultra Dense Wavelength Division Multiplexing (U-DWDM) transmission. A feedback structure based on Decision Feedback Equalizer (DFE) algorithm is proposed to improve the overall bandwidth utilization reducing the undesired spectral guard bands.

Last, digital signal processing (DSP) algorithms are studied to equalize OFDM signal. The experimental demonstrations support Radio-over-Fiber (RoF) transmission system for a stand alone case and mixed modulation mixed bit rates transmission scheme.

In conclusion, this PhD thesis demonstrates the flexibility, upgradeability and robustness offered by rising advanced digital signal processing techniques, for future high-speed, high-capacity optical networking. Furthermore, it opens the prospects for next generation feedback equalization techniques supported by coding such as Turbo Equalization.

Resumé

Denne afhandling omhandler design og evaluering af digitale signalbehandlingsalgoritmer for kohærent optisk kommunikation. Forskningsresultaterne præsenteret rapporterer om transmissionsegenskaber for modulationsformater med høj spektral effektivitet som benytter højere ordens modulationsformater og polarisationsmultipleksing. Avanceret signalbehandling i modtageren åbner mulighed for robuste og fleksible højkapacitets optiske netværk og er derfor et grundelement i næste generations kohærente modtagere

Der er to hovedbidrag i denne afhandling: Det første er brugen af udligning med tilbagekobling og det andet er signalbehandlingsalgoritmer for en optisk kohærent modtager som benytter OFDM og automatisk genkendelse af modulationsformater. Udligning med tilbagekobling kombineret med kodning er blevet undersøgt for transmissionssystemer som benytter højere ordens modulationsformater og for transmissionssystemer med tætpakkede optiske kanaler.

Forskningshøjdepunkter i denne afhandling er evaluering og implementering af en ny metode for fælles kodning og udligning, såkaldt Turbo Equalization (TE) . Denne metode er vist at være meget nyttig til at modvirke signalforvrængning for højere ordens modulationsformater som 16 QAM. Den foreslåede TE algoritme er også blevet demonstreret for dispersionskompenserede links. Endvidere er den udvidede version af TE algoritmen blevet demonstreret for optiske links som ikke benytter dispersionskompenserende fiber. Den nye TE algoritme benytter en mindre kompleks foldningskode i forhold til tidligere publicerede algoritmer.

For at opretholde de strenge krav om spektral effektivitet undersøges også anvendelse af en digital adaptiv udligner til rekonfigurerbare og ultratætte WDM systemer. En algoritme baseret på beslutningstilbagekoblet udligning er anvendt for at forbedre båndbreddeudnyttelsen uden brug af optiske adskillelsesbånd. Digitale signalbehandlingsalgoritmer for udligning

af OFDM signaler er også undersøgt sidst i afhandlingen og er blevet verificeret eksperimentelt for radio-over-fibre systemer og systemer der benytter forskellige modulationsformater.

For at konkludere, denne afhandling demonstrerer den fleksibilitet og robusthed der kan opnås med avancerede digitale signalbehandlingsteknikker for fremtidens højhastigheds optiske netværk med høj kapacitet. Endvidere viser den nogle muligheder for lovende udligningsteknikker der anvender tilbagekobling understøttet af kodning såsom TE.

Acknowledgements

First I would like to thank my supervisors, Professor Idelfonso Tafur Monroy, Professor Knud J. Larsen and Associate Professor Darko Zibar. Idelfonso for the guidance and constant support in this devious PhD journey. Thanks for having me as part of this incredible group of researchers. Knud for always being a reference full of wisdom and knowledge. Thanks also for giving me the possibility to test my preparation and patience as teaching assistant in one of your courses. Darko for teaching me that hard work and organization pay sooner or later. Thanks for always being open to discuss new ideas.

I would also like to express my gratitude to all my colleagues at the Metro-access group: Robert, Bomin, Jesper, Xiaodan, Miguel, Xema, Anna, Alexander, Mario and JJ. Thanks for the time spent together in the lab and the great collaboration. I've learnt from each of you and this PhD work would have not be possible without your help. Thanks to who has been part of this group and this work: Neil, Kamau, Xu, Roberto, Thang, Maisara. Thanks also to all my colleagues at DTU Fotonik, for being an everyday mix of nationalities, knowledge and inspiration.

Thanks to Silvia and Konrad and to the incredible salsa group at DTU. Fun, friendship and good travels are always guaranteed with all of them. A huge thanks to the Egg Deenesh, for all the dances and for reminding me that even if obscure there's always a path. Thanks to all our bachata students, for their patience and the fun of every week class with them. Thanks to all of you salsa and bachata dancers, for making me feel at home and being my family in Denmark. You will always be my first salsa/bachata group in my heart.

Thanks to Luca, Valentina and Enrico. For always being ready to start chatting and gossiping after months of no contacts as if no time has passed. Kilometers of distance have not tackled our friendship and I know I can always count on you.

Thanks to Antonio, for always being here to hold my hand in this difficult travel. I'm not sure I would have managed without you.

There are no words to thank properly all my family, especially my parents, Vito and Rosy, and my sister, Anna Carla, for their uncoditionate love and support. You are and you will always be my rock.

Finally thanks to who is guiding and protecting me from up there. I know in my heart you will always be there.

Summary of Original Work

This thesis is based on the following original publications:

PAPER 1 V. Arlunno, A. Caballero, R. Borkowski, S. Saldaña Cercós, D. Zibar, K. J. Larsen and I. Tafur Monroy, "Turbo Equalization techniques towards robust PDM-16-QAM optical fiber transmission," in *Journal of Optical Communications and Networking*, Vol. 6, No. 2, February 2014.

PAPER 2 V. Arlunno, A. Caballero, R. Borkowski, D. Zibar, K. J. Larsen and I. Tafur Monroy, "Counteracting 16-QAM Optical Fibre Transmission Impairments with Iterative Turbo Equalization ," in *IEEE Photon. Technol. Lett.*, Vol. 25, No. 21, November 2013.

PAPER 3 V. Arlunno, A. Caballero, R. Borkowski, D. Zibar, K. J. Larsen and I. Tafur Monroy, "Turbo Equalization for digital coherent receivers," in *IEEE/OSA J. Lightw. Technol.*, Vol. 32, No. 2, January 2014.

PAPER 4 V. Arlunno, X. Zhang, K. J. Larsen, D. Zibar and I. Tafur Monroy, "Digital non-linear equalization for flexible capacity ultradense WDM channels for metro core networking," in *Optics Express*, Vol. 19, No. 26, December 2011.

PAPER 5 X. Zhang, V. Arlunno, J. Bevensee Jensen, I. Tafur Monroy, D. Zibar, R. Younce, "1.2 Tb/s Ultredense WDM Long Reach and Spectral Efficiency Access Link with Digital Detection," in *Photon-*

ics Conference (PHO), 2011 IEEE, Arlington, USA, 2011, paper ThBB5.

PAPER 6 V. Arlunno, R. Borkowski, N. Guerrero Gonzalez, A. Caballero, K. Prince, J. Bevensee Jensen, D. Zibar, K. J. Larsen and I. Tafur Monroy, "Radio Over Fiber Link With Adaptive Order n-QAM Optical Phase Modulated OFDM And Digital Coherent Detection," in *Microwave and Optical Technology Lett.*, Vol. 53, No. 10, October 2011

PAPER 7 M. Beltran, L. Deng, X. Pang, X. Zhang, V. Arlunno, Y. Zhao, X. Yu, R. Llorente, D. Liu, and I. Tafur Monroy, "Single- and Multiband OFDM Photonic Wireless Links in the 75-110 GHz Band Employing Optical Combs," in *IEEE Photonics Journal*, Vol. 4, No. 5, October 2012

PAPER 8 A. Caballero, N. Guerrero Gonzalez, V. Arlunno, R. Borkowski, T. T. Pham, R. Rodes, X. Zhang, M. B. Othman, K. Prince, X. Yu, J. B. Jensen, D. Zibar, and I. Tafur Monroy, "Reconfigurable Digital Coherent Receiver for Metro-Access Networks Supporting Mixed Modulation Formats and Bit-rates," in *Optical Fiber Technology Journal*, Vol. 19, No. 6, December 2013.

Other scientific reports associated with the project:

[PAPER 9] V. Arlunno, N. Guerrero Gonzalez, A. Caballero, R. Borkowski, T. T. Pham, R. Rodes, X. Zhang, M. Binti Othman, K. Prince, X. Yu, J. B. Jensen, D. Zibar, I. Tafur Monroy, "Reconfigurable Digital Coherent Receiver for Hybrid Optical Fiber/Wireless Metro-Access Networks", in *Proc. 2nd Annual Workshop on Photonic Technologies for Access and Biophotonics*, 2011, Stanford University, USA.

[PAPER 10] N. Guerrero Gonzalez, A. Caballero, R. Borkowski, V. Arlunno, T. T. Pham, R. Rodes, X. Zhang, M. B. Othman, K. Prince, X. Yu, J. B. Jensen, D. Zibar, and I. Tafur Monroy, "Reconfigurable digital coherent receiver for metro-access networks supporting mixed modulation formats and bit-rates," in *Proc. Optical Fiber Communication Conference and Exposition, OFC/NFOEC*, Los Angeles, CA, 2011, paper OMW7.

[PAPER 11] L. Deng, Y. Zhao, X. Yu, V. Arlunno, R. Borkowski, D. Liu, I. Tafur Monroy, "Experimental Demonstration of a Bandwidth Scalable LAN Emulation over EPON Employing OFDMA", in *Proc. Conference on Lasers and Electro-Optics, CLEO*, 2011

[PAPER 12] V. Arlunno, X. Zhang, K. J. Larsen, D. Zibar and I. Tafur Monroy, "Digital non-linear equalization for flexible capacity ultra-dense WDM channels for metro core networking," in *Proc. 37th European Conference on Optical Communication, ECOC'11*, Geneva, Switzerland, 2011, paper Tu.3.K.6.

[PAPER 13] L. Deng, Y. Zhao, X. Yu, V. Arlunno, R. Borkowski, D. Liu, I. Tafur Monroy, "Experimental Demonstration of a Bandwidth Scalable LAN Emulation over EPON Employing OFDMA for bandwidth scalable LAN emulation", *Optical Fiber Technology Journal* vol 17, issue 6, pages 554-557, 2011

[PAPER 14] L. Deng, M. Beltran, X. Pang, X. Zhang, V. Arlunno, Y. Zhao, A. Caballero, A. K. Dogadaev, X. Yu, R. Llorente, D. Liu, I. Tafur

Monroy, "Fiber Wireless Transmission of 8.3-Gb/s/ch QPSK-OFDM Signals in 75-110-GHz Band", *IEEE Photon. Technol. Lett.*, vol 24, issue 5, pages 383-385, 2012

[PAPER 15] L. Deng, D. Liu, X. Pang, X. Zhang, V. Arlunno, Y. Zhao, A. Caballero, A. K. Dogadaev, X. Yu, I. Tafur Monroy, M. Beltran, R. Llorente, "42.13 gbit/s 16qam-OFDM photonics-wireless transmission in 75-110 GHz band", *Journal of Electromagnetic Waves and Applications*, vol 126, pages 449-461, 2012

[PAPER 16] R. Borkowski, F. Karinou, M. Angelou, V. Arlunno, D. Zibar, D. Klonidis, N. Guerrero Gonzalez, A. Caballero, I. Tomkos, I. Tafur Monroy, "Experimental Demonstration of Mixed Formats and Bit Rates Signal Allocation for Spectrum-flexible Optical Networking", in *Proc. Optical Fiber Communication Conference and Exposition, OFC/NFOEC*, 2012, paper OW3A.7

[PAPER 17] L. Deng, X. Pang, M. Beltran, X. Zhang, V. Arlunno, Y. Zhao, R. LLorente, D. Liu, I. Tafur Monroy, "38.2-Gb/s Optical-wireless transmission in 75-110Ghz based on electrical OFDM with optical comb expansion", in *Proc. Optical Fiber Communication Conference and Exposition, OFC/NFOEC*, 2012

[PAPER 18] A. Caballero, J. C. Aguado, R. Borkowski, S. Saldaña Cercos, T. Jiménez, I. de Miguel, V. Arlunno, R. J. Durán, D. Zibar, J. B. Jensen, R. M. Lorenzo, E. J. Abril, I. Tafur Monroy, "Experimental Demonstration of a Cognitive Quality of Transmission Estimator for Optical Communication Systems", in *Proc. 38th European Conference on Optical Communication, ECOC'12*, Amsterdam, Netherlands, paper We.2.D.3

[PAPER 19] D. Zibar, O. Winther, N. Franceschi, R. Borkowski, A. Caballero, V. Arlunno, M. Nørgaard Schmidt, N. Guerrero Gonzales, B. Mao, K. J. Larsen, I. Tafur Monroy, "Nonlinear Impairment Compensation Using Expectation Maximization for PDM 16-QAM Systems", in *Proc. 38th European Conference on Optical Communication, ECOC'12*, Amsterdam, Netherlands, paper Th.1.D.2

[PAPER 20] R. Borkowski, F. Karinou, M. Angelou, V. Arlunno, D. Zibar, D. Klonidis, N. Guerrero Gonzalez, A. Caballero, I. Tomkos, I. Tafur Monroy, "Experimental Study on OSNR Requirements for Spectrum-Flexible Optical Networks", *Journal of Optical Communications and Networking*, vol 4, issue 11, pages B85-B93, 2012

[PAPER 21] A. Caballero, J. C. Aguado, R. Borkowski, S. Saldaña Cercos, T. Jiménez, I. de Miguel, V. Arlunno, R. J. Durán, D. Zibar, J. B. Jensen, R. M. Lorenzo, E. J. Abril, I. Tafur Monroy, "Experimental Demonstration of a Cognitive Quality of Transmission Estimator for Optical Communication Systems", *Optics Express*, vol 20, issue 26, pages B64-B70, 2012

[PAPER 22] D. Zibar, O. Winther, N. Franceschi, R. Borkowski, A. Caballero, V. Arlunno, M. Nørgaard Schmidt, N. Guerrero Gonzales, B. Mao, K. J. Larsen, I. Tafur Monroy, "Nonlinear Impairment Compensation Using Expectation Maximization for PDM 16-QAM Systems", *Optics Express*, vol 20, issue 26, pages B181-B196, 2012

[PAPER 23] R. Borkowksi, D. Zibar, A. Caballero, V. Arlunno, I. Tafur Monroy, "Optical Modulation Format Recognition in Stokes Space for Digital Coherent Receivers" in *Proc. Optical Fiber Communication Conference and Exposition, OFC/NFOEC* 2013, paper OTh3B.3

Other scientific reports:

[C1] J. B. Jensen, A. V. Osadchiy, D. Zibar, R. Rodes, V. Arlunno, N. Guerrero Gonzalez, A. Caballero, X. Yu, I. Tafur Monroy, "Coherent technologies for next generation flexible converged wireless-wireline access networks", in *Proc. Access Networks and In-House Communications* ANIC 2010

[C2] K. Prince, X. Yu, N. Guerrero Gonzalez, A. Caballero, X. Zhang, R. Rodes, V. Arlunno, M. Binti Othman, J. B. Jensen, D. Zibar, I. Tafur Monroy, "Ultra-high throughput converged optical wireless links: challenges and opportunities ", in *Finnish-Russian University Cooperation in Telecommunications* FRUCT 2011

[C3] X. Pang, A. Caballero, A. K. Dogadaev, V. Arlunno, R. Borkowski, J. S. Pedersen, L. Deng, F. Karinou, F. Roubeau, D. Zibar, X. Yu, I. Tafur Monroy, "100 Gbit/s hybrid optical fiber-wireless link in the W-band (75-110 GHz)", *Optics Express*, vol 19, issue 25, pages 24944-24949, 2011

[C4] X. Pang, A. Caballero, A. Dogadaev, V. Arlunno, L. Deng, R. Borkowski, J. S. Pedersen, D. Zibar, X. Yu, I. Tafur Monroy, "25 Gbit/s QPSK Hybrid Fiber-Wireless Transmission in the W-Band (75-110 GHz) With Remote Antenna Unit for In-Building Wireless Networks" *IEEE Photonics Journal*, vol 4, issue 3, pages 691-698, 2012

Contents

Chapter 1

Introduction

1.1 Capacity crunch

The annual global IP traffic will surpass the zettabyte threshold by the end of 2017 [1]. Statistic studies report that the global IP traffic has increased more than 4 times in the past five years and will continue to increase by an expected factor of 3 in the next five years. Moreover, analysis of the IP traffic data for the year 2012 shows that the volume of the internet traffic during busy hours is larger and growing faster than the average one. Furthermore, the increasingly significant role of networks delivering content to the user, such as internet video and online gaming, will fuel the surpassing of the metro traffic over long-haul traffic by 2014. By 2017 metro traffic is expected to count for $\sim$60% of the total IP traffic.

Research in the optical communication industry is therefore focused on transmission architectures able to cope with the evergrowing bandwidth demand from the user side.

There are three major options considered to improve the capacity-distance product [2]. First, by incrementing the spectral efficiency. Spectral efficiency may be increased by using larger signal constellations that transmit more bits per symbol [3]. Dual-polarization m-ary quadrature-amplitude modulation (DP-mQAM) has become the modulation format of choice for long-haul networks, thanks to the very efficient use of the optical spectrum and the capabilities of coherent receivers to enable simpler field equalization. By using all the degrees of freedom available for encoding information, DP-mQAM achieves the best spectral and power efficiency amongst all easy-to-generate modulation formats. However, the use of high order modulations will also affect the transmission system, which will be

less tolerant to noise, and the optical signal power level that can be launched into the fiber without generating excessive nonlinear signal distortions [4], thus limiting the maximum reach and requiring more advanced equalization techniques to counteract those effects. Nevertheless as the modulation level increases, difficulties in system implementation also arise, particularly in terms of complexity of the transmitter structure and digital signal processing hardware.

The second option is to increase the total available bandwidth and to improve network bandwidth utilization. Current Wavelength Division Multiplexing (WDM) systems operate on a fixed ITU grid with guard bands between neighbor channels. Solutions [5, 6] have been proposed to move towards a gridless network scenario, where optical transmission based on superchannels can enable a wider bandwidth signal to continuously occupy an allocated bandwidth, thereby removing the undesired spectral guard bands. Ultra dense WDM systems with reduced spacing between carriers and limited guard bands are therefore considered as a promising major technology towards high capacity transmission link. However, the closed spectral spacing requirements, as well as the reduced guard bands, demand counteracting action to mitigate the detrimental effects of interchannel interference. Another multiplexing solution is Orthogonal Frequency Division Multiplexing (OFDM) which has first been studied in the context of mobile communications mostly as a technique for combating multipath fading. Recently [7], OFDM has received interest in optical fiber transmission for its capability in spectral shaping, reduction of the spectral guard band requirement between neighboring channels. Therefore this increases the bandwidth utilization and spectral efficiency.

The third option to be considered is the reduction of the amount of signal distortion accumulated along the transmission link. To achieve this objective, links will use shorter fiber spans, lower noise amplifiers, distributed Raman amplification, and advanced fibers with ultralow loss and large effective area. Moreover, digital signal processing techniques including nonlinear compensation and advanced forward error-correction coding are nowadays employed to reduce distortion or improve signal sensitivity [8].

Therefore the achievement of high capacity requires also the use of Forward Error Correction (FEC) techniques with high coding gains and high BER thresholds, which are considered as one of the critical enabling technologies for next-generation optical communication systems.

Ultimately, the achievable spectral efficiency, capacity and reachable distance is constrained by optical fiber Kerr nonlinearity. In the absence

of Amplified Spontaneous Emission (ASE) noise, a single-channel signal is mostly limited by self-phase modulation (SPM), whereas WDM systems are dominated by crossphase modulation (XPM) and four-wave mixing (FWM) [9]. In the presence of optical fiber nonlinearity, the existence of an optimal launch power, at which the reachable capacity is maximized, makes power efficiency especially important. Using a modulation format with low SNR requirement increases the achievable capacity. However, the data rate cannot be increased indefinitely due to the limitations set by the Shannon's limit [10].

Next-generation higher capacity systems will use transceivers powered by a key role DSP, where advanced algorithms will be used for compensating fiber impairments and other signal processing that are impractical to perform in analog hardware [3]. DSP can also be used at the transmitter to improve system performance. A software-defined optical system with DSP at both transmitter and receiver enables agile modification and reconfiguration. It allows channel impairments to be compensated by DSP algorithms, as well as new signal (de)multiplexing paradigms. Channel data rate, modulation format, and coding scheme can all be programmed by network management in response to estimated channel conditions. Digital transmitters can also enable advanced spectral shaping, thereby reducing the need for wasteful and undesired guard bands between neighboring channels. This increases bandwidth utilization and spectral efficiency. With precise DSP control, signal constellations generated by digital transmitters will have higher fidelity, enabling higher order modulation to be employed and thereby extending the system reach of high spectral efficiency modulation formats. However, increasing the modulation order or reducing the spacing in a multiplexed system will require the employment of advanced DSP algorithms which can be viewed as a major drawback for practical implementations.

1.2 Transmission systems

1.2.1 High order modulation formats

Research in high-speed fiber-optic systems moved from On-Off Keying (OOK) towards binary and quaternary phase shift keying (BPSK, QPSK) in the late 90s, using direct detection with differential demodulation (DPSK, DQPSK). Moving towards 100 Gb/s capacity target, it became clear that additional techniques were needed. Polarization Division Multiplexed (PDM)

QPSK schemes allowed for a reduction of symbol rates by a factor of 4 compared to the information bit rate, which brought 40 and 100 Gb/s optical signals at around 10 and 25 GBaud which became realizable with fast analog-to-digital converters (ADCs). Furthermore the employment of this modulation format enabled the use of digital coherent detection using robust digital signal processing (DSP) to perform all-electronic chromatic- and polarization-mode dispersion compensation, frequency and phase locking, and polarization demultiplexing. Commercial coherent systems for fiber-optic networks based on PDM-QPSK with custom-designed CMOS ASICs to handle the DSP functionality were introduced at 40 and 100 Gb/s in 2006 [11]. The adoption of advanced coherent communication concepts allowed spectral efficiencies to continue their scaling at ∼1 dB/year using essentially unchanged optical line systems [3, 12]. Therefore higher-order coherent optical modulation formats are considered one of the key technology that has supported the capacity growth over the past ∼5 years. Moreover the use of high-spectral-efficiency, such as Quadrature Amplitude Modulation (QAM), allows increments both in per-channel interface rates and aggregate WDM capacities.

Widely commercially deployed WDM optical networks traditionally operate at a channel bit rate of 10 Gb/s with nonreturn to zero (NRZ) on-off keying (OOK) modulation schemes. The traffic load is currently approaching the maximum capacity of these networks, so solutions aiming to increase the total capacity of their network infrastructure propose the insertion of spectrally efficient solution at 40 or 100 Gb/s. Digital signal processing algorithms enable polarization division multiplexing PDM to be fully exploited without the need of additional complexity at the receiver end. However most telecommunications do not intend to build a specific network for 40 or 100 Gb/s. One possible trend for 10 Gb/s infrastructure is to design an hybrid scenario, where several channels at 40 or 100 Gb/s are progressively inserted in wavelength slots with 50 GHz spacing, without changes in the grid structure or in the resources needed. The process represents an upgrade of the existing network which is able to cope with the increasing demand for bandwidth and capacity from the customer side without the deployment of more infrastructures.

1.2.2 Ultra Dense Wavelength Division Multiplexing

In WDM optical communication systems, increasing the spectral efficiency (SE) is essential to reach higher capacity targets. Higher SE can be achieved by using either high order modulation formats and/or reduction in the chan-

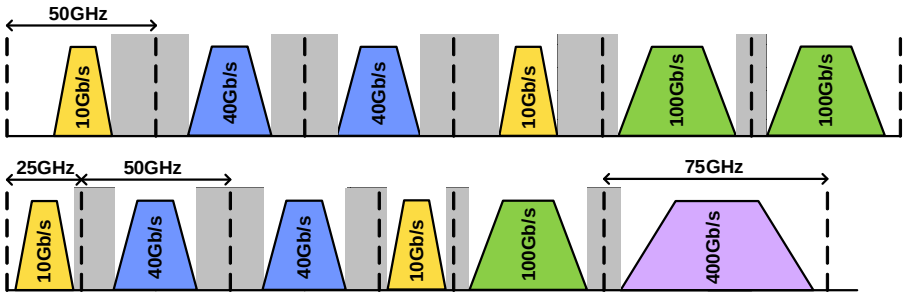

Figure 1.1: Fix grid versus flexible grid. Large guard bands are still employed.

nel spacing. Coherent detection of WDM transmission schemes with digital signal processing (DSP) is attractive for high capacity applications because of its powerful equalization, which is achievable in the electronic domain, of linear distortion, such as Chromatic Dispersion (CD) and Polarization Mode Dispersion (PMD), and its improved tolerance to amplifier noise.

Rigid and coarse granularity of WDM systems leads also to inefficient capacity utilization, which partly results from the lost spectrum due to the difference between the real spectral occupancy of the signal and the bandwidth allocation based on the conventional ITU-T grid. A promising way to overcome this effect would be to introduce the concept of a frequency slot instead of the current fix frequency grid, thus moving towards flexible grid and grid-less solutions. In flexible optical WDM (FWDM), an adjustable amount of spectral resources are dynamically allocated; in addition, channel spacing and center wavelength are not conformed to the ITU-T conventional fix grid, thereby resulting in higher spectral efficiency. Although higher efficiency could be obtained evolving to an allocation adjustable scenario, the bandwidth is still non optimally exploited as large guard bands are employed, as shown in Fig. 1.1. Ultra-dense (UD) WDM with a channel spacing of less than 25 GHz, may provide an evolutionary path from conventional infrastructures towards more scalable and spectrally efficient networks. This trend, supported by the increased demand for more capacity, flexibility and upgradeability of transmission technique while keeping some legacy ones, will also require a re-examination of such network designs.

Increasing the number of wavelengths within a fixed optical bandwidth (e.g., C band), by decreasing the spacing between neighboring channels, allows an increase in the system capacity without requiring of high-speed electronics (e.g., >40 Gb/s), while keeping compatibility with the 10 Gb/s

SONET/SDH equipment. UDWDM systems with no aliasing condition (that is with channel spacing higher than the double the baud rate) have been studied, with particular attention to limitations introduced by fiber nonlinear effects such as Four-Wave Mixing (FWM), Cross-Phase Modulation (XPM), fiber chromatic dispersion-induced symbol intersymbol interference (ISI). However, to cope with the required bandwidth efficiency, future UDWDM schemes will need to use extremely spectral close channel spacing. This implies that more focus has to be put into finding solutions able to mitigate the resultant detrimental effects from crosstalk and neighboring channels interferences.

1.2.3 Orthogonal Frequency Division Multiplexing

OFDM has been proposed in high-speed optical communication link as a possible alternative to standard single carrier modulations [7]. OFDM consists in modulating and demodulating blocks of symbols, previously mapped into a given constellation, for example QPSK or m-QAM, through discrete Fourier transform (DFT), usually employing inverse and direct fast Fourier transform (IFFT/FFT) algorithms. Therefore, symbols in each block are modulated onto subcarriers, whose orthogonality ensures that no intercarrier interference occurs. The transmitted signal, neglecting phase noise and frequency offset, at the receiver can be remapped to the original constellation.

The investigation on OFDM for optical fiber transmission is mostly motivated because of its large immunity to CD and PMD effects, its high spectral efficiency and the implicit parallelization of the processing due to the IFFT/FFT operations. Coherent detection optical OFDM (CO-OFDM) has been therefore proposed as a possible alternative to single carrier schemes. The primary advantage of OFDM over single carrier schemes is its ability to cope with severe channel conditions without complex equalization filters. Furthermore OFDM allows to easily accommodate for transmit filters with a smooth transition band. On the other side, the generation of the analog waveform at the transmitter requires the use of high-speed digital-to-analog converters (DACs). In addition, one of the major drawbacks of this multicarrier transmission, is the high Peak-to-Average Power Ratio (PAPR) of the transmit signal which induces large sensitivity to nonlinearities. Moreover a large PAPR increases the complexity of the analog to digital and digital to analog converter, reduces the efficiency of the radio frequency (RF) power amplifier and the range of the multicarrier transmission. Several techniques have been proposed in literature to re-

duce the PAPR value [13]. In many low-cost applications, the drawback of high PAPR may overshadow all the potential benefits of this multicarrier transmission systems. A solution is presented by coherent detection optical OFDM (CO-OFDM), where maximization of the spectral/power efficiency is reached by exploiting the advantages of software reconfiguration and digital signal processing (DSP) to mitigate for linear and nonlinear fiber impairments in the digital domain.

Radio-over-fiber (RoF) is considered as a possible last-mile solution for the distribution of high capacity and high-frequency RF signals, as it centralizes the radio signal generation and modulation at the central office while keeping the antenna base stations simple with only O/E conversion, RF signal emitting and receiving functionalities. While single-carrier modulated RoF systems have been extensively studied, the multiple-carrier characteristic of OFDM signal requires system linearity and the ability to handle large peak-to-average power (PAPR). Optical phase modulation (PM) has the potential to improve robustness to fiber nonlinearities by encoding the information in the optical phase and thus maintaining a constant optical power. Furthermore, optically phase-modulated links, in transmission of microwave radio frequency (RF) signals over optical fiber links case, can also enable high-capacity, higher spectral efficiency and large dynamic ranges, which can mitigate the drawbacks of high PAPR in OFDM signal.

Phase-modulated RoF coherent optical OFDM systems are therefore a promising solution for applications in converged wireless/wireline service delivery in optical networking scenarios with reconfigurable digital coherent receivers.

1.3 Feedback equalization

Equalization is an essential component of digital signal processing based optical receiver. Intersymbol interference that afflicts serial data transmission is traditionally mitigated by equalization through linear filtering, usually employing transversal structure, and thus the process is called linear equalizer. Due to the tradeoff between equalization of the channel impulse response to remove intersymbol interference (both precursors and postcursors) and noise enhancement at the decision point, a linear equalizer does not always represent the best possible solution. Other types of equalizers have therefore been proposed, based on feedback schemes, which is therefore a nonlinear structure with respect to the received signal [14].

1.3.1 Turbo Equalization

Turbo Equalization (TE) is a joint processing of equalization and decoding steps. A number of iterative receiver algorithms repeat the equalization and decoding tasks on the same set of received data, where feedback information from the decoder is incorporated into the equalization process. First proposed to combat the detrimental effects of intersymbol interference effects in digital communication systems protected by a Convolutional Code [15], TE has been introduced in coherent optical single carrier and OFDM systems.

In this feedback equalization scheme, the data bits must be encoded, interleaved and mapped into symbols before transmission. At the receiver, the feedback part of the turbo equalization includes deinterleaving, decoding and soft re-encoding. The equalized samples are first demapped by a soft demapper that provides the log likelihood ratio for each coded bit followed by deinterleaving and soft output decoding. The latter provides the refined log likelihood ratio by exploiting the properties of the error correcting code. Interleaving follows together with soft mapping that provides a new version of the original received signal. When implemented in the frequency domain, TE can also be viewed as an iterative block decision feedback equalizer integrated with coding/decoding [14]. A feedback equalization based on TE, has been implemented in the DSP receiver for single carrier baseband system presented in **PAPER 1**, **PAPER 2** and **PAPER 3**. Refer to Chapter 2 for the details of the proposed architecture and the state of the art.

1.3.2 Decision Feedback Equalizer

When in a WDM system the channel spacing is reduced, to obtain higher spectral efficiency and capacity, the end-to-end transmission link suffers from Inter-Channel Interference (ICI), thereby resulting in detrimental effects from crosstalk and neighboring channels interferences. In polarization division multiplexed (PDM) optical coherent receivers, Inter-Symbol Interference (ISI) and ICI are partly equalized by the polarization demultiplexing digital signal processing (DSP) block, consisting of feedforward (FF) finite impulse response (FIR) filters updated by a Constant Modulus Algorithm (CMA) [16]. The performance of CMA-FF equalizer structure is comparable to linear equalizers, which are poorly efficient given strong channel selectivity. Therefore the ISI mitigation offered by the traditional polarization demultiplexing DSP block in ultra dense (UD) WDM systems

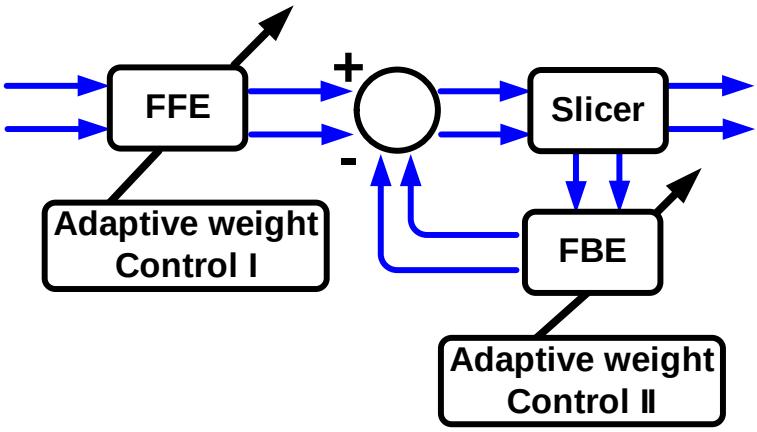

Figure 1.2: Schematic description of Decision Feedback Equalizer (DFE).

is not sufficient. A Decision Feedback Equalizer (DFE) offers a superior ISI mitigation compared to linear equalizer and has been already proven efficient for chromatic dispersion compensation, carrier phase estimation and enhancement of the tolerance of digital signal processing to phase noise.

The interest towards nonlinear receiver, such as decision feedback equalizer, is also driven by the research into suboptimum solutions which are able to provide bit-by-bit detection with significant performance advantages over the linear equalizer, without the high complexity of the optimum solutions [17].

A DFE is a feedback nonlinear adaptive equalizer structure that uses both the received sequence and the previously detected symbols to eliminate the ISI on pulses currently demodulated. The basic idea is that if the values of the symbols previously detected are known, then ISI contributed by these symbols can be canceled out exactly at the output of the forward filter by subtracting past symbol values with appropriate weighting. The nonlinear feature is due to the decision device, which attempts to determine which symbol of a set of discrete levels was actually transmitted. Once the current symbol has been decided, the filter structure calculates the ISI effect it would tend to have on subsequent received symbols and compensate the input to the decision device for the next samples. This postcursor ISI removal is accomplished by the use of a feedback filter structure. The DFE equalizer will not amplify the noise because, according to its structure, the equalization process is done through the feedback, noiseless, data applying symbol-by-symbol detection with successive cancelation of the interference

caused by the detected symbols. A nonlinear DFE, shown in Fig. 1.2, consisting of a feed-forward filter (FFE) and a feed-back filter (FBE) is used in the DSP receiver presented in **PAPER 4** and **PAPER 5**, after the carrier phase recovery block, to improve the system performances [18]. The tap weights of both feed-forward and feed-back equalizer converge through a least mean square (LMS) stochastic algorithm.

1.4 Digital signal processing for receiver structure supporting OFDM and reconfigurable modulation format detection

Next generation metro-access networks will need to support a highly heterogeneous scenario and therefore these systems will need to cope with different broadband services including converged wireless and wireline optical access over a unified fiber platform. Bandwidth requirements, power budget and chromatic dispersion constrains will need to be addressed. Future metro-access networks will also require agile re-configurability to seamlessly accommodate new services and increased bandwidth requirements, allowing co-existence of modulation formats and bitrates. Wavelength-division multiplexed (WDM) combined with coherent detection is considered a promising approach to increase the capacity of passive optical networks (PON). The use of coherent detection allows for closely spaced channels with increased receiver sensitivity to cope with the required large number of users and to extend the reach of metro-access networks. Furthermore, coherent receivers does not require an arrayed waveguide grating (AWG) at the receiver to filter the undesired wavelengths, making this technology compatible with the passive optical splitting of legacy PONs. Digital coherent detection also allows for the detection of wireless signals able to provide the high linearity and high capacity required by next generation wireless networks.

A single receiver could be employed after detection, if advance DSP able to cope with different modulation formats and bit rates is employed. Digital signal processing is therefore a key component towards heterogeneous scenario with co-transmission of baseband single carrier signals, wireless RoF networks and multiband transmission schemes, such as orthogonal frequency division multiplexing OFDM.

Digital signal processing algorithms play a key role in OFDM transmission systems. Synchronization techniques, reduction of PAPR, phase noise

mitigation and carrier frequency offset evaluation are realized in the digital domain because of the use of coherent detection techniques. Similarly, linear and nonlinear fiber impairments compensation can also be accomplished in the digital domain.

The combination of OFDM and coherent all-optical frequency division multiplexed techniques can also support high capacity wireless communications. Conversion of a high-speed optical OFDM baseband signal into the W-band can be accomplished by using a photonic up-conversion technique. This scheme is fully transparent to modulation format and bit-rate, as well as fully scalable to the RF carrier frequency. In such transmission condition the digital signal processing structure, apart from handling the OFDM signal, should also tackle the laser phase noise (from the transmitting laser) and the nonlinearity effects induced from the RF components response, such as photodiodes, amplifiers and electrical mixers.

1.5 State-of-the-art

In this section, the state-of-the-art analysis related to the topic investigated in this thesis is presented. First, high order modulation formats, closed spaced WDM presented in 1.2.2 and decision feedback equalizer solutions reported in Section 1.3.2 will be addressed. Furthermore, comments on state of the art publications related to coherent optical OFDM, as well as in RoF transmission links presented in Section 1.2.3 will be reported. Particular focus is put on literature regarding synchronization techniques in OFDM systems. To conclude, the latest literature on DSP for reconfigurable format detection is reported.

Aiming to increase the capacity, attention has been lately put into identifying schemes capable of achieving high spectral efficiencies (SEs). One of the most prominent approaches, as presented in Section 1.1, is the use of advanced modulation formats and coherent detection combined with multiplexing techniques, such as wavelength division multiplexing (WDM) or orthogonal frequency division multiplexing (OFDM). Solutions based on dual polarization Dual Polarization (DP) 16-QAM have been demonstrated to achieve remarkable SEs [19–21]. In [19] the author reports on the generation and long-haul transmission of WDM coherent detected 112-Gb/s polarization-division-multiplexed (PDM) 16-QAM at 14 Gbaud with spectral efficiencies beyond 4 b/s/Hz. Spectral efficiency of 4.2 b/s/Hz is obtain in [20] where the author present an 11 channels with 224-Gb/s 16-QAM system in a 50 GHz spacing grid. In [21] a spectral efficiency of 5.2

b/s/Hz is obtained in a 160x100G PDM 16-QAM system over transoceanic distance. Scheme based on 16-QAM coherent detection system has been pointed out as a promising compromise between limiting effects and reachable high-speed, high-capacity long-haul optical networking [3]. Intrachannel nonlinear compensation for 112 Gb/s PDM 16-QAM systems has been addressed in [22]. Ongoing research has compared DP 16-QAM to duobinary shaped DP QPSK [23]. Comparisons between transmission of 200 G PDM carrier-suppressed return-to-zero (CSRZ) QPSK and 200 G PDM 16-QAM have been evaluated in [24]. Experimental demonstration based on higher order modulation formats such as 36-QAM [25] and 64-QAM [26] has already been presented. The current capacity record of 101 Tbit/s with a spectral efficiency of 11 b/s/Hz is based on a 128-QAM [27].

In the last decades research efforts has also been put into the development of sub-baudrate-spaced channels moving towards ultra dense WDM. The bandwidth of the pulse shaping filter is decreased below the symbol rate as to avoid linear crosstalk and the ISI has been tackled with equalization techniques [28–30]. Another scenario in which WDM system performance is degraded by the ISI effects, is the case of multiple cascaded Reconfigurable Optical Add-Drop Multiplexers (ROADM). To combat the effect of the ISI, methods based on direct implementation of Maximum a Posteriori (MAP) have been proposed in [28, 31].

Decision feedback equalization schemes have until now been presented to mitigate the detrimental effects of link transmission [32–37]. Polarization-mode dispersion (PMD) mitigation by various types of electronic equalizers, including DFE is discussed in [32]. The state-model-based DFE and its combination with FFE has been proved to considerably reduce OSNR penalty for large dispersions. In [33] a carrier-phase estimation for digital coherent optical receivers, based on the decision-feedback loop and adaptive-equalization algorithm, is investigated; experimental validation has been realized for demodulation of 10-Gsymbols/s QPSK and 16-QAM signals. Chromatic dispersion compensation by DFE routine is discussed in [34]. Performance and implementation complexity are compared to MLSE and FFE for systems combined with phase modulated transmission formats. In [35, 36] DFE is applied for the demodulation in 75- to 110-GHz band of all optical OFDM fiber-wireless system. The proposed DFE structure is combined with a novel digital carrier phase and frequency recovery structure, which is a hybrid between Viterbi-Viterbi algorithm and digital phase-locked loop. The authors of [37] proposes a DFE scheme to enhance the tolerance of the employed DSP scheme to phase noise. More

recently, DFE based DSP solutions have been also considered for Nyquist Wavelength division multiplexing (N-WDM), a promising scheme where the channel bandwidth and spacing are selected to maximize the spectral efficiency while maintaining acceptable levels of inter-carrier and inter symbol interference [38]. Furthermore the FFE+DFE equalization structure has been demonstrated effective in Gb/s Polymer Optical Fiber (POF) transmission systems [39].

Optical intensity modulation for CO-OFDM has been dominantly employed due to its simplicity; however, it suffers from higher sensitivity to fiber nonlinearities due to the relative large PAPR. Therefore different approaches and experimental demonstrations to overcome technological issues in optical OFDM schemes have been reported. The resilience of the coherent optical OFDM signal to PMD in the transmission fiber is confirmed in [40], where nonlinear phase noise mitigation based on receiver digital signal processing is experimentally demonstrated for coherent optical OFDM transmission. In optical fiber communications, phase noise due to transmitter and receiver lasers [41], as well as the presence of a residual uncompensated carrier frequency offset (CFO) [42], are expected to degrade the performance of OFDM, due to the fact that ICI arises in this scenario. RF-pilot based phase noise compensation has been introduced in [43] and a novel pilot subcarrier based structure has been proposed in [44]. An extension of pilot-based phase noise mitigation scheme to compensate for sampling frequency offset (SFO) is proposed in [45]. The impact of fiber nonlinear impairments, such as self-phase modulation (SPM), cross-phase modulation (XPM), and fourwave mixing (FWM), has also been addressed in the literature, as it is known that, in dispersion-compensated links, the high PAR characterizing OFDM signals has a more detrimental effect on system performance than in SC transmission [46].

The increased interest in OFDM systems also raises attention towards synchronization in these systems. In such transmission schemes synchronization errors can destroy the orthogonality among the subcarriers and result in performance degradation. Several approaches take advantage of a special structure of training symbols to achieve faster timing and frequency synchronization. A preamble-aided method for timing and frequency offset estimation has been presented in [47]. The structure of the original preamble has been modified in [48] and a symmetrical correlation scheme has been then introduced in [49]. Multistage method for timing and frequency synchronization, based on the cross correlation characteristics presented in [50], is reported in [51]. A multistage scheme that works in time domain

and is independent of the preamble structure is proposed in [52]. The aim of [46] is to carry out an extensive investigation of the practical potential of OFDM for use over optical communication links at 100 Gb/s, through both analytical characterization and computer simulations. Specifically, comparison in terms of BER performance, complexity, and overall state-of-the-art feasibility is carried out between an OFDM communication system with a single-carrier communication scheme. High speed transmission systems enabling flexible modulation formats, flexible bandwidth and adaptive FEC have been reported in [53]. The author stressed that adaptable DSP algorithms are crucial in order to optimize resources and achieve good performances. Channel estimation and equalization, carrier phase recovery and nonlinearity mitigation for flexible transceivers have been investigated. Investigation of digitally generated OFDM performance and the required DSP algorithms has been presented in [54]. Furthermore the work presents comparison to another high spectral efficiency multiplexing technique such as Nyquist pulse generation. This system aim to obtain a trade-off between spectral confinement, pulse shaping, filter impulse response length, PAPR, appropriately oversampled DAC resolution, and ultra-dense WDM or optical superchannel system performance [55, 56].

Recently, some reported publications have been carried in the demonstration of wideband OFDM transmission using RoF techniques for the 60 GHz band [57–60] and ultra wide band over fiber systems [61]. The transmission performance of 16-QAM OFDM signal over 25-km fiber and 5-m air distance using 60 GHz RoF technology is firstly investigated in [57]. The feasibility of a simple multi-gigabit-per-second (Gb/s) RoF system using multilevel OFDM signalat 60 GHz and a single-electrode Mach–Zehnder modulator (MZM) is reported in [58]. Wireless data transmission of 31.4 Gb/s within 7 GHz license-free band at 60 GHz fiber transmission distances beyond 5 km is experimentally demonstrated in [59] using adaptive bit-loading OFDM modulation. In [60] the author adopts a companding transform coding technique to reduce the PAPR of the OFDM radio-over-fiber system. However, these results are achieved using expensive high-bandwidth optical modulators and photo-detectors. Due to the linearity requirement, the modulation depth is very low and the optical received power is relatively high, which leads to power wastage. A report on a scalable system by combining OOFDM and coherent all-optical frequency division multiplexed techniques to achieve high capacity wireless communications in the 75–110 GHz band is presented in PAPER 14 with transmission over 22.8 km SMF and up to 2 m air distance. A radio over fiber

link design for distributed antenna applications with wide radio channel bandwidth, complex modulation, a high number of OFDM subcarriers and several MIMO channels is presented in [62]. Subcarrier multiplexing is adopted in order to minimize cost.

Digital signal processing is also of crucial importance in receiver structure supporting reconfigurable format detection. The use of multiplexing techniques will put more stress on DSP techniques due to the coexistence and transmission of different modulation formats and bit rates. Particular interest has been latey put into elastic optical networks and in scenario with mixed modulation formats and bit rates. In [63] the author presents a WDM system with mixed modulation formats such as ASK and QPSK. An extensive experimental study on adaptive allocation of superchannels in spectrum-flexible heterogeneous optical network is reported in PAPER 20, where PDM QPSK and 16-QAM are the modulation formats considered. The first testbed demonstration of a flexible bandwidth network with a real-time adaptive control plane has been reported in [64,65] and an evaluation of elastic optical networking for next optical transmission systems is presented in [66]. Product solution has also been presented, like the scheme presented by Ciena [67], which has been demonstrated able to scale from 100 G to 400 G and switch between BPSK, QPSK and 16-QAM.

Furthermore digital signal processing algorithms able to blindly evaluate and estimate the modulation format transmitted are also under consideration. Particular focus has lately been put into Stokes space solution presented in [68] and PAPER 23.

1.6 Beyond state-of-the-art

The work presented in this thesis has extended the state-of-the-art in the area digital signal processing for different coherent optical transmission systems.

PAPER 1, **PAPER 2** and **PAPER 3** extend the state of the art introducing TE based solutions for high order modulation formats transmission links. Complete evaluation of the state-of-the-art and the results achieved is presented in Chapter 2.

In the area of ultra dense WDM systems, this PhD work focuses on implementing decision feedback equalizer to mitigate the interchannel interference induced by the extremely closed spacing. This work uses a similar scheme to the one presented in [35,36] where it is employed for the demodulation in 75- to 110-GHz band of all optical OFDM. This work extends the

state-of-the-art by introducing it for an UD-WDM system based on PM-QPSK modulation format and commercial DFB laser spaced at 12.5 GHz. The use of the proposed non-linear equalization is proven to reduce inter-channel interference and improve overall system performance in terms of OSNR. These achievements are presented in **PAPER 4**. In **PAPER 5** an experimental implementation of a long reach ultradense WDM system is reported. The DFE algorithm has been applied to mitigate the effects of inter-channel interference (ICI) and to guarantee system bit error rate (BER) back to back performance below the 7% overhead FEC threshold for all 30 sub-channels with DP QPSK modulation generated from a single DFB laser.

This work have also extended the state-of-the-art of PM RoF links assisted with coherent detection, employing multiplexing techniques such as OFDM. The digital signal processing algorithms have been accomplished based on state-of-the-art experiment and using a time synchronization scheme adapted from [47, 48]. The electrically generated OFDM link has been evaluated for its application in different scenarios for next generation broadband access networks. First, in **PAPER 6**, it is reported on the use of OFDM for phase modulated RoF link at an RF frequency of 5 Ghz. Successful demodulation of 4-QAM and 16-QAM OFDM signals after fiber transmission has been experimentally demonstrated by using a single reconfigurable digital receiver. The easy reconfigurability of the implemented digital receiver is proven also for PM CO-64QAM-OFDM and CO adaptive n-QAM OFDM where no hardware changes has been introduced in the experimental setup.

Elaborating further on the application of OFDM for RoF links, **PAPER 7** reports on the photonic generation of electrical OFDM modulated wireless signals in the 75-110 GHz band with in-phase/quadrature electrooptical modulation and optical heterodyn upconversion. Wireless transmission of 16-QAM OFDM signals is also experimentally demonstrated.

PAPER 8 reports on a converged wireless and optical fiber transport with experimental validation of different modulation formats, including Vertical-Cavity Surface-Emitting laser (VCSEL) based OOK, baseband QPSK, RoF OFDM, based on the scheme presented in **PAPER 6**, and wireless Impulse Radio (IR)-Ultra-Wide Band (UWB) over a 78 km deployed fiber link. A single, reconfigurable, digital coherent receiver is proposed and experimentally demonstrated for the demodulation of mixed modulation formats and bit-rates.

The overall scientific results and technical achievements presented in

this Ph.D. thesis have therefore significantly contributed to current state-of-the-art.

1.7 Main contribution and outline of the thesis

The main contributions of this thesis are in the area of digital signal processing for high capacity coherent optical transmission. First, this thesis proposes, studies and experimentally demonstrated feedback equalization techniques for high order modulation formats and ultra dense WDM systems. Secondly, it contributes on the evaluation and realization of digital signal processing for receiver structure supporting OFDM and the first ever demonstration of single reconfigurable receiver supporting mixed bit rates and modulation formats.

This thesis is structured as follows. Chapter 1 introduces the context of the main research papers included. It provides a short overview on the topic of capacity crunch in optical fiber transmission and digital signal processing algorithms. Feedback equalization and digital signal processing for coherent receiver are explained. The impact of the proposed scheme on mitigating impairments due to optical transmission are also evaluated. Chapter 2 describes the Turbo Equalization architecture and its benefit in optical fiber coherent transmission. Chapter 3 presents the novelty of the main contributions of the thesis. To conclude, chapter 4 summarizes the main achievements of this thesis and provides an outlook of further work on the prospects of the digital signal processing algorithms evaluated.

Chapter 2

Turbo Equalization

The employment of Quadrature Amplitude Modulation (QAM) modulation formats to increase both per-channel rate as well as WDM capacities is considered the next evolutionary step towards higher spectral efficiency and therefore higher data rates. A reliable compromise between various limiting factor is represented by 16-QAM, which still enables high-speed and high-capacity long-haul optical networking [3]. Furthermore Polarization Division Multiplexing (PDM) 16-QAM is considered as a promising candidate for doubling the bit rate per channel with respect to PDM Quadrature Phase-Shift Keying (QPSK). The major concerns associated with high data rates over transmission distances are the signal quality degradation due to linear and non-linear impairments. Linear fiber channel impairments, such as Chromatic Dispersion (CD), group velocity dispersion and polarization mode dispersion [69], can be effectively mitigated by using digital linear signal processing techniques as it has been demonstrated both for QPSK and higher order QAM signaling [8, 69]. Focus has been put on CD compensation and several methods to counteract its detrimental effects have been proposed, such as optical performance monitoring [70], CMA and autocorrelation based schemes and Maximum-Likelihood Sequence Estimation (MLSE) based criterion [71]. However transmitter and receivers imperfections, not entirely mitigated by linear techniques, still need to be addressed.

Nonlinear effects are also a major limiting factor for high data rates transmission in metro and long haul optical fiber links. Linear processing algorithms are shown to be less effective for compensation of such performance impairments stemming from optical fiber nonlinearities, such as self phase modulation, four-wave mixing and cross-phase modulation, and laser

phase noise [72, 73]. Several techniques have been reported in literature to mitigate for nonlinear optical fiber impairments. Digital backpropagation (DBP) has been presented as a universal method for jointly compensating dispersion and nonlinear impairments in optical fibers [74]. It is applicable to signals of any modulation format and has been reported for single channel and OFDM [74], WDM systems [75] and PDM 16-QAM [76]. In [77] the author directly compare (DBP) with spectral inversion (SI) and demonstrate that predispersed SI outperforms traditional SI, and approaches the performance of computationally exhaustive ideal DBP. The DBP method requires high-complexity processing based on split-step Fourier methods (SSFM) and solution to reduce its computational complexity in dispersion managed links have been proposed in [78]. Maximum likelihood sequence estimation (MLSE) has been proposed for the implementation of maximum likelihood (ML) detection in the presence of linear phase noise and Nonlinear Phase Noise (NLPN) [79]. It has also been proposed as nonlinear mitigator in long-haul 112 Gb/s PDM-QPSK transmission after linear impairment compensation block [80]. Pre- and post- compensation, such as multiplier-free predistortion [81], have been used for intrachannel nonlinearity compensation. Expectation maximization has been exploited in PAPER 19 and PAPER 22 for compensation of fibre nonlinearities, I/Q modulator imperfections and laser linewidth. However, most of these methods suffer from complexity and depend on particular optical fiber transmission scenarios. Therefore there is a need for efficient equalization techniques to enhance the benefit of the aforementioned non-linear techniques and to allow to search for new lower-complexity solution.

Additionally, in mixed modulation format transmission links, nonlinear impairments induced by co-existing 10 Gb/s Amplitude Shift-Keying (ASK) channels introduce a serious degradation to the overall system performance [82, 83]. Moreover, when long transmission reach is targeted, higher power levels launched into the fiber might be required to guarantee extended reach; however such high optical power level fiber transmission conditions enhance the generation of nonlinear optical fiber impairments. As the level of the M-ary modulation increases, higher optical signal-to-noise ration (OSNR) is required due to the reduced Euclidean distance between each signal point which gives rise to difficulties associated with distinguish between the states [84]. Forward error correction can compensate for the low OSNR, but the employment of a powerful FEC is not enough for transmitted signals affected by linear and nonlinear effects. The interplay between equalization and FEC becomes then a key technology for

future high speed transmission solutions [85].

2.1 State-of-the-art

Inspired by Turbo Codes, TE was firstly introduced to combat the detrimental effects of intersymbol interference effects in digital communication systems protected by a Convolutional Code (CC) [15]. A TE system consists of an iterative joint equalization and decoding technique in the receiver structure. Fig. 2.1 presents the two possible receiver structures.

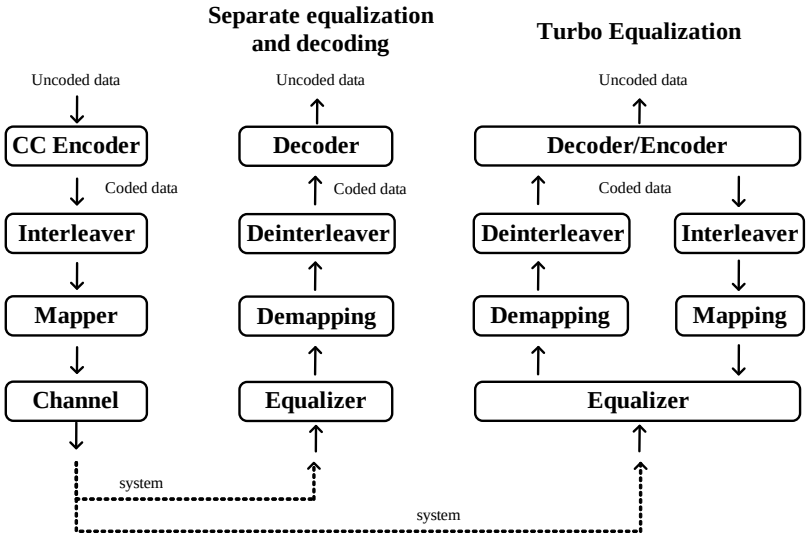

Figure 2.1: Turbo Equalization.

The standard approach is to split the detection problem into two separate parts, equalization and decoding. The latter could be based on hard or soft decoding. TE is instead an approach to jointly address the equalization and decoding tasks. A number of iterative receiver algorithms repeat the equalization and decoding tasks on the same set of received data, where feedback extrinsic information from the decoder is incorporated into the equalization process. The key point if this scheme is the iterative exchange of information between the two Soft-Input Soft-Output (SISO) modules, the equalizer and decoder which form the receiver.

In [15], Turbo Equalization (TE) has been realized through a $R = \frac{1}{2}$ CC with Soft Output Viterbi Algorithm (SOVA). Afterwards several methods for minimizing the bit error rate (BER) have been exploited, mostly based

on maximum likelihood (ML) estimation, which turns into a maximum a posteriori (MAP) probability estimation in the presence of a priori information of the transmitted data. Efficient algorithms exist for the MAP/ML sequence estimation, such as the Viterbi algorithm and for MAP/ML symbol estimation such as BCJR [86] algorithm. Both MAP/ML-based solutions often suffer from high computational load. A major research issue is thus towards the complexity reduction of such iterative algorithms [87, 88]. In [87] a simplification of the Log-Map algorithm has been addressed through numerical investigations. A novel technique to reduced the complexity of the BCJR algorithm in TE schemes is presented in [88]. Numerical results are reported for BPSK transmission over different transmission channels. Specific studies on the channel estimator have also been reported in literature. Analysis of soft input Kalman channel estimator and soft input weighted Recursive Least Squares (RLS) are presented in [89]. The aim of [90] is to show that many of the linear SISO equalizer can be interpreted as specific instances of the generic variational free energy minimization (VFEM) algorithm. It should be noted that in [90] the TE problem is addressed from a statistical physics perspective. Several approaches presented in other fields, such as magnetic recording channels and acoustic underwater, address the complexity and thus suggest to replace the MAP with a linear or a decision feedback equalizer [91, 92].

In optical communication field, TE routines have been first proposed and numerically evaluated for direct detection optical communication systems in order to mitigate the effects of Polarization Mode Dispersion (PMD) [93–96]. In [93] iterative TE is investigated to mitigate the effects of PMD in non return-to-zero (NRZ) intensity modulated optical fiber transmission systems. The performance of Symbol-by-symbol Maximum a Posteriori (sbs-MAP) SISO decoders is studied and compared to Soft Output Viterbi Equalizer (SOVE). Monte Carlo simulations of TE are proposed in [94]. Turbo equalization routines based on MAP solutions are proven to outperform the performances of separate decoding/equalization techniques based on MLSE and FEC. Investigation of Low-Density Parity-Check (LDPC) codes, as to replace the CC, is presented in [95]. Comparison of MLSE and TE based on LDPC codes of direct detected Differential Group Delay (DGD) channels and NRZ signaling is proposed in [96].

In coherent detection optical fiber communications the employment of systems based on Low-density parity-check (LDPC) coded TE have been numerically [97–99] and experimentally [98, 100, 101] presented. The technique presented by these groups of publications is a TE scheme based on

LDPC codes and BCJR equalizer. In [97] simulation results are reported for different DGD values and different LDPC codes for a return-to-zero ON-OFF keying (RZ-OOK). A MAP TE based on sliding-window multilevel BCJR algorithm and large-girth LDPC codes [102] is proposed in [98]. The scheme is proven suitable for simultaneous linear and nonlinear impairment mitigation in multilevel coded-modulation. PMD compensation by the proposed scheme is experimentally validated in a QPSK transmission. LDPC coded TE scheme in [99] is presented as a universal scheme for simultaneous mitigation of fiber nonlinearities, PMD, PDL, CD and I/Q imbalance effects in multilevel coded modulation schemes. The efficiency of LDPC-coded TE in suppression of fiber nonlinearities, chromatic dispersion compensation and PMD compensation is demonstrated and reported in [100]. To verify the efficiency of the proposed scheme, PMD compensation is experimentally demonstrated for a NRZ system operating at 10 Gb/s. Experimental validation of polarization multiplexed BPSK at 10 Gb/s is reported in [101]. A multilevel maximum a posteriori probability TE (MTE) is proposed and employed. More recently LDPC-coded TE has also been evaluated in electrical generated PDM Orthogonal Frequency Division Multiplexing (OFDM) 16-QAM for transoceanic transmission with large-core/ultralow loss fiber [103]. The experiment results suggest that 16-QAM OFDM modulation format could be employed in transoceanic optical transmission with the development of strong FEC coding capabilities and sophisticated DSP algorithms, such as TE.

Even though LDPC codes can be very powerful, as the works reported suggest, their implementation remains a challenge due to the complex structure of the decoder and alternative works are looking for simplified low complexity solutions [104].

2.2 Beyond the State-of-the-art

The work presented in this thesis has extended the state-of-the-art introducing a structure based on convolutional codes and normalized least mean square equalizer for high speed optical fiber transmission. Fig. 2.2 shows the receiver structure for TE employed in **PAPER 1**, **PAPER 2** and **PAPER 3**. At the transmitter side random generated data are created with offline processing and encoded by a convolutional code (CC) described by a states trellis. Rate $R = \frac{1}{2}$ for paper **PAPER 1**, **PAPER 2** and $R = \frac{1}{2}$,$R = \frac{2}{3}$ and $R = \frac{3}{4}$ for **PAPER 3** have been considered. The coded bits are then interleaved to suppress burst errors, and sent to the optical modulator at

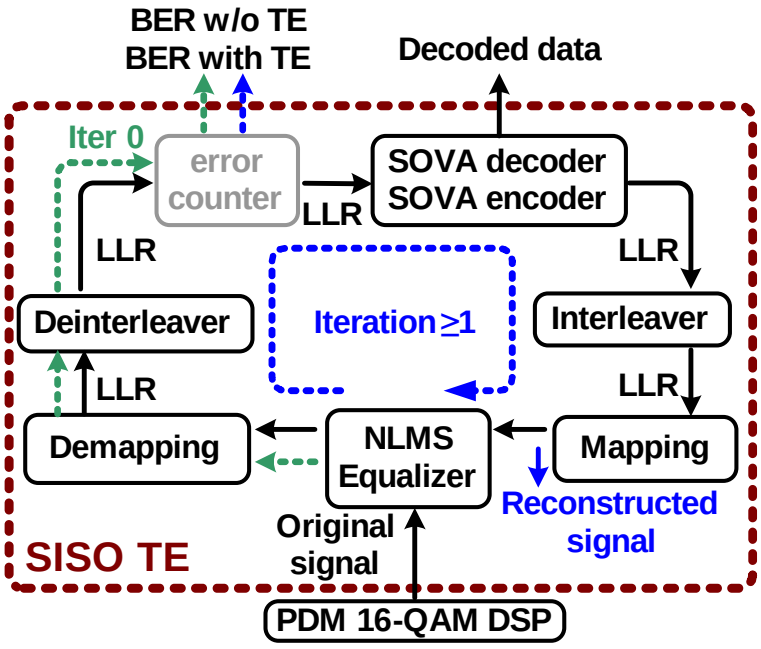

Figure 2.2: Schematic description of Turbo Equalization.

the transmitter in the physical layer.

Convolutional codes have up to now only been incompletely explored for optical communications. The drawback of such codes in optical transmission is their high coding overhead compared to high-rate block codes, such as Reed-Solomon (RS) codes and Low-Density Parity Check (LDPC) codes. On the other hand CC codes present attractive features such as simple and straightforward encoding and hard and soft decision decoding algorithms. The large overhead can be alleviated by using CC codes together with bandwidth-efficient modulation. Similar performance to RS codes has been obtained, with the benefit of simpler encoding electronics [105].

On the receiver side, the received signal after optical transmission and detection is then processed offline. After a 16-QAM DSP receiver, the received data is fed into the SISO TE structure presented in Fig. 2.2. A Normalized Least Mean Squared (NLMS) adaptive equalizer is applied due to the unknown nature of the transmission channel. The number of taps and the step is optimized to obtain the best performance in terms of bit error rate (BER). Soft information on all the coded bits in the form of log-likelihood-ratios (LLRs) is provided by the demapper. Two different

demapper blocks have been realized according to the mapping, Gray or Non-Gray resulting from the typical setup configuration on optical systems based on independent binary electronics. In the second mapping, not all the neighbor symbols differ by only one bit and therefore this requires a specific LLR calculation on which Section 2.2.1 focuses. After the mapping stage a deinterleaver process, symmetrical to the one employed at the transmitter side, is applied. An error counter will provide the system performance of the coded data in terms of BER.

Detailed description of the proposed TE scheme is reported in **PAPER 1**, Section II, **PAPER 2**, Section II and in **PAPER 3**, Section II.

In **PAPER 1**, **PAPER 2** and **PAPER 3** the BER performance without TE, is calculated at this point and is also called "iteration 0" and "w/o TE", to highlight that no complete iteration has been accomplished and the exiting of the loop. The values obtain at this moment represent the reference on which we calculate the gain in terms of BER. Moving forward with the TE iteration, decoding is performed using a soft output Viterbi algorithm (SOVA) binary decoder with a 64 states depth, for the $R = \frac{1}{2}$ case, to obtain soft estimation of both information and parity bits. The obtained decoded version of our signal is then re-encoded to create a reconstructed signal. After passing through an interleaving and mapping stage, to reproduce the original constellation, new soft estimates of the original transmitted symbols are obtained. An NLMS equalization process is then realized using the information of the original and reconstructed signal. Demapping, deinterleaving and decoding can be performed as for the first iteration. In every iteration the BER is evaluated at the error counter stage. The performance of one complete loop are named "TE 1st iter". The use of a Non-Gray mapping influences also the reconstruction part of the loop and due to this difficulties can arise difficulties to accomplish more iteration.

TE systems make use of knowledge of the channel together with the available redundancy introduced to protect the data, in the form of forward error correction (FEC). Therefore the benefit introduce by this technique rely on exchanging reliability information between the SISO equalizer and the SISO decoder, the so-called extrinsic information expressed in log-likelihood ratio (LLR) form. The encoder stage will give in return information in LLR form which will be used to create a reconstructed signal to be fed into the equalizer with the original received signal. The knowledge and reliability of the LLRs is therefore one of the key point of TE techniques. The proposed scheme based on TE has been experimentally

and numerically proven effective in mitigating accumulated noise induced by link amplification and the effects induced by fiber non-linearities. This TE approach features low complexity stemming from the use of a convolutional code, and its ability to accomplish for each new decoding iteration a more accurate channel estimation.

PAPER 1 is the first report of the proposed structure in optical fiber transmission. Compensated transmission, with and without interfering OOK neighboring channels, is experimentally verified, while uncompensated transmission is numerically investigated. In **PAPER 2** we present experimental demonstration of uncompensated link transmission up to 497 km in a WDM scenario. Gains and effectiveness of additional iterations are also reported. **PAPER 3** reports on the TE scheme proposed in its totality. Compensated and uncompensated transmissions are experimentally demonstrated, and numerical investigations are also reported. Three different convolutional codes have also been considered.

Table 2.1 gathers the experimental results achieved during this work on TE techniques and it shows the comparison with the latest state-of-the-art. It shows the chosen modulation format, Forward Error Correction (FEC) (LDPC or CC), equalization/turbo scheme (BCJR or NMLS VA), whether it is an experimental or numerical investigation, and the aim that each of the reported results wants to tackle. The research performed during this work has led to the demonstration of TE schemes for high order modulation formats, such as 16-QAM, which comprises of the current state-of-the-art.

2.2.1 Mapping and LLRs calculation

In Fig. 2.3 two different mapping for 16-QAM are shown. On the left side the Gray mapping and on the right side the Non-Gray mapping. In **PAPER 1** we report on TE scheme with Non-Gray mapping resulting from the typical setup configuration of optical systems based on binary electronics. The experimental results obtained in **PAPER 2** are instead based on the Gray mapped 16-QAM TE scheme. In Fig. 2.3 the value of the first two bits according to the region they belong to is also shown, for both mappings. As we can see in the Gray mapping design, if one moves from left to right, only one bit of the two is changed every time one passes from one region to another. On the other side, in the Non-Gray mapping, this feature is not present. It has been observed that moving from region 2 to region 3 requires changing both bits at the same time. This fact influences also the LLR calculation. The LLR calculation is realized for all the four bits that constitutes the 16-QAM signal and is based on the formulation

Table 2.1: State-of-the-art and main contribution reported in this thesis.

	Format	Scheme	Type	Aim
[97]	OOK	LDPC BCJR	Sim	PMD
[100]	OOK	LDPC BCJR	Sim/Exp	nonlinearities, CD, PMD
[101]	BPSK	LDPC BCJR	Sim/Exp	PMD
[98]	QPSK	LDPC BCJR	Sim/Exp	PMD
[99]	QPSK	LDPC BCJR	Sim/Exp	nonlinearities, PMD, PDL, CD, I/Q imb
[103]	OFDM 16-QAM	LDPC BCJR	Exp	record transmission
PAPER 1	PDM 16-QAM	CC NMLS VA	Sim/Exp	TX/RX imb ASE&NL noise
PAPER 2	PDM 16-QAM	CC NMLS VA	Exp	TX/RX imb ASE&NL noise
PAPER 3	PDM 16-QAM	CC NMLS VA	Sim/Exp	TX/RX imb ASE&NL noise

reported in [106]. We indicate the four bits as $b_{Re,k}$ $b_{Re,k}$ $b_{Im,k}$ $b_{Im,k}$ and $k = 0, 1$. The first two bits are derived from the real part of the signal, while the last two are derived from the imaginary part of the signal. The idea is demapping the received signal into soft bits which have the same sign as provided by a hard detector and whose absolute value represents the reliability of the decision. The optimum hard decision on bit $b_{Re,k}$ is given by the rule:

$$b_{Re,k} = \beta \quad if \quad P[b_{Re,k} = \beta | r] > P[b_{Re,k} = (1-\beta) | r] \quad \beta = 0, 1 \tag{2.1}$$

where r represents the received signal

$$r = G_{ch} \cdot a + w \tag{2.2}$$

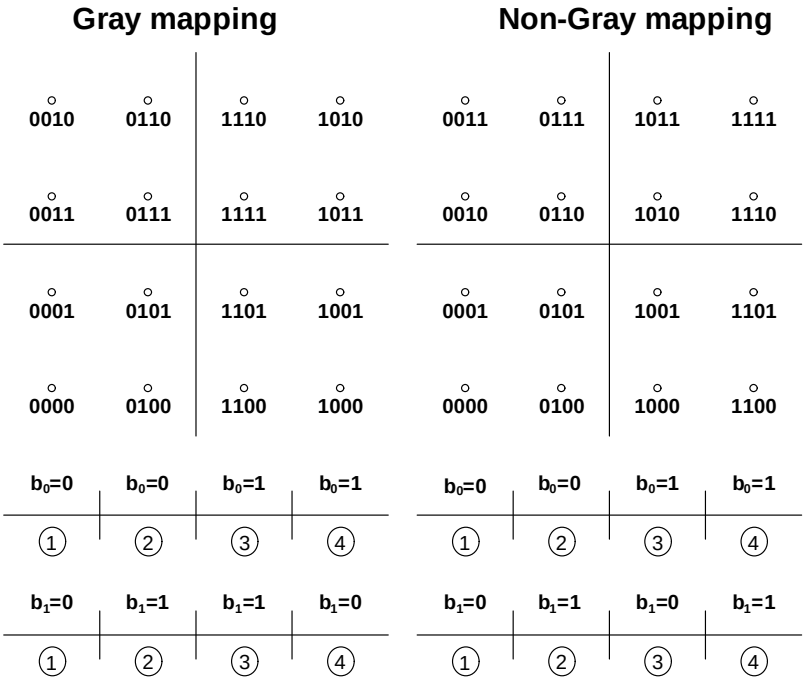

Figure 2.3: Schematic description of mapping.

where G_{ch} is the channel frequency response and w is the complex AWGN noise. If we set $\beta = 1$ we can rewrite 2.1 as

$$\hat{b}_{Re,k} = 1, \quad if \quad log\frac{P(r|b_{Re,k}=1)}{P(r|b_{Re,k}=0)} > 0 \tag{2.3}$$

As example, we consider $k = 0$, the first bit of the real part. As shown in Fig. 2.3 for both case this bit is mapped with the same rule for both studied cases. Therefore we obtain

$$\frac{P(r|b_{Re,0}=1)}{P(r|b_{Re,0}=0)} = \frac{e^{\frac{-(y_{Re}-1)^2}{2\sigma^2}} + e^{\frac{-(y_{Re}-3)^2}{2\sigma^2}}}{e^{\frac{-(y_{Re}+1)^2}{2\sigma^2}} + e^{\frac{-(y_{Re}+3)^2}{2\sigma^2}}} \tag{2.4}$$

The formulation in 2.4 has been obtained considering that when $b_{Re,0} = 0$ the real part of the 16QAM can only assume negative values, that is -3 or -1, and when $b_{Re,0} = 1$ the real part of the 16-QAM can only assume positive values, that is $+1$ or $+3$. Therefore the LLR formulation for $b_{Re,0}$ is the same reported in [106].

When a particular region is considered, one can assume that some of the relative contribution in the numerator or denominator can be ignored.

Table 2.2: LLRs formulas for $b_{Re,0}$ and $b_{Re,1}$. Upper part Gray mapping, lower part non-Gray mapping

Region		$LLR(b_{Re,0})$	$LLR(b_{Re,1})$
1	$y < -2$	$\frac{4}{\sigma^2}(y_{Re}+1)$	$\frac{2}{\sigma^2}(y_{Re}+2)$
2	$-2 \leq y < 0$	$\frac{2}{\sigma^2}y_{Re}$	$\frac{2}{\sigma^2}(y_{Re}+2)$
3	$0 \leq y < +2$	$\frac{2}{\sigma^2}y_{Re}$	$\frac{2}{\sigma^2}(-y_{Re}+2)$
4	$y \geq +2$	$\frac{4}{\sigma^2}(y_{Re}-1)$	$\frac{2}{\sigma^2}(-y_{Re}+2)$
1	$y < -2$	$\frac{4}{\sigma^2}(y_{Re}+1)$	$\frac{2}{\sigma^2}(y_{Re}+2)$
2	$-2 \leq y < 0$	$\frac{2}{\sigma^2}y_{Re}$	$\frac{2}{\sigma^2}(-y_{Re})$
3	$0 \leq y < +2$	$\frac{2}{\sigma^2}y_{Re}$	$\frac{2}{\sigma^2}(-y_{Re})$
4	$y \geq +2$	$\frac{4}{\sigma^2}(y_{Re}-1)$	$\frac{2}{\sigma^2}(y_{Re}-2)$

According to the 4 possible regions one can therefore obtain the following possibilities:

$$LLR_{Re,0} = \begin{cases} \frac{4}{\sigma^2}(y_{Re}[i]+1), & y_{Re}[i] < -2, \quad region1 \\ \frac{2}{\sigma^2}(y_{Re}[i]), & y_{Re}[i] \leq 2, \quad region2\&3 \\ \frac{4}{\sigma^2}(y_{Re}[i]-1), & y_{Re}[i] > +2, \quad region4 \end{cases} \tag{2.5}$$

Similarly to what obtained for $b_{Re,0}$ one can obtain the formulations for $b_{Re,1}$. In this case, the calculation is mapping dependent. For a Gray mapping one obtains

$$\frac{P(r|b_{Re,0}=1)}{P(r|b_{Re,0}=0)} = \frac{e^{\frac{-(y_{Re}+1)^2}{2\sigma^2}} + e^{\frac{-(y_{Re}-1)^2}{2\sigma^2}}}{e^{\frac{-(y_{Re}+3)^2}{2\sigma^2}} + e^{\frac{-(y_{Re}-3)^2}{2\sigma^2}}} \tag{2.6}$$

For a non-Gray mapping instead one obtains

$$\frac{P(r|b_{Re,0}=1)}{P(r|b_{Re,0}=0)} = \frac{e^{\frac{-(y_{Re}-3)^2}{2\sigma^2}} + e^{\frac{-(y_{Re}+1)^2}{2\sigma^2}}}{e^{\frac{-(y_{Re}-1)^2}{2\sigma^2}} + e^{\frac{-(y_{Re}+3)^2}{2\sigma^2}}} \tag{2.7}$$

Using the presented reductions and expressing the LLRs in logarithmic form one obtains Table 2.2 for $b_{Re,0}$ and $b_{Re,1}$ for the two mapping

The LLR formulas calculation for $b_{Im,0}$ and $b_{Im,1}$ follows the same rules as for $b_{Re,0}$ and $b_{Re,1}$. Similar equations are therefore obtained on the imaginary part of the signal. In **PAPER 1**, **PAPER 2** and **PAPER 3** it is assumed that all the clusters have the same variance and therefore the factor $2\sigma^2$ is removed from all the LLR formulas. A study on the different variances of the 16 clusters can lead to a more precise calculation of the LLR and therefore to a better performance.

The mapping block realizes the inverse operation of the demapping block. The encoder creates a new encoded signal based on the obtained decoded version of the original received data. After passing through an interleaving stage, the mapping block uses the new soft estimates of the original transmitted symbols to create a reconstructed signal based on the inverse formulas reported in Table 2.2.

Detailed description of mapping and LLRs calculation is reported in **PAPER 1**, Appendix, and in **PAPER 3**, Section III.

2.3 Conclusions

Turbo Equalization (TE) techniques based on Convolutional Codes (CC) and Normalized Least Mean Squared (NLMS) equalizer have been demonstrated as promising techniques to compensate for accumulated noise induced by link amplification, the effects induced by fiber nonlinearities and transmitter/receiver imperfections. Experimental investigations show that gain exceeding one order of magnitude in terms of BER can be obtain for compensated and uncompensated link transmission of up to 700 km. In addition numerical investigations has been conducted to confirm the results experimentally obtained. Furthermore it has been reported on the LLR calculation based on 16QAM Gray and Non-Gray mapping. In conclusion it has been demonstrated that lower complexity TE is still effective in high speed long haul fiber transmission.

Chapter 3

Description of papers

This thesis is based on a set of articles already published or submitted for publication in peer-reviewed journals and conference proceedings. These articles present the results obtained during the course of my doctoral studies on feedback equalization techniques for impairments mitigation and flexible modulation schemes and on digital signal processing (DSP) for receiver structure. The papers are grouped in two categories. Feedback equalization techniques for high modulation formats and WDM techniques are studied and demonstrated experimentally in **PAPER 1** to **PAPER 5**. **PAPER 6** to **PAPER 8** present the experimental results for DSP for receiver structure supporting OFDM and reconfigurable format detection.

3.1 Feedback equalization

PAPER 1 presents experimental results for Turbo Equalization (TE) applied to high modulation formats uncompensated coherent system. The main novelty of this paper is the use of a simple TE technique based on Convolutional Code (CC) and Normalized Least Mean Squared (NLMS) equalizer. **PAPER 1** includes theoretical and experimental investigation of dispersion managed link transmission also in the presence of interfering co-propagating OOK channels. A 80 Gb/s 16-QAM signal, previously encoded, has been transmitted through 640 km long coherent transmission link consisting of spans of standard single mode fiber (SSMF) and dispersion compensated fiber (DCF). At the receiver side a Soft-Input Soft-Output (SISO) TE routine has been proven to guarantee a 2 dB increment in link input power tolerance and a gain of about half order of magnitude at the best operational point in terms of BER.

PAPER 2 reports on the experimental verification of TE applied to high modulation formats in dispersion uncompensated coherent links. The system consists of a 100 GHz grid WDM transmission with a central PDM 16-QAM signal and surrounding QPSK channels. The proposed TE structure, based on rate $R = \frac{1}{2}$ CC and NLMS equalizer, is able to counteract PDM 16-QAM transmission impairments in dispersion uncompensated coherent transmission links. Gains exceeding one order of magnitude in terms of BER are obtained through experimental validation up to 497 km SSMF link transmission. Furthermore, the use of more iterations, due to the Gray mapping, is proven to enhance the performance in terms of BER.

PAPER 3 presents a complete work reporting on the theoretical model, computer simulation and experimental results for a 16-QAM link with TE. A turbo loop with CC and NLMS equalizer is considered. Computer simulation and experimental results are reported for dispersion compensated coherent links. Experimental demonstrations have been conducted based on CC with different rate ($R = \frac{1}{2}$, $R = \frac{2}{3}$ and $R = \frac{3}{4}$). The considered TE technique can provide gains exceeding one order of magnitude in terms of BER for uncompensated transmission up to 750 km of SSMF for all the considered codes. Furthermore dispersion managed link transmission is also experimentally investigated. Gains of about half order of magnitude are obtained also with co-propagating OOK channels.

PAPER 4 presents the use of Decision Feedback Equalizer (DFE) in an Ultra Dense WDM transmission scheme. In order to allocate extremely closed carriers, it is suggested to use of the proposed digital non-linear equalization to mitigate inter-channel interference and improve overall system performance in terms of OSNR. The scheme is experimentally demonstrated in a 80 km optical fiber uncompensated transmission system. The solution reported allows also the use of independent tunable DFB lasers spaced at 12.5 GHz for ultradense WDM PM-QPSK flexible capacity channels for metro core networking. Furthermore the efficiency of the algorithm proposed is experimentally verified in a system with 3 coherent carriers.

PAPER 5 reports on an experimental implementation of a long reach ultradense WDM system based on a single distributed feedback (DFB) laser to generate 30 sub-channels with DP QPSK modulation. A WDM 30x40 Gb/s DP QPSK achieving 1.2 Tb/s on a bandwidth of 300 GHz is demonstrated. A DFE algorithm has also been implemented in the DSP to

mitigate the effects of Inter-Channel Interference (ICI) for this ultradense WDM system. The employment of non-linear DFE equalizer guarantees system bit error rate (BER) back to back performance below the 7% FEC overhead threshold for all 30 sub-channels.

3.2 Digital Signal processing for receivers structure

PAPER 6 reports on the use of phase modulated coherent detected orthogonal frequency-division multiplexing (OFDM) supported by a reconfigurable DSP receiver that allows for adaptation of the modulation order of the transmitted signal. Successful digital coherent demodulation of optical phase-modulated adaptive order QAM (4, 16, and 64) OFDM signals is achieved by a single reconfigurable digital receiver after 78 km of optical deployed fiber transmission. Also reported is the ease of reconfiguring the implemented digital receiver capable of achieving BER values conform to the 7% FEC overhead for back-to back PM CO-64QAM-OFDM and CO adaptive n-QAM OFDM, without hardware changes in the experimental setup.

PAPER 7 presents the wireless transmission of 16-QAM electrical orthogonal frequency-division multiplexing (OFDM) modulated signals in the 75-110 GHz band employing in-phase/quadrature electrooptical modulation and optical heterodyn upconversion. Signals of 19.1 Gb/s in 6.3 GHz bandwidth are transmitted over up to 1.3 m wireless distance. Optical comb generation is further implemented to support different channels and therefore different users. Transmission is also demonstrated in the multiband system. Electrical OFDM modulation with a high number of subcarriers has been chosen and implemented in this work to benefit from its high spectral efficiency, flexibility, and robustness against fiber dispersion impairments and wireless multipath fading. Detection is furthermore compensated by baseband Digital Signal Processing (DSP).

PAPER 8 reports on the application of a reconfigurable digital coherent receiver for unified heterogeneous metro-access network. 4 signals from different optical access technologies are WDM multiplexed onto the same optical fiber, transported through 78 km of installed optical fiber and detected using a single reconfigurable digital coherent receiver. The heterogeneous metro access network is composed of the following subsystems: 1) 5 Gb/s directly modulated Vertical-Cavity Surface-Emitting laser (VCSEL). 2) Baseband 20 Gb/s non return-to-zero (NRZ)-Quadrature Phase Shift Keying (QPSK). 3) Optically phase-modulated 2 Gb/s Impulse Radio (IR) Ultra-Wide Band (UWB) and 4) PM-Coh link with 500 Mb/s OFDM at 5 GHz RF frequency. The robustness of the OFDM transmission is here

therefore verificated in a mixed modulation and bit rated scenario. The original work presented in PAPER 10 has been awarded the Honorable Mentions of the Corning Outstanding Student Paper Competition at the Optical Fiber Communication Conference (OFC) in 2011.

Chapter 4

Conclusion

4.1 Conclusions

This thesis addresses the design and performance evaluation of advance Digital Signal Processing (DSP) in coherent optical transmission systems. The focus of the thesis is on the use of digital signal processing as a technique for compensation of transmission impairments and interchannel interference, as well as on the design of digital signal processing for receiver structure supporting Orthogonal Frequency Division Multiplexing (OFDM) and reconfigurable format detection. The research results presented in this thesis are pioneering in two main areas. First, in the evaluation of feedback equalizer structure based on Turbo Equalization (TE) techniques and Decision Feedback Equalizer (DFE) schemes. Experimental verification of the approach has been realized through 16-QAM coherent optical transmission, for TE schemes, and ultra dense WDM, for DFE. Second, the design of digital signal processing for receiver structure supporting OFDM and reconfigurable format detection has been experimentally demonstrated. These achievements fulfill the requirements on digital signal processing evolution towards high capacity next generation coherent optical fibre networks.

4.1.1 Feedback equalization

Feedback equalization schemes are shown in this thesis to be an effective solution for high order modulation formats. The results in **PAPER 1**, **PAPER 2** and **PAPER 3** provide experimental demonstration of the capabilities of TE routines to counteract the detrimental effects of fibre transmission in a PDM 16-QAM transmission system. The presented DSP

algorithm can be used as an alternative or complementary technique to high gain forward error correction structure. This conclusion is based on the results shown in **PAPER 1**, reporting experimental validation for compensated link transmission, in **PAPER 2**, for uncompensated link transmission case, and in **PAPER 3**, where different codes are presented. The employment of the TE routine guarantees gain of half order of magnitude in **PAPER 1** and gain exceeding one order of magnitude in **PAPER 2** and **3** in terms of BER.

The integration of DFE structure into the DSP algorithm scheme, is reported in **PAPER 4** and **PAPER 5**. The presented digital non-linear equalization, able to mitigate inter-channel interference and improve overall system performance in terms of OSNR, is presented in **PAPER 4**. Experimental implementation of a long reach ultradense WDM system employing DFE equalization is also presented in **PAPER 5**.

4.1.2 Digital signal processing for receiver structure supporting OFDM and reconfigurable format detection

Digital signal processing is proven to be a key component towards heterogeneous scenario with co-transmission of baseband single carrier signals, wireless Radio-over-Fiber (RoF) networks and multiband transmission schemes, such as OFDM. The investigation on OFDM for optical fiber transmission is mostly motivated by its large immunity to Chromatic Dispersion (CD) and Polarization Mode Dispersion (PMD) effects, by its high spectral efficiency and by the implicit parallelization of the processing due to the IFFT/FFT operations. The multiple-carrier characteristic of OFDM signal requires system linearity and the ability to handle its large peak-to-average power (PAPR) that can be guarantee by the proposed phase modulated RoF system presented in **PAPER 6**. Extension of this system is proposed in **PAPER 7** where the wireless transmission of 16-QAM electrical OFDM modulated signals in the 75-110 GHz band employing in-phase/quadrature electrooptical modulation and optical heterodyn upconversion is presented.

The integration of the proposed Phase Modulated RoF link assisted with Coherent Detection (PM-Coh) OFDM RoF with baseband access networks was also demonstrated in **PAPER 8**, where four different signals, with different modulation formats and bit rates, were transmitted and detected with a single reconfigurable digital receiver.

4.2 Future work

In this section a view of the future work that could be pursued for further development and benefit assessment of the digital signal processing techniques reported in this thesis is provided.

4.2.1 Digital signal processing for high order modulation format

Further work is suggested on the use of DSP algorithm to enable the employment of larger constellation sizes and thus extending the system reach of such modulation formats [2]. The use of advanced forward error correction based on Low-Density Parity-Check (LDPC) codes and reduced-complexity decoding algorithms will enable next-generation systems to have higher coding gains and higher bit-error rate thresholds, resulting in system performance closer to channel capacity.

Turbo loops of combined equalizer/detector/FEC decoder will enhance the receiver performance in future multi level optical transmission systems and thus TE routines are believed to be a key technology for the deployment of 100 G and to enable 400 G transmissions [84, 85]. However, the interplay of the TE scheme with high gain FEC structure still need to be addressed. Evaluation of complexity and implementation possibility in Field Programmable Gate Array (FPGA) and coherent ASIC also need to be considered. Collaboration within TE and nonlinear mitigator structures should also be evaluated. Challenges for digital coherent receivers are mostly related to A/D convertors speed, limited bandwidth and effective number of bits, and the real time implementation of DSP algorithms at the receiver.

When the capacity of single-core single-mode fibers becomes exhausted, space-division multiplexing will be required to satisfy the user's bandwidth demand. Multicore and multimode fibers, which nowadays present numerous challenge to be solved, are therefore an open topic research for new advance multiple-input multiple-output digital signal processing techniques [12]. New paradigm and challenges will then need to be addressed to avoid drastic increase in the DSP complexity when the number of spatial modes is increased [107, 108].

4.2.2 Multiplexing systems: WDM and OFDM

Future optical networks will no longer be constrained to a fixed wavelength grid, thus they will require the ability to dynamically allocate network resources to different users in response to their traffic demands. Future optical systems will require higher capacity, flexibility and indispensable ease of control and management. One arising solution is the use of superchannels [109, 110]. However advance DSP techniques able to create orthogonal optical subcarriers to be modulated and detected via parallel transmitters and receivers also need to be developed. Furthermore, the data rate per-channel will not be anymore constrained by the bandwidth limitations of the electronic components, introducing new challenges to be tackled by DSP solutions.

The user bandwidth demand will claim an additional reduction of the spectral guard bands between neighboring channels. Advanced spectral shaping techniques, able to increase the spectral utilization and spectral efficiency, are therefore required.

The challenges for digital signal processing are many. Digital coherent receivers will need to handle not only mixed bit rates and modulation formats, but will also be needed to reduce their latency as to allocate the network resources required in the shortest possible time. Utra dense WDM and OFDM with even narrower guard bands will require more algorithms to reduce the induced impairments. Challenges in terms of DSP complexity will arise in order to maintain solution commerciable and upgreadable.

Finally future optical systems need to be self-adjustable as to support the continuing demand of new and diverse services. Cognitive optical networks based on models of human-brain abilities and with reduced man intervention for their control and management, are expected to be integrated into the network to implement future optical communication networks.

Paper 1: Turbo Equalization techniques towards robust PDM-16-QAM optical fiber transmission

V. Arlunno, A. Caballero, R. Borkowski, S. Saldaña Cercós, D. Zibar, K. J. Larsen and I. Tafur Monroy, "Turbo Equalization techniques towards robust PDM-16-QAM optical fiber transmission," *Journal of Optical Communications and Networking*, Vol. 6, No. 2, February 2014.

Turbo Equalization Techniques Toward Robust PDM 16-QAM Optical Fiber Transmission

Valeria Arlunno, Antonio Caballero, Robert Borkowski, Silvia Saldaña Cercós, Darko Zibar, Knud J. Larsen, and Idelfonso Tafur Monroy

***Abstract*—In this paper, we show numerically and experimentally that turbo equalization (TE) is an efficient technique to mitigate performance degradations stemming from optical fiber propagation effects in both optical fiber dispersion managed and unmanaged coherent detection links. The effectiveness of the proposed solution can be appreciated in both linear and nonlinear regimes for either scenario. We report on a system employing a polarization division multiplexing (PDM) 16-quadrature amplitude modulation (QAM) format for which we accomplish an increment in tolerance to link input power of up to 3 dB that represents a substantial improvement margin. The best bit error rate (BER) performances will therefore be guaranteed in a larger window, 6 dB, of link input power thanks to the implemented TE scheme. Moreover, our proposed approach is also proven to effectively mitigate interchannel impairments from surrounding amplitude shift-keying interfering channels in a dispersion managed link achieving also in this case an increment in power tolerance of 3 dB. Furthermore, in terms of BER performances, our proposed TE approach guarantees a gain of about a half order of magnitude at the best operational point. As TE can be included in the current coherent detection transceiver technologies and complement other equalization techniques, it has prospects for application in next-generation high-capacity and long-reach optical transmission links.**

***Index Terms*—Coherent detection; Convolutional codes; Equalizers; Optical transmission; Signal processing algorithms; Turbo equalization.**

I. Introduction

Higher-order modulation formats constitute an attractive solution toward capacity upgrade of the existing optical fiber infrastructure by exploiting their important feature of high spectral efficiency [1–5]. For example, polarization division multiplexing (PDM) 16-quadrature amplitude modulation (QAM) is considered as a promising candidate for doubling the bit rate per channel with respect to PDM quadrature phase-shift keying (QPSK). In these transmission systems, linear fiber channel impairments, such as chromatic dispersion, group velocity dispersion, and polarization mode dispersion (PMD), can be effectively mitigated using digital linear signal processing techniques, as has been demonstrated for both QPSK and higher-order QAM signaling [6]. However, transmitter and receiver imperfections, not entirely mitigated by linear techniques, still need to be addressed. Linear processing algorithms are shown to be less effective for compensation of performance impairments stemming from optical fiber nonlinearities, such as self-phase modulation, four-wave mixing, cross-phase modulation, and laser phase noise. Additionally, in mixed modulation format transmission links, nonlinear impairments induced by coexisting 10 Gb/s amplitude shift-keying (ASK) channels introduce a serious degradation to the overall system performance [7]. Moreover, when long transmission reach is targeted, higher power levels launched into the fiber might be required to guarantee extended reach; however, such high optical power level fiber transmission conditions enhance the generation of nonlinear optical fiber impairments.

Several techniques have been reported in the literature to mitigate for nonlinear optical fiber impairments, such as digital backpropagation, maximum likelihood sequence estimation (MLSE), use of radio frequency pilot, pre- and post-compensation, or expectation maximization [8–14]. However, these methods suffer from complexity and depend on particular optical fiber transmission scenarios. Therefore there is a need for efficient equalization techniques to enhance the benefit of the aforementioned nonlinear techniques or to allow us to search for a new lower-complexity solution.

In this paper, we present a scheme based on turbo equalization (TE) equally effective in mitigating accumulated noise induced by link amplification and the effects induced by fiber nonlinearities. We realize a digital signal processing (DSP) structure based on convolutional code (CC), normalized least mean square (NLMS) equalization, and a soft-input soft-output (SISO) routine. TE routines have been proposed for direct detection optical communication systems in order to mitigate the effects of PMD [15,16]. In coherent detection optical fiber communications, until now, experimental demonstration of low-density parity-check (LDPC) coded TE [17–19] has been presented for polarization multiplexed binary phase-shift keying (BPSK) and QPSK. More recently LDPC-coded TE has also been

Manuscript received May 2, 2013; revised December 18, 2013; accepted December 22, 2013; published January 31, 2014 (Doc. ID 189917).

The authors are with DTU Fotonik, Department of Photonics Engineering, Technical University of Denmark, Ørsteds Plads 343, 2800 Kgs. Lyngby, Denmark (e-mail: vaar@fotonik.dtu.dk).

http://dx.doi.org/10.1364/JOCN.6.000204

evaluated in electrical generated PDM orthogonal frequency division multiplexing (OFDM) 16-QAM for transoceanic transmission with large-core/ultra-low-loss fiber [20]. Even though LDPC codes can be very powerful, their implementation remains a challenge due to the complex structure of the decoder, and alternative works are looking for simplified low-complexity solutions [21].

We expand the state of the art by introducing TE for coherent optical links using an advanced modulation format, 16-QAM, including the transmission scenario with unmanaged and managed optical links with standard single-mode fiber (SSMF) and also in the presence of legacy channels in a 100 GHz spectral grid. We perform experimental and numerical validation of the performance of our proposed TE for different fiber transmission lengths. We evaluate the performance both in the linear regime, where the performance is mostly degraded by chromatic dispersion and amplified spontaneous emission (ASE) noise introduced by the amplifier of the transmission link, and in the nonlinear regime, where nonlinearities are the dominant effects of performance degradation. Nevertheless further investigations should be realized to better evaluate the proposed scheme when specific nonlinear effects are targeted. Our TE approach features low complexity stemming from the use of a CC, and its ability to accomplish for each new decoding iteration a more accurate channel estimation. Concatenated Reed–Solomon (RS), Bose–Chaudhuri–Hocquenghem (BCH), and LDPC codes are employed as error correcting schemes in current optical communication products. In our case the employment of a simple and weaker code, i.e., CC, has been chosen to show the advantages of the TE routine and to avoid complexity challenges that solutions based on the other codes would present.

All the presented results in this paper have been obtained employing a PMD 16-QAM coherent detection system. We first implement a TE scheme in a simulation tool, and then we perform experimental validation. For completeness of results we study the effectiveness of our approach in a dispersion uncompensated link, through numerical investigations, and in a dispersion compensated link, through experimental investigations. Both experiment and simulation show that an increment in power tolerance up to 3 dB and a bit error rate (BER) gain of a half order of magnitude can be accomplished, confirming the efficiency of our approach for both scenarios. Additionally we perform experimental validation for PDM 16-QAM transmission surrounded by neighbor 10 Gb/s ASK channels in a 100 GHz spectral grid, a situation in which the transmission reach is severely distorted by cross nonlinear impairments due to the interactions with the copropagating ASK channels. A total increment in power tolerance of up to 3 dB is also accomplished in this case. Both CC and the equalizer contribute in the TE routine to achieve the obtained improvements.

II. Turbo Equalization

Inspired by turbo codes, TE was first introduced to combat intersymbol interference effects in digital communication systems [22]. A TE system consists of an iterative joint equalization and decoding technique that can achieve impressive performance gains in terms of signal-to-noise ratio (SNR) for communication systems.

Figure 1 shows the pre-encoder and receiver structure for TE employed in this work. Random generated data 1000 bits long are created with offline processing and encoded by a CC with rate $R = ½$ and 16 states trellis. The 2000 coded bits are then interleaved to suppress burst errors and sent to the optical modulator at the transmitter in the physical layer. CCs have up to now only been incompletely explored for optical communications. The drawback of such codes in optical transmission is their high coding overhead compared to high-rate block codes, such as RS codes and LDPC codes. On the other hand, CC codes present attractive features such as simple and straightforward encoding and hard and soft decision decoding algorithms. The large overhead can be alleviated by using CC codes together with bandwidth-efficient modulation. Similar performance to RS codes has been obtained, with the benefit of simpler encoding electronics [23]. In this work we present a simple CC not only for the features presented, but also for convenience purposes in demonstrating its benefits and the advantages of TE. However, a more complex code can be designed and evaluated in the future.

On the receiver side, the received signal after optical transmission and detection is then processed offline. After a 16-QAM DSP receiver [12], the received data are fed into a SISO TE structure. A NLMS adaptive equalizer is applied due to the unknown nature of the transmission channel. We optimize the number of taps and the step to obtain the best performance. Soft information on all the coded bits in the form of log-likelihood ratios (LLRs) is provided by the demapper. A nongray 16-QAM mapping results due to the typical setup configuration on optical systems based on independent binary electronics, requiring a specific

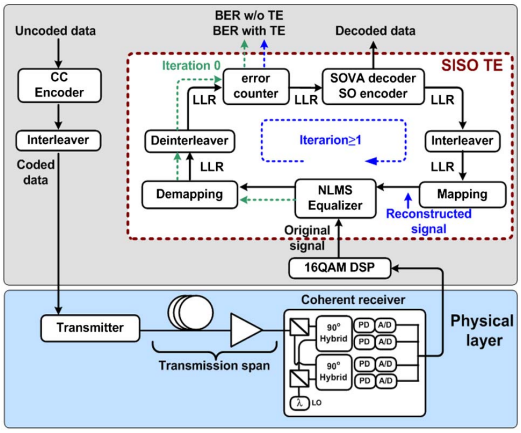

Fig. 1. Pre-encoding and receiver structure of the SISO turbo equalizer algorithm. CC, convolutional code; LO, local oscillator; PD, photodiode; A/D, analog-to-digital converter; DSP, digital signal processing; NLMS, normalized least mean square; LLR, log-likelihood ratio; SOVA, soft-output Viterbi algorithm; SO, soft output; SISO, soft-input soft-output; TE, turbo equalization.

demapper implementation. In this mapping, not all the neighbor symbols differ in only one bit, thus requiring a specific LLR calculation. For more details regarding mapping and LLR calculation, please refer to Appendix A. Thereafter we apply a deinterleaver process, symmetrical to the one employed at the transmitter side. An error counter will then give us the performance of the system in terms of BER. The performance without TE, later presented in this work, is calculated at this point and is also called "iteration 0" and "w/o TE," to highlight that no complete iteration has been accomplished and we are exiting the loop. Moving forward with the TE iteration, we perform decoding using a soft-output Viterbi algorithm (SOVA) binary decoder with 64 states to obtain soft estimation of both information and parity bits. We then re-encode the obtained decoded version of our signal to create a reconstructed signal. After passing through an interleaving and mapping stage, to reproduce the original constellation, new soft estimates of the original transmitted symbols are obtained. We then realize an NLMS equalization process using the information of the original and reconstructed signal. Demapping, deinterleaving and decoding can be performed as for the first iteration. In every iteration we evaluate the BER at the error counter stage. In this work the results presented as "with TE" represent just the first complete iteration of the TE routine. The use of a nongray mapping also influences the reconstruction part of the loop and therefore could originate difficulties in the realization of more iteration, as explained in Appendix A.

III. Simulation and Experimental Setup

A. Simulation Setup

The setup used for the numerical simulations is presented in Fig. 2. The numerical setup is composed of three main blocks: 4-pulse amplitude modulation (PAM) generation and transmitter, link transmission, coherent receiver, and DSP modules. At the transmitter side the output of a 100 kHz linewidth laser is passed through an optical I/Q modulator driven by two four-level PAM electrical signals to generate the optical 16-QAM single polarization (SP) signal. The 4-PAM module consists of an encoding process, signal mapping, upsampling, pulse shaping, digital-to-analog conversion, attenuators, and electrical amplifiers. The baud rate is kept at 28 Gbaud. The orthogonal polarization, Y, is created with the same procedure. The two signals are then combined with a polarization beam combiner (PBC) to create a PDM 16-QAM signal. In the link transmission block the PDM 16-QAM signal is amplified and launched into the fiber span link. The transmission link consists of spans of SSMF of 100 km length. Three link lengths of 1000, 1500, and 2000 km, corresponding to a number of spans equal to 10, 15, and 20, respectively, are evaluated. For the SSMF we have the following fiber parameters: $\alpha_{\text{smf}} = 0.2$ dB/km, $D_{\text{smf}} = 17$ ps/nm/km, and the nonlinear coefficient is $\gamma_{\text{smf}} = 1.3\ \text{W}^{-1}\ \text{km}^{-1}$. Erbium-doped fiber amplifier (EDFA) amplification is employed after each span, compensating fully the fiber losses. At the receiver side we apply coherent detection and DSP modules. The received PDM 16-QAM signal is coherently detected in a 90 deg optical hybrid, photodetected, and sampled at twice the baud rate by the analog-to-digital converter. We consider a 100 kHz linewidth laser as the local oscillator (LO). The DSP module includes a digital filter, CD compensation, radius directed equalization (RDE), polarization demultiplexing, and frequency and carrier phase recovery [12]. After demodulation the signal is fed into the SISO TE structure presented earlier.

B. Experimental Setup

The setup used for the experimental evaluations for the PDM 16-QAM coherent optical system is presented in Fig. 3. It is composed of three main blocks: 16-QAM generation and transmitter, link transmission, and coherent receiver and DSP modules. A 2000 bit data frame encoded by a CC is applied to the system. The data are pre-encoded offline and loaded into the memory of a programmable pulse pattern generator (PPG). The data outputs at 10 Gbaud are delayed to guarantee decorrelation, subsequently combined to create a four-level electrical signal,

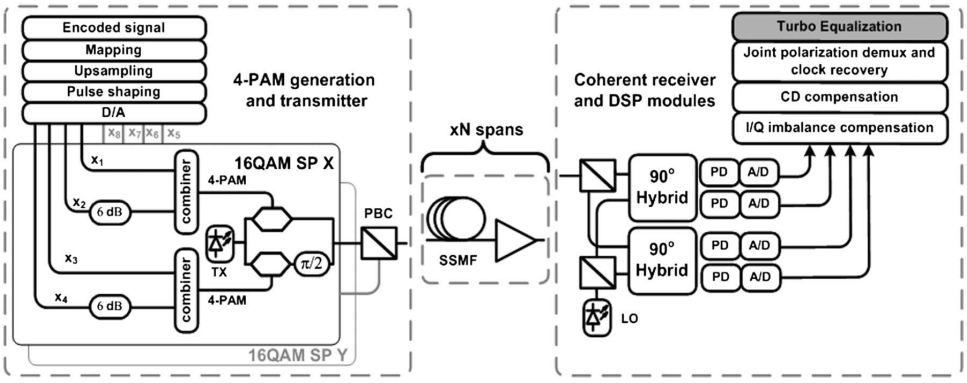

Fig. 2. Simulation setup. D/A, digital-to-analog converter; SP, single polarization; PBC, polarization beam combiner; PD, photodetector; A/D, analog-to-digital converter.

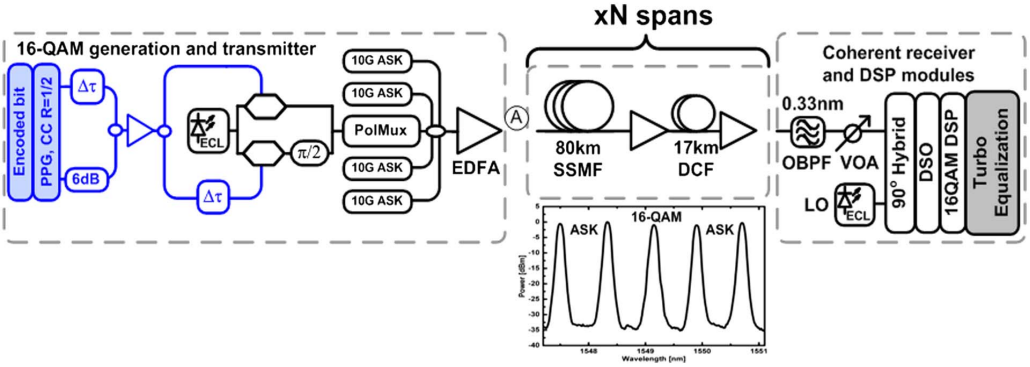

Fig. 3. Experiment setup. PPG, pulse pattern generator; CC, convolutional code; ECL, external cavity laser; EDFA, erbium-doped fiber amplifier; A, launch power measurement point; OBPF, optical bandpass filter; VOA, variable optical attenuator.

amplified, and split into two branches to be fed to an I/Q optical modulator. An external cavity laser (ECL) with a linewidth of 100 kHz is employed at the transmitter. The optical 16-QAM signal is then sent to a polarization multiplexing stage to generate the PDM 16-QAM signals. The experimental evaluations are reported for a baud rate of 10 Gbaud and a bit rate of 80 Gb/s. Four 10 G transponders are then multiplexed with the 16-QAM signal to emulate the interfering channels, which have been placed symmetrically around the central signal with a spacing of 100 GHz. The spectrum of the signal with the neighboring four legacy ASK channels is presented as an inset of Fig. 3. In the center is placed the PDM 16-QAM encoded signal, surrounded by two ASK channels on both sides in a 100 GHz spacing grid. An EDFA is used to adjust the launch power to the link, including a precompensation of the dispersion equivalent to 40 km of SSMF. The transmission link block consists of spans of SSMF of 80 km length and dispersion compensated fiber (DCF) of 17 km length. EDFA amplification is used for span loss compensation. Three link lengths 240, 400, and 640 km, corresponding to a number of spans equal to 3, 5, and 8, respectively, are evaluated. The input power to the link, measured at point A, is varied between −4 and 4 dBm with a granularity of 1 dB. At the receiver side, we apply coherent detection and DSP modules. We employ an ECL with 100 kHz linewidth as the LO and a variable optical attenuator at the signal input to maintain a constant ratio between the signal received and the LO. A 40 GSa/s sampling rate digital signal oscilloscope (DSO) with 13 GHz bandwidth is employed to sample the received signals, and then offline signal processing is performed. The PDM 16-QAM DSP-based receiver earlier presented for the numerical validation case, with exception of the CD compensation module not present for the compensated link, is then applied followed by the SISO TE structure presented above.

C. Metodology

The measured curve for the BER as a function of the link input power, presented in Figs. 3, 5, 6, and 7, and the measured curve for the BER as a function of the lasers' linewidth, presented in Fig. 4, show results without (w/o) TE and with TE. The first case, when no TE is employed, corresponds to "iteration 0." After demodulating the signal, we apply the hard decision to obtain the stream of bits that forms the received signal. This stream is then directly compared to the one used at the transmitter side in the BER counter block. When TE is applied, we employ the SISO TE structure, using therefore the LLR information of the received signals and making a full iteration. We will then exit the loop at the BER counter stage, as shown in Fig. 1, before starting a new iteration. In both cases, iteration 0 and iteration 1, the error counter is placed before the soft decoder; therefore the results reflect the performance of the original bits, w/o TE, and of the reconstructed bits, with TE, and not the performance of the CC. This also means that the results reported all have the same line rate, and baud rate, chosen at the transmission side, while the decoded results, not reported in this work, would show better performances but with a net rate equal to half the line rate, due to the rate chosen for the CC.

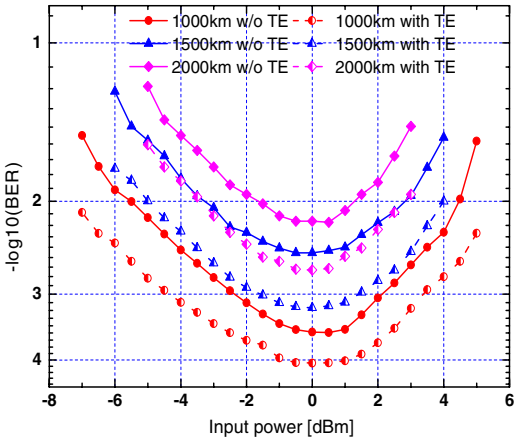

Fig. 4. BER as a function of link input power to the transmission span with and without TE for 1000, 1500, and 2000 km uncompensated SSMF transmission.

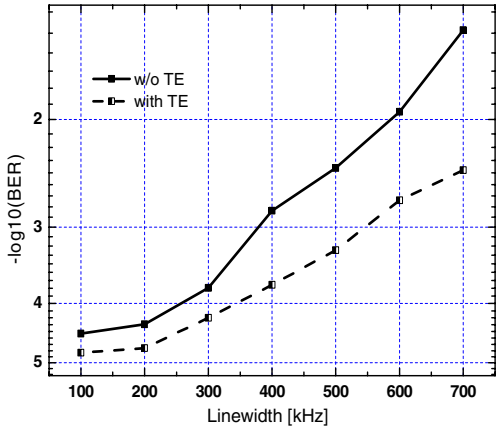

Fig. 5. BER as a function of transmitter and local oscillator laser linewidth for back-to-back with a fixed OSNR value of 25 dB.

For the numerical evaluation of the PDM 16-QAM signal we have created three different realizations, while for the experimental results we have evaluated three different traces of the transmitted signal. That holds for all the results presented and for all the transmission distances considered. In all of them, for both polarizations and for all four bits that constitute the 16-QAM signal, 52 frames of the encoded original data were retrieved. This gives an amount of processed data equal to $\sim 2.5 \times 10^6$ bits, which guarantees sufficient bits for error count of the BER values reported for both numerical and experimental results.

IV. Performances Over Uncompensated Link

We first evaluate the performance for the dispersion uncompensated link scenario, through numerical investigations. We study the effectiveness of our approach for

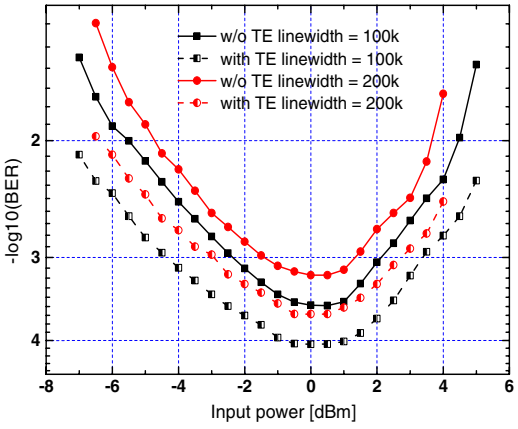

Fig. 6. BER as a function of link input power to the transmission span with and without TE for 100 and 200 kHz linewidth for 1000 km uncompensated SSMF transmission.

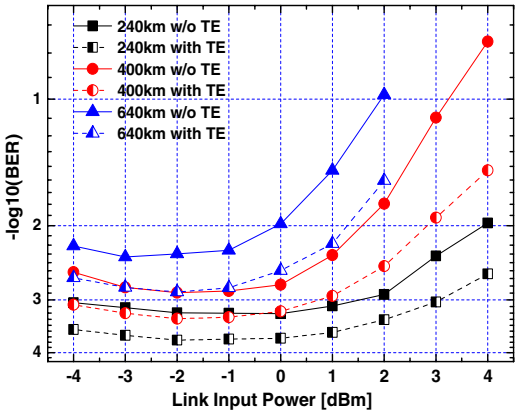

Fig. 7. Performance of single channel. BER as a function of link input power to the transmission span with and without TE for 240, 400, and 640 km compensated link.

different transmission lengths. We then demonstrate that similar performance obtained can be expected with a more commercial laser with higher laser linewidth through numerical investigations of back-to-back and 1000 km total link length scenario.

We consider a transmission link consisting of spans of SSMF of 100 km length. The 16-QAM DSP modules block includes CD compensation, polarization demultiplexing, frequency, and carrier recovery. For the case in which TE is not used, the so-called iteration 0, hard decision BER evaluation is applied. For the case when TE is used, the SISO TE structure explained above is employed after demodulation. We employ a NLMS adaptive equalizer; the number of taps and step size is kept constant throughout all the numerical investigations. A SOVA, based on the soft information provided by the LLR and with 64 states, is used as the decoder. The results of the BER performances as a function of link input power for three different distances are shown in Fig. 4. A total link reach of 1000, 1500, and 2000 km, corresponding to a number of spans of 10, 15, and 20, respectively, has been investigated. We can evaluate the results both on link input power accomplished tolerance and on BER performance gain. It is observed from Fig. 4 that by employing the TE, we accomplish an increment in tolerance to link input power of up to 2 dB. If we consider as an example the case of 1000 km transmission, the best operational point is obtained for a link input power equal to 0 dBm. The same BER performance can be obtained for a link input power to 2 dBm when the TE routine is applied, resulting in the mentioned total increment in tolerance of 2 dB. The same BER performance can be obtained for −2 dBm, and therefore the best operational point BER performance can now be obtained over a window of link input power of 4 dB, from −2 to 2 dBm. In terms of BER performance, our proposed TE approach guarantees a gain of about a half order of magnitude at the best operational point. It should also be noted that this algorithm can extend the maximum total length by 500 km, which corresponds to five spans. We can notice that the results

obtained employing the TE scheme in a 2000 km link outperform the results of a 1500 km length link when no TE is applied.

We then demonstrate that the performances obtained are not related to the laser linewidth value. First we evaluate a back-to-back case, no transmission, and we vary the value of the linewidth parameter of both the transmitter and the LO laser from 100 to 700 kHz with a granularity of 100 kHz. In Fig. 5, we numerically evaluate the BER performances as a function of the value for laser linewidth for a fixed optical signal-to-noise ratio (OSNR) of 25 dB. The results obtained show that our TE routine has similar behavior for all the laser linewidth values considered and can therefore be implemented with commercial distributed feedback lasers. It should also be noted that the TE routine is more effective in the low-performance region, from 400 to 700 kHz, where an improvement of almost one order of magnitude can be seen.

Next we demonstrate the independence from the laser linewidth also in the transmission scenario. We consider uncompensated link transmission with 1000 km of total distance length, and we vary the value of the linewidth parameter of both the transmitter and LO lasers from 100 to 200 kHz. The results are shown in Fig. 6. In this case it is observed that by employing the TE, we accomplish an increment in tolerance to link input power of up to 2 dB, and the best operational point BER performance can now be obtained over a window of link input power of 4 dB. Figure 6 also shows that by employing the TE routine, the results obtained with a linewidth value of 200 kHz outperform the ones with 100 kHz when no TE has been applied. This means that the use of our proposed solution can relax the requirements in terms of laser linewidth value for the transmitter and receiver.

V. Experimental Result for Compensated Optical Fiber Transmission Link

We evaluate the dispersion compensated link scenario through experimental investigations. We study the effectiveness of our approach for different transmission lengths; we then evaluate its effects in the presence of copropagating interfering ASK channels.

We consider a dispersion managed transmission link consisting of spans of SSMF of 80 km length. The dispersion effect is compensated optically by 17 km of DCF. The 16-QAM DSP modules block includes polarization multiplexing, frequency, and carrier recovery. For the case in which TE is not used, the so-called iteration 0, hard decision BER evaluation is applied. For the case in which TE is used, the SISO TE structure explained above is employed after demodulation. We employ a NLMS adaptive equalizer; we optimize the number of taps and the step for all the realizations. A SOVA, based on the soft information provided by the LLR and with 64 states, is used as the decoder.

A. Performances of Single Channel Transmission

First, we evaluate the BER performances obtained through experimental investigations for a single channel transmission scenario. In Fig. 7 the BER performance is plotted as a function of the link input power. We evaluate three link transmission lengths: 240, 400, and 640 km, corresponding to 3, 5, and 8 spans, respectively. We vary the value of the link input power from −4 to +4 dBm with a granularity of 1 dBm. We then evaluate the results both on link input power accomplished tolerance and on BER performance gain. It is observed that by employing the TE, we accomplish an increment in tolerance to link input power of up to 3 dB, and the best operational point BER performance can now be obtained over a window of link input power of 6 dB. The use of the CC can provide a maximum improvement of ∼5 dB in the loop, which is seen in the following way. A performance of 10^{-3} after the soft encoder corresponds to ∼6 dB of SNR. Before the soft encoder we have a BER of $(1/7) \times 10^{-3}$ (since the generator has 7 ones) corresponding to an Eb/N0 of ∼4 dB. To obtain the aforementioned BER, ∼1 dB in entrance to the SOVA block is required. Thus a maximum gain of ∼5 dB is provided by the presence of the CC in the loop. The 6 dB increment in the launch power window is therefore provided by the use of the complete TE scheme. In terms of BER performances our proposed TE approach also guarantees a gain of about a half order of magnitude at the best operational point. It should also be noted that the results obtained using the TE routine for 400 and 640 km have similar performances to the results obtained with 240 and 400 km, respectively, when no TE has been applied. For all the transmission lengths, we observe that larger improvement in terms of BER is achieved when the original performances are worse, in this case between 2 and 4 dBm of link input power, where the performance degradation is also dominated by nonlinear effects.

B. Performances With Interfering Channels

In Fig. 8, the BER performance as a function of the link input power is plotted for a multichannel transmission scenario employing PDM 16-QAM and 10 Gb/s ASK surrounding channels in a 100 GHz grid. The 16-QAM signal is placed in the center, while the four interfering channels are placed two on each side. The spectrum is reported as an inset of the experimental setup in Fig. 3. As for the single channel transmission scenario we evaluate three link transmission lengths, 240, 400, and 640 km, and we vary the value of the link input power from −4 to +4 dBm with a granularity of 1 dBm. It is observed that also in this case by employing the TE, we accomplish an increment in tolerance to link input power of up to 3 dB, and the best operational point BER performance can now be obtained over a window of link input power of 6 dB. In terms of BER performances, our proposed TE approach guarantees a gain of about a half order of magnitude at the best operational point. It should also be noted that the results obtained using the TE routine for

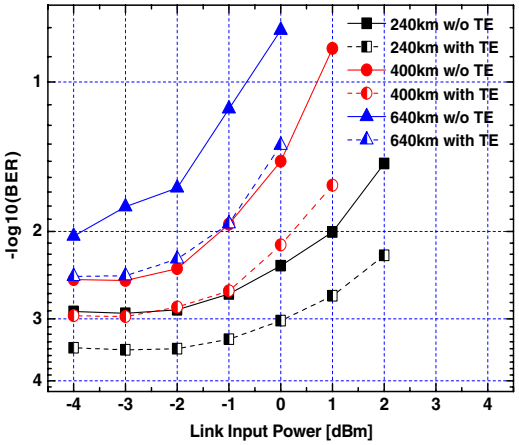

Fig. 8. Performance with interfering OOK channels. BER as a function of link input power to the transmission span with and without TE for 240, 400, and 640 km compensated link.

400 and 640 km show performance similar to the results obtained with 240 and 400 km, respectively, when no TE has been applied. For all the transmission lengths, we observe that larger improvement in terms of BER is achieved for higher link input power, between 2 and 4 dBm, which is the region where the performance degradation is strongly dominated by nonlinear effects. If we consider, for example, 400 km transmission at +1 dBm link input power, we achieve an improvement of almost one order of magnitude in terms of BER performance.

Comparing this result with the single channel reported above, we notice that the total performance is affected by the presence of the ASK interfering channels, which cause a penalty of 3 dB in terms of input power. As an example, it can be pointed out that similar performance for 240 km and 3 dB of input power obtained with a single channel is now reported for the same distance with 0 dB of input power in the presence of ASK interfering channels.

VI. Comparison

The BER performance has been evaluated for three different situations: uncompensated link transmission, through numerical simulations, and compensated link transmission, through experimental investigations, for both single and multichannel scenarios. The performances reported in Figs. 4, 7, and 8 have been obtained for the same sets of link input powers, from −4 to +4 dBm with a granularity of 1 dBm. Therefore we can compare the above-mentioned results in terms of gain system tolerance, which are reported in Table I. Power tolerance, in Table I, represents the accomplished tolerance to link input power obtained through the TE routine. From Table I, we observe that a 2 dB power increment in tolerance is guaranteed for all the numerical evaluations with an unmanaged transmission link. A maximum increment of 3 dB is obtained for the 1500 km transmission case. In the case of the dispersion managed link, investigated through experimental validation, we have evaluated single channel and multichannel transmission with interfering ASK channels, reported as 100 GHz in Table I. For both of these cases and for all the transmission link lengths considered, TE results in a reported increment in power tolerance of 3 dB. Similar to what we obtain for numerical validations, link transmission distances longer than the ones considered in this experimental validation should result in smaller increments. The column labeled "window" represents the sets of link input power for which the best operational point BER performance can be obtained. From Figs. 7 and 8 we can analyze only the right half of the tolerance, 3 dB in all cases, but the results should present the same properties as the numerical investigations, in which case the tolerance on the left side was equal to that on the right side. Δ BER represents the gain in terms of BER obtained by applying TE for the best operational values. We notice that an improvement of about a half order of magnitude has been obtained for numerical investigation. If we consider 1500 km, at the best operational point the system presents a BER performance of 3.1×10^{-3} without TE and of 6.8×10^{-4} after the TE routine, for a total Δ BER of 6.9 dB. This value represents the numerical evaluation of the BER improvement in terms of order of magnitude. Since one order of magnitude would correspond to 10 dB, the results obtained confirm an improvement greater than a half order of magnitude. For the experimental validation we also obtain an improvement of almost a half order of magnitude for all the cases considered. The performance improvement is also reported in terms of the Q factor.

TABLE I
Summary of Transmission Results

	Distance [km]	Increment Tolerance [dB]	Window [dB]	Δ BER [dB]	Q [dB]
Numerical single channel	1000	2.5	5	5.1	0.75
	1500	3	6	6.8	1.36
	2000	2	4	5.2	1.30
Experiment single channel	240	3	6	4.6	0.75
	400	3	6	4.5	0.81
	640	3	6	5.2	1.01
Experiment 100 GHz	240	3	6	5.4	0.97
	400	3	6	4.7	0.97
	640	3	6	4.6	1.17

VII. Conclusion

We have reported the impact of the TE structure for mitigation of transmission impairments in a coherently detected PDM 16-QAM system. A CC has been employed at the transmitter side, while at the receiver the investigated TE is based on a NLMS as equalizer and on a SOVA as a decoder. We observe from our studies that TE is effective in mitigating fiber transmission impairments in a single channel PDM 16-QAM. We have accomplished up to 3 dB of increment in power tolerance and about a half order of magnitude BER gain for both unmanaged and managed transmission links. The first scenario has been evaluated by numerical investigations, the latter by experimental validation. The use of a TE routine can therefore also improve the maximum total and span length; 500 km longer transmission has been obtained in the numerical validation case. On the other hand, the benefit of this method can be addressed to relax the optical component, such as the laser linewidth; evaluation of the effect of the transmitter and receiver lasers' linewidth has been realized for a 1000 km unmanaged SSMF transmission realized by numerical validation. Additionally our proposed solution is proven to be effective in the transmission scenario where performance and reach are severely distorted by cross nonlinear impairments due to the interactions with the copropagating ASK channels in a 100 GHz spectral grid. An increment in system tolerance of 3 dB is also reported in this case. Both the CC and equalizer in the TE loop contribute to the achieved improvements.

The results show the potential of the proposed TE routine for promising high-speed, high-capacity optical networking, such as PDM 16-QAM, over unmanaged and managed systems based on SSMF. Further improvement and some future research directions of the results could be (i) the use of gray mapping, (ii) the use of more powerful codes, and (iii) concatenation of the CC, and therefore of the TE scheme, with high-rate block codes.

Appendix A

In this appendix we show that the nongray mapping results in a specific calculation of the LLR values. In Fig. 9 two different mappings are shown: on the left side the gray mapping, and on the right side the nongray 16-QAM mapping resulting from the typical setup configuration of optical systems based on binary electronics. In Fig. 9 the value of the first two bits according to the region they belong to is also shown, for both mappings. As we can see, in the gray mapping design, if we move from left to right, only one bit of the two is changed every time we pass from one region to another. On the other side, in the nongray mapping, this feature is not present. We can notice that moving from region 2 to region 3 requires changing both bits at the same time. This fact also influences the LLR calculation.

The LLR calculation is realized for all four bits that constitute the 16-QAM signal and is based on the formulation reported in [24]. We indicate the four bits as $b_{\mathrm{Re},k}b_{\mathrm{Re},k}b_{\mathrm{Im},k}b_{\mathrm{Im},k}$ and $k = 0,\ 1$. The first two bits are

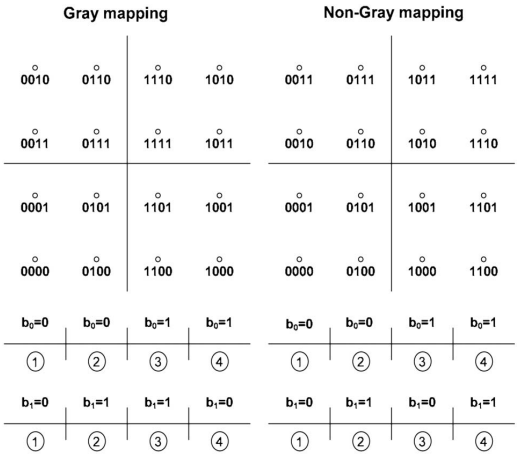

Fig. 9. Gray, left side, and nongray, right side, mapping employed in the system.

derived from the real part of the signal, while the last two are from the imaginary part of the signal. The idea is demapping the received signal into soft bits that have the same sign as provided by a hard detector and whose absolute value represents the reliability of the decision. The optimum hard decision on bit $b_{\mathrm{Re},k}$ is given by the rule

$$\hat{b}_{\mathrm{Re},k} = \beta \quad \text{if } P[b_{\mathrm{Re},k} = \beta | r] > P[b_{\mathrm{Re},k} = (1-\beta)|r], \qquad \beta = 0, 1, \tag{A1}$$

where r represents the received signal

$$r = G_{\mathrm{ch}} \cdot a + w, \tag{A2}$$

where G_{ch} is the channel frequency response and w is the complex additive white Gaussian noise (AWGN). If we set $\beta = 1$, we can rewrite Eq. (A1) as

$$\hat{b}_{\mathrm{Re},k} = 1, \quad \text{if } \log \frac{P(r|b_{\mathrm{Re},k} = 1)}{P(r|b_{\mathrm{Re},k} = 0)} > 0. \tag{A3}$$

When we consider $k = 0$ we obtain

$$\frac{P(r|b_{\mathrm{Re},0} = 1)}{P(r|b_{\mathrm{Re},0} = 0)} = \frac{e^{\frac{-(y_{\mathrm{Re}}-1)^2}{2\sigma^2}} + e^{\frac{-(y_{\mathrm{Re}}-3)^2}{2\sigma^2}}}{e^{\frac{-(y_{\mathrm{Re}}+1)^2}{2\sigma^2}} + e^{\frac{-(y_{\mathrm{Re}}+3)^2}{2\sigma^2}}}. \tag{A4}$$

The formulation in Eq. (A4) has been obtained considering that when $b_{\mathrm{Re},0} = 0$ the real part of the 16-QAM can only assume negative values, −3 or −1, and when $b_{\mathrm{Re},0} = 1$ the real part of the 16-QAM can only assume positive values, +1 or +3. Therefore the LLR formulation for $b_{\mathrm{Re},0}$ is the same as reported in [24]

$$\mathrm{LLR}_{\mathrm{Re},0} = \begin{cases} \frac{4}{\sigma^2}(y_{\mathrm{Re}}[i]+1), & y_{\mathrm{Re}}[i] < -2, \quad \text{region 1} \\ \frac{2}{\sigma^2} y_{\mathrm{Re}}[i], & |y_{\mathrm{Re}}[i]| \le 2, \quad \text{regions 2 \& 3} \\ \frac{4}{\sigma^2}(y_{\mathrm{Re}}[i]-1), & y_{\mathrm{Re}}[i] > +2, \quad \text{region 4} \end{cases}. \tag{A5}$$

Similarly to what is obtained for $b_{\mathrm{Re},0}$, we can obtain the formulations for $b_{\mathrm{Re},1}$:

$$\frac{P(r|b_{\mathrm{Re},1}=1)}{P(r|b_{\mathrm{Re},1}=0)} = \frac{e^{\frac{-(y_{\mathrm{Re}}-3)^2}{2\sigma^2}} + e^{\frac{-(y_{\mathrm{Re}}+1)^2}{2\sigma^2}}}{e^{\frac{-(y_{\mathrm{Re}}-1)^2}{2\sigma^2}} + e^{\frac{-(y_{\mathrm{Re}}+3)^2}{2\sigma^2}}}. \tag{A6}$$

The LLR formulation in Eq. (A6) has been obtained considering that when $b_{\mathrm{Re},1}=0$ the real part of the 16-QAM can only assume values -3 or $+1$, and when $b_{\mathrm{Re},1}=1$ the real part of the 16-QAM can only assume values -1 or $+3$.

We now consider $b_{\mathrm{Re},1}$. In region 2, when $-2 \le y_{\mathrm{re}} < 0$, we can assume that the relative contribution by constellation point $+3$ in the numerator [Eq. (A8)] can be ignored. Therefore the likelihood ratio reduces to

$$\frac{P(r|b_{\mathrm{Re},1}=1)}{P(r|b_{\mathrm{Re},1}=0)} \approx \frac{e^{\frac{-(y_{\mathrm{Re}}+1)^2}{2\sigma^2}}}{e^{\frac{-(y_{\mathrm{Re}}+3)^2}{2\sigma^2}} + e^{\frac{-(y_{\mathrm{Re}}-1)^2}{2\sigma^2}}}. \tag{A7}$$

Expressing Eq. (A7) in logarithm form and considering negligible the added term $e^{((-8)/2\sigma^2)}$, we obtain the LLR formula for $b_{\mathrm{Re},1}$ in region 2 as

$$\mathrm{LLR}(b_{\mathrm{Re},1})_{\mathrm{reg}\,2} = \frac{2}{\sigma^2}(-y_{\mathrm{Re}}). \tag{A8}$$

Considering all four regions for $b_{\mathrm{Re},0}$ and $b_{\mathrm{Re},1}$ we obtain the LLR formulas summarized in Table II.

The LLR formulas calculation for $b_{\mathrm{Im},0}$ and $b_{\mathrm{Im},1}$ follows the same rules as for $b_{\mathrm{Re},0}$ and $b_{\mathrm{Re},1}$. The results obtained are therefore the same, but on the imaginary part of the signal. We assume that all the clusters have the same variance and we therefore remove the factor $2/\sigma^2$ from all the LLR formulas. A study on the different variances of the 16 clusters can lead to a more precise calculation of the LLR and therefore to better performance.

The remapping block, placed after the SOVA decoder in the TE routine, works with the inverse formula reported in Table II. The four LLR values are then used to reconstruct the real and imaginary signals. It should be noted that only one of the LLR values between $b_{\mathrm{Re},0}$ and $b_{\mathrm{Re},1}$ is necessary to reconstruct the real part, and only one between $b_{\mathrm{Im},0}$ and $b_{\mathrm{Im},1}$ to reconstruct the imaginary part. Due to this fact and to the mapping scheme, the reconstruction process may present jumps beyond the nearest cluster of the constellation. For example, let us consider the complex signal $+1.3+1.3j$. It will be demapped into 1010, and the LLRs are calculated with the formulas presented. Let us now assume that we have a decoder/re-encoder error, and the new bits are 0010. In this case we can notice that the corrections of the error forced us to move from region 3 to region 1 for the real part of the signal, and therefore not to the nearest clusters.

TABLE II
LLR FORMULAS FOR $b_{\mathrm{Re},0}$ AND $b_{\mathrm{Re},1}$

		$\mathrm{LLR}(b_{\mathrm{Re},0})$	$\mathrm{LLR}(b_{\mathrm{Re},1})$
Region 1	$y < -2$	$(4/\sigma^2)(y_{\mathrm{Re}}+1)$	$(2/\sigma^2)(y_{\mathrm{Re}}+2)$
Region 2	$-2 \le y < 0$	$(2/\sigma^2)y_{\mathrm{Re}}$	$(2/\sigma^2)(-y_{\mathrm{Re}})$
Region 3	$0 \le y < +2$	$(2/\sigma^2)y_{\mathrm{Re}}$	$(2/\sigma^2)(-y_{\mathrm{Re}})$
Region 4	$y \ge +2$	$(4/\sigma^2)(y_{\mathrm{Re}}-1)$	$(2/\sigma^2)(y_{\mathrm{Re}}-2)$

REFERENCES

[1] D. van den Borne, V. Sleiffer, M. S. Alfiad, and S. L. Jansen, "Towards 400G and beyond: How to design the next generation of ultra-high capacity transmission systems," in *Proc. of OptoElectronics and Communications Conf.*, July 2011, pp. 429–432.

[2] P. J. Winzer, "Beyond 100G Ethernet," *IEEE Commun. Mag.* vol. 48, no. 7, pp. 26–30, July 2010.

[3] X. Zhou and L. E. Nelson, "400G WDM transmission on the 50 GHz grid for future optical networks," *J. Lightwave Technol.*, vol. 30, no. 24, pp. 3779–3792, Dec. 2012.

[4] J. Yu, Z. Dong, H. C. Chien, Z. Jia, X. Li, D. Huo, M. Gunkel, P. Wagner, H. Mayer, and A. Schippel, "Transmission of 200G PDM-CSRZ-QPSK and PDM-16QAM with a SE of 4 b/s/Hz," *J. Lightwave Technol.*, vol. 31, no. 4, pp. 515–522, Feb. 2013.

[5] P. J. Winzer, "High-spectral-efficiency optical modulation formats," *J. Lightwave Technol.*, vol. 30, no. 24, pp. 3824–3835, Dec. 2012.

[6] S. J. Savory, "Digital coherent optical receivers: Algorithms and subsystems," *IEEE J. Sel. Top. Quantum Electron.*, vol. 16, no. 5, pp. 1164–1179, Sept.–Oct. 2010.

[7] T. Inoue, E. Mateo, F. Yaman, T. Wang, Y. Inada, T. Ogata, and Y. Aoki, "Low complexity nonlinearity compensation for 100G DP-QPSK transmission over legacy NZ-DSF link with OOK channels," in *38th European Conf. on Optical Communication*, Sept. 2012, paper Mo.1.C.5.

[8] E. Ip and J. Kahn, "Compensation of dispersion and nonlinear impairments using digital backpropagation," *J. Lightwave Technol.*, vol. 26, no. 20, pp. 3416–3425, Oct. 2008.

[9] A. Lau and J. Kahn, "Signal design and detection in presence of nonlinear phase noise," *J. Lightwave Technol.*, vol. 25, no. 10, pp. 3008–3016, Oct. 2007.

[10] Z. Tao, L. Dou, W. Yan, L. Li, T. Hoshida, and J. C. Rasmussen, "Multiplier-free intrachannel nonlinearity compensating algorithm operating at symbol rate," *J. Lightwave Technol.*, vol. 29, no. 17, pp. 2570–2576, Sept. 2011.

[11] N. Stojanovic, Y. Huang, F. N. Hauske, Y. Fang, M. Chen, C. Xie, and Q. Xiong, "MLSE-based nonlinearity mitigation for WDM 112 Gbit/s PDM-QPSK transmissions with digital coherent receiver," in *Proc. of Optical Fiber Communication Conf.*, 2011, paper OTu3C.5.

[12] D. Zibar, O. Winther, N. Franceschi, R. Borkowski, A. Caballero, V. Arlunno, M. N. Schmidt, N. Guerrero Gonzalez, B. Mao, Y. Ye, K. J. Larsen, and I. Tafur Monroy, "Nonlinear impairment compensation using expectation maximization for PDM 16-QAM systems," *Opt. Express*, vol. 20, no. 26, pp. B181–B196, 2012.

[13] E. Ip, P. Ji, E. Mateo, Y. Huang, L. Xu, D. Qian, N. Bai, and T. Wang, "100G and beyond transmission technologies for evolving optical networks and relevant physical-layer issues," *Proc. IEEE*, vol. 100, no. 5, pp. 1065–1078, 2012.

[14] D. Rafique, J. Zhao, and A. D. Ellis, "Digital back-propagation for spectrally efficient WDM 112 Gbit/s PM m-ary QAM transmission," *Opt. Express*, vol. 19, no. 6, pp. 5219–5224, 2011.

[15] M. Jäger, T. Rankl, J. Speidel, H. Bülow, and F. Buchali, "Performance of turbo equalizers for optical PMD channel," *J. Lightwave Technol.*, vol 24, no. 3, pp. 1226–1236, Mar. 2006.

[16] H. F. Haunstein, T. Schorr, A. Zottmann, W. Sauer-Greff, and R. Urbansky, "Performance comparison of MLSE and iterative equalization in FEC systems for PMD channels with respect to implementation complexity," *J. Lightwave Technol.*, vol. 24, no. 11, pp. 4047–4054, Nov. 2006.

[17] I. B. Djordjevic, L. L. Minkov, and H. G. Batshon, "Mitigation of linear and nonlinear impairments in high-speed optical networks by using LDPC-coded turbo equalization," *IEEE J. Sel. Areas Commun.*, vol. 26, no. 6, pp. 73–83, Aug. 2008.

[18] L. L. Minkov, I. B. Djordjevic, L. Xu, and T. Wang, "PMD compensation in polarization-multiplexed multilevel modulations by turbo equalization," *IEEE Photon. Technol. Lett.*, vol. 21, no. 23, pp. 1773–1775, Dec. 2009.

[19] L. L. Minkov, I. B. Djordjevic, L. Xu, and T. Wang, "Suppression of fiber nonlinearities and PMD in coded-modulation schemes with coherent detection by using turbo equalization," *J. Opt. Commun. Netw.*, vol. 1, no. 6, pp. 555–564, Nov. 2009.

[20] S. Zhang, Y. Zhang, M. Huang, F. Yaman, E. Mateo, D. Qian, L. Xu, Y. Shao, and I. B. Djordjevic, "Transoceanic transmission of 40 × 117.6 Gb/s PDM-OFDM-16QAM over hybrid large-core/ultralow-loss fiber," *J. Lightwave Technol.*, vol. 31, no. 4, pp. 498–505, Feb. 2013.

[21] M. N. Sakib, V. Mahalingam, W. J. Gross, and O. Liboiron-Ladouceur, "Optical front-end for soft-decision LDPC codes in optical communication systems," *J. Opt. Commun. Netw.*, vol. 3, no. 6, pp. 533–541, June 2011.

[22] C. Douillard, M. Jézéquel, C. Berrou, A. Picart, P. Didier, and A. Glavieux, "Iterative correction of intersymbol interference: Turbo-equalization," *Eur. Trans. Telecommun.*, vol. 6, no. 5, pp. 507–511, 1995.

[23] T. Wuth, E. Agrell, M. Karlsson, and M. Sköld, "Fiber communications using convolutional coding and bandwith-efficient modulation," *Opt. Express*, vol. 14, no. 2, pp. 542–555, 2006.

[24] F. Tosato and P. Bisaglia, "Simplified soft-output demapper for binary interleaved COFDM with application to HIPERLAN/2," in *Proc. of IEEE Int. Conf. on Communications*, 2002, p. 664.

Valeria Arlunno was born in Gattinara, Italy, in 1984. She received her B.Sc. in 2006 and M.Sc. from the Politecnico di Torino, Torino, Italy, in 2009. In 2009 she joined the Optcom group at Politecnico di Torino as a research assistant. She is currently pursuing a Ph.D. in optical communications engineering at DTU Fotonik, Technical University of Denmark, with the Metro-Access and Short Range Systems research group of the Department of Photonics Engineering. Her research interests are in the areas of coherent optical communications and digital signal processing.

Antonio Caballero was born in 1985 in Zaragoza, Spain. He received B.Sc. and M.Sc. degrees in telecommunications engineering from Centro Politécnico Superior, Zaragoza, Spain, in 2008. He received his Ph.D. in optical communications engineering at DTU Fotonik, Technical University of Denmark, in September 2011, with a thesis on high-capacity radio-over-fiber links. He was a visiting researcher at The Photonics and Networking Research Laboratory at Stanford University from February to June 2010, under supervision of Prof. Leonid G. Kazovsky. He is currently a postdoctoral researcher at DTU Fotonik. His research interests are in the area of coherent optical communications as well as radio-over-fiber links.

Robert Borkowski was born in Lodz, Poland, in 1987. He received the M.Sc. degree in telecommunications from the Technical University of Denmark in 2011 and the M.Sc. degree in electronics and telecommunications from the Technical University of Lodz in 2012. He is now working toward his Ph.D. degree in the field of optical communications in the Metro-Access and Short Range Systems group at DTU Fotonik, Department of Photonics Engineering, Technical University of Denmark. He is involved in the EU FP7 project CHRON (Cognitive Heterogeneous Reconfigurable Optical Networks). His research interests are in the areas of optical performance monitoring, coherent transmission systems, and digital signal processing for fiber-optic communications.

Silvia Saldaña Cercós was born in Barcelona, Spain, in 1985. She received her B.Sc. in 2009 from Universitat Politècnica de Catalunya, Spain, and her M.Sc. from DTU Fotonik, Technical University of Denmark, in 2011. She is currently pursuing a Ph.D. in optical communications engineering at DTU Fotonik, Technical University of Denmark, with the Metro-Access and Short Range Systems research group of the Department of Photonics Engineering. Her research interests are in the areas of energy efficiency in coherent optical communications and digital signal processing.

Darko Zibar was born in Belgrade, in the former Yugoslavia, on September 9, 1978. He received the M.Sc. degree in telecommunication and the Ph.D. degree in optical communications from the Technical University of Denmark, Lyngby, Denmark, in 2004 and 2007, respectively. He was a visiting researcher with the Optoelectronic Research Group, University of California, Santa Barbara, during January–August 2006 and in January 2008, where he was involved in coherent receivers for phase-modulated analog optical links. From February to July 2009, he was a visiting researcher with Nokia-Siemens Networks, where he worked on 112 Gbit/s polarization multiplexed systems. He is currently an associate professor at DTU Fotonik, Technical University of Denmark. His research interests include coherent optical communication, with an emphasis on digital demodulation and compensation techniques.

Dr. Zibar is the recipient of the Best Student Paper Award at the IEEE Microwave Photonics Conference 2006, the Villum Kann Rasmussen Postdoctoral Research Grant in 2007, and the Villum Foundation Young Investigator Program in 2011.

Knud J. Larsen received M.S.E.E. and Ph.D. degrees from the Technical University of Denmark, Lyngby, Denmark. He was a senior engineer and project manager at Ericsson Signal Systems, where he was involved in design and implementation of communication systems and traffic control systems. Since 1986, he has been a professor at the Technical University of Denmark (previously the Institute of Telecommunication, now the Department of Photonics), teaching and performing research in communication theory and coding. He has worked extensively on studies of error correction for the European Space Agency and is currently involved in projects related to optical transmission.

Dr. Larsen together with four colleagues received the Information Theory Society Paper Award in 1991 for a paper on algebraic geometry codes.

Idelfonso Tafur Monroy is currently a professor and the head of the Metro-Access and Short Range Systems group of the Department of Photonics Engineering at the Technical University of Denmark. He graduated from the Bonch-Bruevitch Institute of Communications, St. Petersburg, Russia, in 1992, where he received an M.Sc. degree in multichannel telecommunications. In 1996 he received a Technology Licentiate degree in telecommunications theory from the Royal Institute of Technology, Stockholm, Sweden. In the same year he joined the Electrical Engineering Department of the Eindhoven University of Technology, The Netherlands, where he earned a Ph.D. degree in 1999 and worked as an assistant professor until 2006. He has participated in several European research framework projects in photonic technologies and their applications to communication systems and networks. At the moment he is involved in the ICT European projects GigaWaM and EURO-FOS and is the technical coordinator of the CHRON project. His research interests are in hybrid optical–wireless communication systems, high-capacity optical fiber communications, digital signal processing for optical transceivers for baseband and radio-over-fiber links, application of nanophotonic technologies in the metropolitan and access segments of optical networks, and short range optical–wireless communication links.

Paper 2: Counteracting 16-QAM Optical Fibre Transmission Impairments with Iterative Turbo Equalization

V. Arlunno, A. Caballero, R. Borkowski, D. Zibar, K. J. Larsen and I. Tafur Monroy, "Counteracting 16-QAM Optical Fibre Transmission Impairments with Iterative Turbo Equalization ," *IEEE Photon. Technol. Lett.*, Vol. 25, No. 21, November 2013.

Counteracting 16-QAM Optical Fiber Transmission Impairments With Iterative Turbo Equalization

Valeria Arlunno, Antonio Caballero, Robert Borkowski, Darko Zibar, Knud J. Larsen, and Idelfonso Tafur Monroy

***Abstract*— A turbo equalization (TE) scheme based on convolutional code and normalized least mean square equalizer for coherent optical communication links is proposed and experimentally demonstrated. The proposed iterative TE technique is proved effective for counteracting polarization-division-multiplexing 16 quadrature amplitude modulation impairments in dispersion uncompensated coherent transmission links. Gains exceeding one order of magnitude in terms of bit error rate are obtained in experimental validation up to 497 km-standard single mode fiber link transmission.**

***Index Terms*— Digital signal processing, forward error correction, optical fiber communication.**

I. Introduction

MULTI-LEVEL modulation formats, such as 16 Quadrature Amplitude Modulation (QAM) with polarization-division-multiplexing (PDM), in combination with coherent detection, are considered to be the next evolutionary step towards fiber transmission links with capacities beyond 100 Gb/s [1]. However as the baud rate increases, the performance of multilevel modulation formats faces challenges stemming from optical fiber transmission impairments. While chromatic dispersion (CD) and polarization mode dispersion (PMD) can be easily mitigated by linear equalizers, fiber nonlinearities are still very challenging and their compensation capability is marginal [2]. Furthermore, imperfections of transmitters and receivers not entirely compensated by linear techniques still need to be addressed. Even though several techniques have been demonstrated successful against nonlinear impairments, performance and implementation complexity remain a challenge. Therefore efficient equalization solutions able to enhance the results of linear techniques and to reduce the complexity of non-linear equalizers are still an open research topic to be explored. As the order of modulation increases, higher optical signal-to-noise ratio (OSNR) is required due to the reduced Euclidean distance between each signal point. Although forward error correction can compensate for low OSNR, the employment of a powerful Forward Error Correction (FEC) is not enough for transmitted signal affected from linear and nonlinear effects. The interplay between equalization and FEC becomes then a relevant topic of investigation for future high speed transmission solution [3].

In this letter we present a scheme based on Turbo Equalization (TE) equally effective in counteracting accumulated noise induced by link amplification and for transmission in the regime where fibre non-linearities start to impair the overall system performance. The low complexity of the solution proposed, thanks to the presence of a simple convolutional code, and its ability to accomplish for each new iteration a more accurate estimation of the unknown channel, make it a promising solution for high speed, high capacity optical networking. We demonstrate that in a PDM 16 QAM transmission over 251 and 497 km of standard single mode fibre (SSMF) link the use of a Turbo Equalization algorithm improves the bit error rate (BER) performance by more than one order of magnitude, which overcomes previous results reported for compensated link transmission [4]. Moreover we demonstrate that further improvement can be obtained employing additional iterations of the Gray mapping based soft-input soft-output (SISO) TE structure presented.

II. Turbo Equalization

Inspired by Turbo Codes, TE was firstly introduced [5] to improve the performance of digital communication systems in presence of intersymbol interference (ISI). A TE system consists of an iterative joint equalization and decoding technique. While TE techniques have been widely exploited for PMD compensation in direct detection schemes, their employment in coherent detection optical fiber transmission schemes is still limited. Until now experimental demonstrations are only reported for low density parity check (LDPC) coded TE polarization multiplexed Binary phase-shift keying (BPSK) [6] and Quadrature phase-shift keying (QPSK), and PDM orthogonal frequency division multiplexing (OFDM) 16 QAM [7]. Even though LDPC based TE scheme can be very powerful, alternative works are looking for simplified solution to overcome their high complexity [8], [9]. Convolutional Code (CC) codes have been proven to obtain similar performances to block codes [10]. The performance can be comparable to that of RS codes, but with the benefit of simpler encoding electronics and the potential of using soft decision decoding.

In this letter we consider communication of frames CC encoded in 4 Pulse amplitude modulation (PAM) format quadrature modulated to 16 QAM and polarization-division-multiplexed (PDM). On the receiver side, after a PDM

Manuscript received June 8, 2013; revised August 23, 2013; accepted September 2, 2013. Date of publication September 10, 2013; date of current version October 9, 2013.

The authors are with DTU Fotonik, Department of Photonics Engineering, Technical University of Denmark, Lyngby 2800, Denmark (e-mail: vaar@fotonik.dtu.dk; acaj@fotonik.dtu.dk; rbor@fotonik.dtu.dk; dazi@fotonik.dtu.dk; knjl@fotonik.dtu.dk; idtm@fotonik.dtu.dk).

Color versions of one or more of the figures in this letter are available online at http://ieeexplore.ieee.org.

Digital Object Identifier 10.1109/LPT.2013.2281239

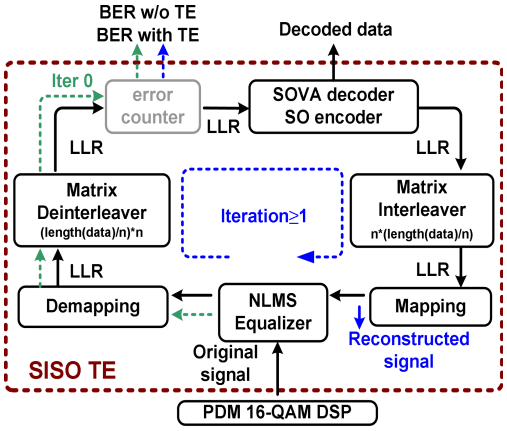

Fig. 1. Receiver structure of the SISO Turbo Equalizer algorithm.

16 QAM digital signal processing (DSP) receiver, the signal is fed into a soft input soft output (SISO) TE structure presented in Fig. 1. The received data is passed through a normalized least mean square (NLMS) adaptive equalizer, due to the unknown nature of the transmission channel. The equalizer has a similar structure to the one presented in [11]. Number of taps and step size are optimized as to guarantee the best performances in terms of BER. The equalizer output is demapped in order to provide soft information on all the coded bits in the form of log-likelihood-ratios (LLRs). After a deinterleaver process, symmetrical to the one at the transmitter side, a standard error counter provides the system performance in terms of BER. Decoding is then performed using a soft output 64 states Viterbi algorithm (SOVA) binary decoder to obtain soft estimation of both information and parity bits. A traditional DSP scheme would now provide the BER performance. The novelty and benefit of the TE scheme is to use the information in a soft encoding block. The aim is to obtain a new version of the original received signal to drive accordingly the equalizer. After the soft output (SO) encoder, to create the reconstructed signal, an interleaving and mapping stage are required to reproduce the original signal. After the NLMS equalizer, based on the original and reconstructed signal information, deinterleaving, demapping and decoding can be performed as for the first iteration.

III. Experimental Setup

The general outline of the experimental setup for the polarization-division-multiplexing (PDM) 16 QAM coherent optical (CO) system is shown in Fig. 2. The data pattern employed for the experiment is generated offline. Random generated data of 5000 bits length is created in Matlab. The data is then encoded with a rate R = 1/2 convolutional code. The chosen code has a constrain length of 5 and is based on a 16 states trellis. The resulting coded data, with 10000 bits length, is interleaved to avoid block errors, and employed to generate two independent Gray mapped 4-PAM signals with a 24 Gbit/s Arbitrary Waveform Generator. The central optical channel under test is then a 12 Gbaud PDM 16 QAM, generated by driving a MZM with the two decorrelated 4-PAM electrical data signals. Polarization-division multiplexing was emulated by multiplexing the signal with its delayed copy in the orthogonal polarization to obtain a total bit rate of 96 Gbit/s. Six 24 Gbaud PDM QPSK channels, with the same total bit rate per channel of 96 Gbit/s, are then combined with the PDM 16 QAM channel resulting in a 7 channel system on 100 GHz grid. The optical spectrum of the transmitted WDM signal is reported as an inset of Fig. 1. High spectral efficiency could have been achieved with 25 GHz WDM. However the aim of this experiment was not to achieve high SE but to demonstrate the improvement achievable of TE in a WDM scenario. Fiber transmission was realized over a maximum of 6 standard single mode fiber (SSMF) spans, each approximately 80 km, for a total length of 497 km, without dispersion compensation and amplified using double-stage Erbium Doped Fibre Amplifiers (EDFAs). The noise figure of the amplifiers is 6 dB. Three and six amplification stages are employed respectively for the 251 km and 497 km links. At the receiver side, the coherent front end consists of a polarization diverse 90-degree hybrid with integrated balanced photodiodes. An External-cavity laser (ECL) is employed as local oscillator (LO). A Digital sampling oscilloscope (DSO) with 40 GS/s of sampling rate and 13 GHz bandwidth is used to sample the received signals. The acquired data are processed offline with a digital signal processing-based receiver that included: digital filter, CD compensation, timing recovery, multi-modulus algorithm for polarization demultiplexing and residual fiber impairment compensation and carrier phase recovery. The SISO TE structure earlier presented is then applied. The BER results are calculated by the error counter at each iteration. The performance without TE is also referred to as "iteration 0" as to indicate that no complete iteration has been accomplished. For all the results reported, three different traces have been evaluated to obtain a total number of processed data equal to $\sim 2.5 \cdot 10^6$ bits. With this amount of bits a confidence level over 99% is guaranteed for all the resulting BER values presented, including the maximum value of $1.25 \cdot 10^{-5}$ (B2B case TE 2nd iter, OSNR = 28 dB).

IV. Result and Discussion

First, we evaluate the effect of the TE scheme for back-to-back (B2B) measurements, reported in Fig. 3. BER performances are presented as a function of the OSNR values in dB. The black squared curve represents the results for "iteration 0", when no TE is applied, the case where after the demodulation a hard decision BER counter provides the results as reported in Fig. 1. The red circled curve represents the first iteration of the TE routine and the triangle blue curve represents the second iteration. It is observed that the proposed TE routine guarantees a gain higher than one order of magnitude for all the OSNR values considered. The performance obtained without TE is due to pre-equalization imperfection at the transmitter side. Furthermore the TE routine is able to tackle transmitter and receiver imperfections not completely mitigated by a traditional DSP. Additional gain can be obtained incrementing the iterations number of the studied scheme, as

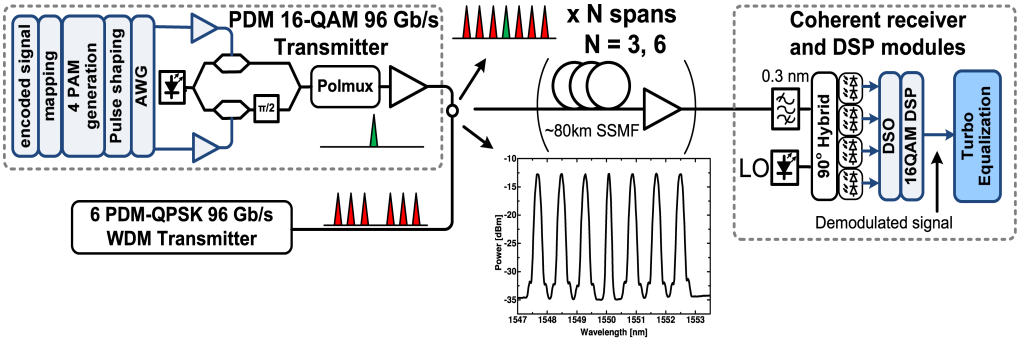

Fig. 2. Description of the experimental setup.

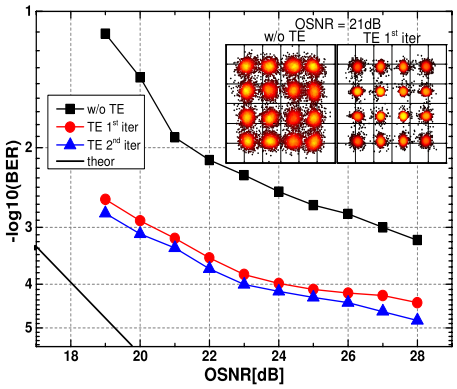

Fig. 3. BER as a function of OSNR for B2B measurements.

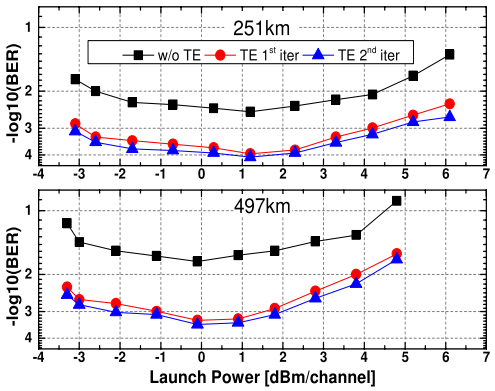

Fig. 4. BER as a function of link input power for 251 and 497 km uncompensated link transmission.

the results obtained in the second iteration confirm. It can also be observed that the use of the suggested TE routine drastically reduces the gap between the experimental results and the theoretical curve for 12 Gbaud PDM 16-QAM. As an inset of Fig. 3 is also shown the constellation diagram obtained at 21 dB of OSNR without TE and after the first iteration. It is observed that already after one iteration, the spread of the signal in each cluster is visibly reduced. For the B2B case, the number of taps is kept constant to 3 for all the OSNR considered, while the step size is chosen separately for each OSNR value between a minimum of 0.01 and a maximum of 0.55. The chosen number of taps is kept constant also for the additional iteration, while the step size is chosen in a window of 0.1 around a central value which is the step value employed in the previous iteration.

We then evaluate the performance for dispersion uncompensated link transmission. Two different transmission distances are measured, 251 and 497 km, which correspond to 3 and 6 spans respectively. The BER performance as a function of the link launch power for the two considered distances is reported in Fig. 4. The effectiveness of the TE routine can be observed on BER performances and as well on extending the values of link input power that can guarantee a given BER performance. For both the presented distances and for all the link input power values considered, the use of the TE algorithm ensures an improvement of more than one order of magnitude in terms of BER. It is noticed that the solution proposed is slightly less effective for launch power exceeding 3 dBm, when the signal is highly affected by non linearities. However, we can still accomplish an improvement of almost one order of magnitude in terms of BER. It is also observed that after using the TE algorithm proposed we obtain the same BER performance for a higher launch power in dB. If we consider as example the 251 km transmission case, we obtain the best operational point at 1 dBm/channel when no TE is employed. After the first iteration we obtained the same BER performance for −3 dBm/channel and for +5 dBm/channel. For the transmission cases, the number of taps has a value of 3 for 251 km and 5 for 497 km and it's kept constant for all the launch powers considered. The step size is chosen separately for each launch power as to guarantee the best performance in terms of BER. The values of the step size are chosen between a minimum of 0.01 and a maximum of 0.55. The chosen number of taps is kept constant also for the additional iteration, while the step size is chosen in a window of 0.1 around a central value which is the step value employed in the previous iteration. At a chosen launch power of 0 dBm, the received OSNR is 24.5 dB for 251 km transmission and 21.4 dB for 491 km transmission.

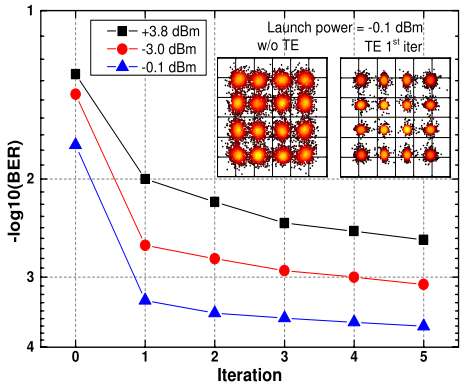

Fig. 5. BER as a function of iteration number for three different launch power values for 497 km.

Last we evaluate the gain in terms of BER of multiple TE iterations. Fig. 5 shows BER as a function of the iteration number for three different values of launch power, −3.0 dBm, −0.1 dBm and +3.8 dBm for uncompensated transmission of 497 km. It is also observed that the first and second iterations have the highest gains and that the BER keeps decreasing with the iteration number. For the cases −3.0 dBm and −0.1 dBm the employment of additional iteration provides similar improvement, from $6{\cdot}10^{-3}$ to 10^{-3} and from $3{\cdot}10^{-4}$ to $6{\cdot}10^{-4}$ respectively. The situation is different for the case of +3.8 dBm, when the signal is affected by nonlinearities. Iteration 1, 2 and 3 give substantial gain, while the consecutive iterations give moderate gains, because the signal quality improves. In this case the total improvement is higher compared to other two values reported, from 10^{-2} of iteration 2 to $5{\cdot}10^{-3}$ of iteration 5.

V. Conclusion

In this letter, the performance of an iterative Turbo Equalization (TE) technique for different transmission distances of 96 Gb/s PDM 16 QAM in a WDM scenario is experimentally investigated. The results show that a significant improvement in terms of BER can be achieved with the use of the proposed TE algorithm. Gains exceeding one order of magnitude in terms of BER were obtained for both 251 and 497 km uncompensated link transmission distances. Furthermore, the employment of more iterations is proven to enhance the performance in terms of BER.

References

[1] P. J. Winzer, "High-spectral-efficiency optical modulaion formats," *J. Lightw. Technol.*, vol. 30, no. 24, pp. 3824–3835, Dec. 15, 2012.

[2] O. Bertran-Pardo, *et al.*, "Linear and nonlinear impairment mitigation for enhanced transmission performance," in *Proc. OFC*, 2011, pp. 1–3, paper OMR1.

[3] T. Sugihara, T. Yoshida, and T. Mizouchi, "Collaborative signal processing with FEC in digital coherent systems," in *Proc. OFC/NFOEC*, Mar. 2013, pp. 1–3, paper OM2B.3.

[4] V. Arlunno, *et al.*, "Turbo equalization techniques towards robust PDM-16-QAM optical fiber transmission," *J. Opt. Commun. Netw.*, to be published.

[5] C. Douillard, M. Jézéquel, C. Berrou, A. Picart, P. Didier, and A. Glavieux, "Iterative correction of intersymbol interference: Turbo equalization," *Eur. Trans. Telecom.*, vol. 6, no. 5, pp. 507–511, Sep./Oct. 1995.

[6] L. L. Minkov, I. B. Djordjevic, X. Lei, and W. Ting, "PMD compensation in polarization-multiplexed multilevel modulations by turbo equalization," *IEEE Photon. Technol. Lett.*, vol. 21, no. 23, pp. 1773–1775, Dec. 1, 2009.

[7] S. Zhang, *et al.*, "Transoceanic transmission of 40×117.6 Gb/s PDM-OFDM-16QAM over hybrid large-core/ultralow-loss fiber," *J. Lightw. Technol.*, vol. 31, no. 4, pp. 498–505, Feb. 15, 2013.

[8] M. Tüchler and A. C. Singer, " Turbo equalization: An overview," *IEEE Trans. Inf. Thoery*, vol. 57, no. 2, pp. 920–952, Feb. 2011.

[9] C. Duan, *et al.*, "A low-complexity sliding-window turbo equalizer for nonlinearity compensation," in *Proc. OFC*, 2012, pp. 1–3, paper JW2A.59.

[10] T. Wuth, E. Agrell, M. Karlsson, and M. Sköld, " Fiber communications using convolutional coding and bandwidth-efficient modulation," *Opt. Express*, vol. 14, no. 2, pp. 542–555, Jan. 2006.

[11] Y. Mori, C. Zhang, K. Igarashi, K. Katoh, and K. Kikuchi, "Unrepeated 200-km transmission of 40-Gbit/s 16-QAM signals using digital coherent optical receiver," *Opt. Express*, vol. 17, no. 3, pp. 1435–1441, 2009.

Paper 3: Turbo Equalization for digital coherent receivers

V. Arlunno, A. Caballero, R. Borkowski, D. Zibar, K. J. Larsen and I. Tafur Monroy, "Turbo Equalization for digital coherent receivers," *IEEE/OSA J. Lightw. Technol.*, Vol. 32, No. 2, January 2014.

Turbo Equalization for Digital Coherent Receivers

Valeria Arlunno, Antonio Caballero, Robert Borkowski, Darko Zibar, Knud J. Larsen, and Idelfonso Tafur Monroy

***Abstract*—High order modulation formats allow to reach higher spectral efficiency and data rate. However, their practical implementation is limited by their reduced tolerance to noise and to the optical signal power that can be launched into the fiber without generating excessive nonlinear signal distortions. In this paper, it is demonstrated that Turbo Equalization routines can be used to mitigate performance degradations stemming from optical fiber propagation effects both in optical fiber dispersion managed and unmanaged coherent detection links. The effectiveness of this solution is analyzed both numerically and experimentally for different transmission systems.**

***Index Terms*—16-quadrature amplitude modulation (16-QAM), coherent detection, spectral efficiency (SE), turbo equalization (TE).**

I. Introduction

THE employment of high order modulation formats and advanced digital signal processing (DSP) techniques is considered the next evolutionary deployed step towards higher spectral efficiency and higher data rates. A good compromise between various limiting factor is represented by 16-QAM, which can still enable high-speed, high-capacity long-haul optical networking [1]. The major concern for such high data rates over transmission distance is the signal quality degradation due to linear and non-linear impairments. Linear fiber channel impairments, such as chromatic dispersion (CD), group velocity dispersion and polarization mode dispersion [2], can be effectively mitigated by using digital linear signal processing techniques as it has been demonstrated both for QPSK and higher order QAM signaling [2], [3].

When long transmission reach is targeted, higher power levels launched into the fiber might be required to guarantee extended reach; however such high optical power levels enhance the generation of nonlinear fiber impairments, which are a major limiting factor for high-rate data transmission in metro and long haul optical fiber links. As the level of the M-ary modulation increases, a higher optical signal-to-noise ratio (OSNR) is required due to the reduced Euclidean distance between each signal point which arises difficulties in distinguishing between the states [4]. Linear processing algorithms are shown to be less effective for compensation of impairments stemming from optical fiber nonlinearities, such as self phase modulation, four-wave mixing, cross-phase modulation and laser phase noise [5], [6]. Several techniques have been reported in the literature to mitigate nonlinear optical fiber impairments, such as digital backpropagation [7], maximum likelihood sequence estimation [8], [9], multiplier-free predistortion [10] and expectation maximization [11]. However, most of these methods suffer from complexity. Forward error correction can compensate for low OSNR, but the employment of a powerful FEC is not enough for signals affected from linear and nonlinear effects. The interplay between equalization and FEC becomes then a key technology for future high speed transmission solutions [12].

Turbo Equalization (TE) is a joint approach to address the equalization and decoding task. A number of iterative receiver algorithms repeat the equalization and decoding tasks on the same set of received data, where feedback of extrinsic information from the decoder is incorporated into the equalization process. Inspired by Turbo Codes, TE was firstly introduced to combat the detrimental effects of intersymbol interference effects in digital communication systems protected by a convolutional code (CC) [13]. In the optical communication field, TE routines have first been proposed and numerically evaluated for direct detection optical communication systems in order to mitigate the effects of PMD [14]–[17].

TE schemes based on low-density parity-check (LDPC) coded TE have been numerically [18]–[20] investigated. Experimental validation have been reported in [19]–[22], but the performance in single carrier high order modulation coherent systems has not yet been evaluated. More recently LDPC-coded TE has also been evaluated in electrical generated polarization-division-multiplexed (PDM) Orthogonal Frequency Division Multiplexing 16-QAM for transoceanic transmission with large-core/ultralow loss fiber [23]. Even though LDPC codes can be very powerful, as the work reported suggested, their implementation remains a challenge due to the complex structure of the decoder and alternative works are looking for simplified low complexity solutions [24].

In this paper, we propose to use a TE scheme based on CCs and least mean square equalizer to combat the signal quality degradation due to fiber transmission and transmitter-receiver imperfections. Preliminary experimental results have been presented in [25], [26]. In this paper we give a complete study of the TE adopted in different transmission schemes. The outline of the paper is as follows. In Section II, we detail the TE structure employed to conduct the investigation. In Section III, we formulate analytically the demapper steps to obtain the log-likelihood-ratios (LLR) of the received bits. The effect of TE in an uncompensated scenario is studied by simulation in Section IV. The obtained results are then experimentally verified in a WDM scenario in Section V. In this section we moreover report on the independence from the CC rate. Finally in Section VI,

Manuscript received June 30, 2013; revised September 30, 2013; accepted October 31, 2013. Date of publication November 19, 2013; date of current version December 16, 2013.

The authors are with the DTU Fotonik, Department of Photonics Engineering, Technical University of Denmark, Kgs. Lyngby 2800, Denmark (e-mail: vaar@fotonik.dtu.dk; acaj@fotonik.dtu.dk; rbor@fotonik.dtu.dk; dazi@fotonik.dtu.dk; knjl@fotonik.dtu.dk; idtm@fotonik.dtu.dk).

Color versions of one or more of the figures in this paper are available online at http://ieeexplore.ieee.org.

Digital Object Identifier 10.1109/JLT.2013.2291956

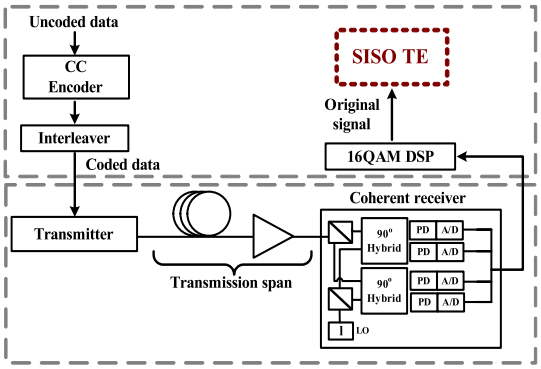

Fig. 1. Pre-encoding and receiver structure of the SISO Turbo Equalizer algorithm. CC: Convolutional Code, LO: local oscillator, PD: Photodiode, A/D: Analog to Digital converter, DSP: Digital Signal Processing, SISO: Soft Input Soft Output, TE: Turbo Equalization.

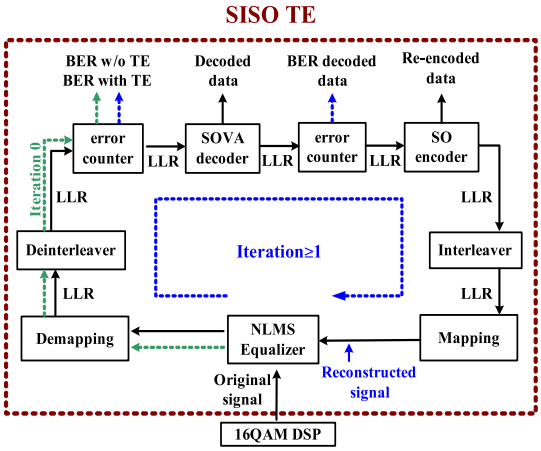

Fig. 2. Schematic description of TE. SISO: Soft input soft output, TE: turbo equalization, NLMS: Normalized least mean square, LLR: Log likelihood ratio, SOVA: Soft output viterbi algorithm, SO: Soft output.

we extend the experiment validation to a dispersion managed transmission case with co-propagating legacy channels.

II. Turbo Equalization

In this paper, we base our investigations on TE structure based on CCs and normalized least mean square equalizer for high speed optical fiber transmission. The encoder and receiver structure of the transmission system is illustrated in Fig. 1. At the transmitter side, random generated data are created with offline processing and encoded by a CC described by a state trellis. After encoding the coded bits are interleaved to suppress burst errors, and sent to the optical modulator at the transmitter.

CCs have up to now only been incompletely explored for optical communications. The drawback of such codes in optical transmission is their high coding overhead compared to high-rate block codes, such as Reed–Solomon (RS) codes and LDPC codes. On the other hand, CC codes present attractive features such as simple and straightforward encoding together with hard and soft decision decoding algorithms. The large overhead can be alleviated by using CC codes together with bandwidth-efficient modulation. Similar performance to RS codes has been obtained, with the benefit of simpler encoding electronics [27]. In this paper most of the results are presented for a rate $R = \frac{1}{2}$ CC code with a 16 state trellis. Furthermore, $R = \frac{2}{3}$ rate CC and $R = \frac{3}{4}$ rate CC are considered in the uncompensated transmission case to prove the independence of the TE from the chosen rate.

On the receiver side, the received signal after optical transmission and detection is processed offline. After a 16 QAM DSP receiver, the received data is fed into the soft-input soft-output (SISO) TE structure illustrated in Fig. 2. A normalized least mean square (NLMS) adaptive equalizer is applied due to the unknown nature of the transmission channel. The NLMS is given by

$$c(n+1) = c(n) + \frac{\mu e^*(n)x(n)}{x^H(n)x(n)} \tag{1}$$

$$e(n) = d(n) - c^H(n)x(n) \tag{2}$$

where $x(n)$ is the signal and $d(n)$ the desired one. We optimize the number of taps and the step size to obtain the best performance in terms of bit error rate (BER). The choice of the step size parameter reflects a tradeoff between fast convergence and good tracking ability. As the step size parameter is chosen based on the current input values, the NLMS algorithm shows good stability with unknown signals. This combined with fast convergence speed and relative computational simplicity [28] makes NLMS the algorithm our choice.

Soft information on all the coded bits in the form of LLRs is provided by the demapper, as explained in details in Section III. In this paper two different mapping schemes have been experimentally investigated and therefore two different demapper blocks have been realized according to the mapping. Gray or non-gray mapping have been investigated. Non-gray mapping results from the typical setup configuration on optical systems based on independent binary electronics without precoding. After the demapping stage a deinterleaver process is employed, symmetrical to the one at the transmitter side, followed by a first error counter to provide the system performance in terms of BER.

The performance without TE, is calculated at this point. This value is reported as “iteration 0” in Fig. 2 and “w/o TE” in the simulations and experimental validations. The name is chosen to highlight that no complete iteration has been realized. The values obtained after the first error counter represent therefore the reference on which we calculate the gain in terms of BER.

Moving forward with the TE iteration, we perform decoding using a soft output Viterbi algorithm (SOVA) binary decoder, with 64 states depth for the $R = \frac{1}{2}$ case, to obtain soft estimation of both information and parity bits. This algorithm is a modification of the general Viterbi scheme that takes into account soft information and provides not only a decision, but also its reliability. It is based on branch and path metric calculation.

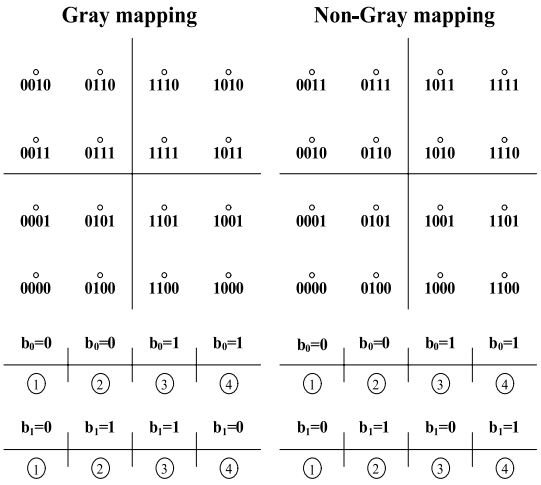

Fig. 3. Schematic description of mapping.

When the Viterbi detection is completed, the survivor path can be traced back at the starting time or time of interest. A second error counter provides the decoded system performance in terms of BER. A soft output (SO) encoder will then create a new encoded signal based on the obtained decoded version of the original received data. After passing through an interleaving stage, the mapping block uses the new soft estimates of the original transmitted symbols to create a reconstructed signal. We then realize an NLMS equalization process using the information of the original and reconstructed signal. Demapping, deinterleaving and decoding can be performed as for the first iteration. In every iteration we evaluate the BER at the first error counter stage. The performance of one complete loop are named "TE 1st iter". The use of a Non-Gray mapping influence also the reconstruction part of the loop and therefore could arise difficulties to accomplish more iterations.

III. LLR Calculation

In Fig. 3, two different mapping for 16QAM are shown: on the left side the Gray mapping, on the right side the Non-Gray mapping. The results included in this study are obtained in both cases. The experimental results obtained for uncompensated link transmission are based on Gray mapped 16QAM TE scheme. The four bits in each constellation point can be considered as 2 bits each on independent 4 pulse amplitude modulation (PAM) on I-axis and Q-axis, respectively. The LLR calculation is then realized for all the four bits that constitute the 16QAM signal and is based on the formulation reported in [29]. We indicate the four bits as $b_{Re,0}b_{Re,1}b_{Im,0}b_{Im,1}$. The first two bits are derived from the real part of the signal, while the last two are from the imaginary part of the signal. In Fig. 3 the value of the first two bits according to the region they belong to are shown, for both mappings. The values that the first two bits, $b_{Re,0}b_{Re,1}$, assume according to the region they belong to are also reported in Table I. As we can see, in the Gray mapping design, if we move from left to right, from top to bottom in Table I, only one bit of the two is changed every time we pass from one region to another. On the other side, in the non-Gray mapping, this feature is not present. We can notice that moving from region 2 to region 3 requires changing both bits at the same time. This fact influences also the LLR calculation. The Non-Gray mapping case is evaluated in dispersion managed link where the reported mapping results from the typical setup configuration of optical systems based on binary electronics.

TABLE I
Hard Detection Real Part

Region		$b_{Re,0}b_{Re,1}$
1	$y < -2$	00
2	$-2 \le y < 0$	01
3	$0 \le y < +2$	11
4	$y \ge +2$	10
1	$y < -2$	00
2	$-2 \le y < 0$	01
3	$0 \le y < +2$	10
4	$y \ge +2$	11

Upper part Gray mapping, lower part non-Gray mapping.

The received signal is demapped into soft bits which have the same sign as provided by a hard detector and whose absolute value represents the reliability of the decision. The optimum hard decision on bit $b_{Re,k}$ is given by the rule

$$b_{Re,k} = \beta \text{ if } P[b_{Re,k} = \beta | r] > P[b_{Re,k} = (1-\beta) | r] \qquad \beta = \{0, 1\} \tag{3}$$

where r represents the received signal

$$r = G_{ch} \cdot a + w \tag{4}$$

where G_{ch} is the channel frequency response and w is the complex AWGN noise. If we set $\beta = 1$ and we assume equally likely β we can rewrite 3 as

$$\hat{b}_{Re,k} = 1, \text{ if } \log \frac{P(r|b_{Re,k}=1)}{P(r|b_{Re,k}=0)} > 0. \tag{5}$$

As example, we consider $k = 0$, the first bit of the real part. As shown in Fig. 3 (top) for both case this bit is mapped with the same rule. Therefore we obtain

$$\frac{P(r|b_{Re,0}=1)}{P(r|b_{Re,0}=0)} = \frac{e^{\frac{-(y_{Re}-1)^2}{2\sigma^2}} + e^{\frac{-(y_{Re}-3)^2}{2\sigma^2}}}{e^{\frac{-(y_{Re}+1)^2}{2\sigma^2}} + e^{\frac{-(y_{Re}+3)^2}{2\sigma^2}}}. \tag{6}$$

The formulation in (6) has been obtained considering that when $b_{Re,0} = 0$ the real part of the 16QAM can only assume negative values, -3 or -1, and when $b_{Re,0} = 1$ the real part of the 16QAM can only assume positive values, $+1$ or $+3$. Therefore the LLR formulation for $b_{Re,0}$ is the same as reported in [29].

TABLE II
LLRs FORMULAS FOR $b_{Re,0}$ AND $b_{Re,1}$

Region		$LLR(b_{Re,0})$	$LLR(b_{Re,1})$
1	$y<-2$	$\frac{4}{\sigma^2}(y_{Re}+1)$	$\frac{2}{\sigma^2}(y_{Re}+2)$
2	$-2\le y<0$	$\frac{2}{\sigma^2}y_{Re}$	$\frac{2}{\sigma^2}(y_{Re}+2)$
3	$0\le y<+2$	$\frac{2}{\sigma^2}y_{Re}$	$\frac{2}{\sigma^2}(-y_{Re}+2)$
4	$y\ge+2$	$\frac{4}{\sigma^2}(y_{Re}-1)$	$\frac{2}{\sigma^2}(-y_{Re}+2)$
1	$y<-2$	$\frac{4}{\sigma^2}(y_{Re}+1)$	$\frac{2}{\sigma^2}(y_{Re}+2)$
2	$-2\le y<0$	$\frac{2}{\sigma^2}y_{Re}$	$\frac{2}{\sigma^2}(-y_{Re})$
3	$0\le y<+2$	$\frac{2}{\sigma^2}y_{Re}$	$\frac{2}{\sigma^2}(-y_{Re})$
4	$y\ge+2$	$\frac{4}{\sigma^2}(y_{Re}-1)$	$\frac{2}{\sigma^2}(y_{Re}-2)$

Upper part gray mapping, lower part non-gray mapping.

According to the 4 possible regions we therefore have the following possibilities

$$\mathrm{LLR}_{Re,0}=\begin{cases}\dfrac{4}{\sigma^2}(y_{Re}[i]+1), & y_{Re}[i]<-2, \quad \text{region1}\\ \dfrac{2}{\sigma^2}(y_{Re}[i]), & y_{Re}[i]\le 2, \quad \text{region2\&3}\\ \dfrac{4}{\sigma^2}(y_{Re}[i]-1), & y_{Re}[i]>+2, \quad \text{region4}\end{cases}. \tag{7}$$

Similarly to what obtained for $b_{Re,0}$ we can obtain the formulations for $b_{Re,1}$. In this case, the calculation is mapping dependent. For a Gray mapping we obtain

$$\frac{P(r|b_{Re,0}=1)}{P(r|b_{Re,0}=0)}=\frac{e^{\frac{-(y_{Re}+1)^2}{2\sigma^2}}+e^{\frac{-(y_{Re}-1)^2}{2\sigma^2}}}{e^{\frac{-(y_{Re}+3)^2}{2\sigma^2}}+e^{\frac{-(y_{Re}-3)^2}{2\sigma^2}}}. \tag{8}$$

For a non-Gray mapping we obtain instead

$$\frac{P(r|b_{Re,0}=1)}{P(r|b_{Re,0}=0)}=\frac{e^{\frac{-(y_{Re}-3)^2}{2\sigma^2}}+e^{\frac{-(y_{Re}+1)^2}{2\sigma^2}}}{e^{\frac{-(y_{Re}-1)^2}{2\sigma^2}}+e^{\frac{-(y_{Re}+3)^2}{2\sigma^2}}}. \tag{9}$$

When we consider a particular region, we can assume that some of the relative contribution in the numerator or denominator can be ignored. Therefore using these reductions and expressing the LLRs in logarithmic form we obtain Table II for $b_{Re,0}$ and $b_{Re,1}$ for the two mappings.

The LLR calculation for $b_{Im,0}$ and $b_{Im,1}$ follows the same rules as for $b_{Re,0}$ and $b_{Re,1}$. Similar equation are therefore obtained on the imaginary part of the signal. We assume that all the clusters have the same variance and we therefore remove the factor $2\sigma^2$ from all the LLR formulas.

The remapping block, placed after the SO encoder and interleaver in the TE routine, works with the inverse formula reported in Table II. The four LLR values are then used to reconstruct the real and imaginary signal. It should be noted that only one of the LLR values between $b_{Re,0}$ and $b_{Re,1}$is necessary to reconstruct the real part, and only one between $b_{Im,0}$ and $b_{Im,1}$ to reconstruct the imaginary part.

As already mentioned, the use of a non-gray mapping could arise difficulties in the reconstruction part of the loop. Due to the fact that only one of the bits is needed for remapping purpose and to the mapping scheme, the reconstruction process may present jumps beyond the nearest cluster of the constellation. For example, let us consider the complex signal +1.3+1.3j. It will be demapped into 1010 and the LLRs are calculated with the formulas presented. Let us now assume that we have a decoder/re-encoder error, and the new bits are 0010. In this case we can notice that the corrections of the error forced us to move from region 3 to region 1 for the real part of the signal, and therefore not to the nearest clusters.

IV. NUMERICAL RESULTS

A. Setup

The numerical simulations setup is reported in Fig. 4. Three are the main blocks: 4-PAM generation and transmitter, link transmission, coherent receiver and DSP modules. At the transmitter side the output of a 100 kHz linewidth laser is passed through an optical I/Q modulator driven by two four level Pulse Amplitude Modulation (PAM) electrical signals to generate the optical 16-QAM single polarization (SP) signal. The 4-PAM module consists of encoding process, signal mapping, upsampling, pulse shaping, digital to analog conversion, attenuators and electrical amplifiers. A $R=\frac{1}{2}$ CC with a 16 states trellis is employed to encode a 1000 bits data frame. The data frame is tested to guarantee a rather equal symbol distribution. The same data frame is later employed in the experimental validation. The baud rate is kept at 28 Gbaud. The same procedure is employed to realize the orthogonal polarization Y. The two signals are combined with a polarization beam combiner (PBC) to create a PDM 16-QAM signal. In the link transmission block the PDM 16-QAM signal is amplified and launched into the fiber span. The transmission link consists of spans of standard single mode fiber (SSMF) of 100 km length each. Three link lengths of 1000, 1500, and 2000 km, corresponding to a number of spans equal to 10, 15 and 20 respectively, are evaluated. The simulation parameters of the fiber link are listed in Table III. Erbium-doped fiber amplifier (EDFA) amplification is employed after each span compensating fully the fiber losses. At the receiver side we apply coherent detection and DSP modules. The received PDM 16-QAM signal is coherently detected in a 90° optical hybrid, photodetected and sampled at twice the baud rate by the analog-to-digital converter. We consider a 100 kHz linewidth laser as local oscillator (LO). The DSP module includes digital filter, CD compensation, radius directed equalization (RDE), polarization demultiplexing, frequency and carrier phase recovery [11].CD compensation is performed in frequency domain. Blind equalization is then performed based on RDE based on the equalizer output and the nearest constellation radius. An equalizer driven first by the constant modulus algorithm and then by the multi modulus algorithm (MMA) is used for polarization demultiplexing. A decision directed phase locked loop for frequency and offset estimation then follows. After demodulation the signal is fed into the SISOTE, structure presented.

B. Results

In the following results we assess the performance of TE in terms of BER. In this section only the performance of

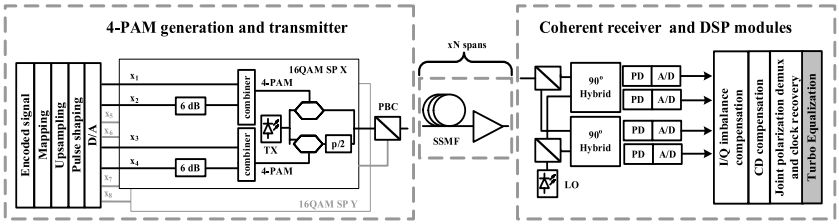

Fig. 4. Simulation setup. D/A: Digital to Analog converter, SP: Single PolarizationPBC: Polarization Beam Combiner, PD: Photodetector, A/D: Analog to Digital converter.

TABLE III
SIMULATION PARAMETERS

Parameter	Value
Modulation type	PDM 16-QAM
Baudrate	28 Gbaud
attenuation	0.2 dB/km
Chromatic dispersion	17 ps/nm/km
nonlinear coefficient	1.3 $W^{-1}km^{-1}$
Laser linewidth	100 kHz

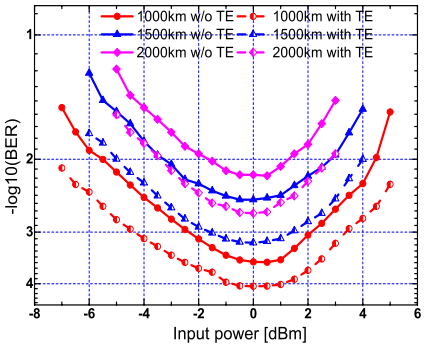

Fig. 5. BER as a function of link input power to the transmission span with and without TE for 1000, 1500 and 2000 km uncompensated SSMF transmission.

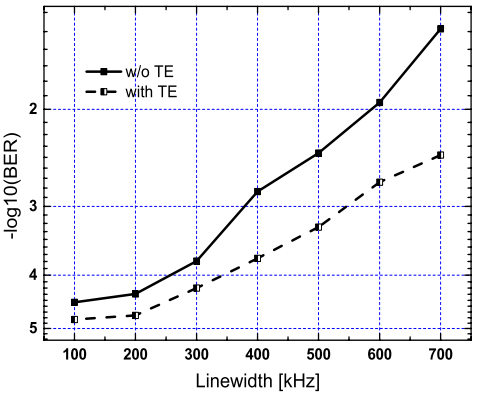

Fig. 6. BER as a function of transmitter and local oscillator laser linewidth for back-to-back with fix OSNR value of 25 dB.

simulation is assessed, and the experimental verification will be reported in Section V. In Fig. 5, we present the performance of the TE for a single channel transmission case. The results are shown in terms of BER as a function of the link input power. Both performance obtained without TE and with one iteration are presented. The performance without TE is obtained with hard decision BER accomplished by the first error counter in Fig. 2. When TE is employed, the SISO TE presented follows the 16-QAM DSP algorithms. The digital signals are equalized by an adaptive NLMS. The optimum number of taps and step size is evaluated for 0 dBm link input power and is thereafter kept constant throughout all the numerical investigations. The SOVA decoder is based on the soft information provided by the LLR and on a depth of 64 states.

Fig. 5 shows that the system after one TE performs better than when no TE is applied for the same link input power. In terms of BER performance the TE approach guarantee a gain of about half order of magnitude at the best operational point and similar values for all the considered link input power values. The validity of the proposed scheme are assessed through validation of its performance for three different lengths. A total link reach of 1000, 1500, and 2000 km, corresponding to a number of spans of 10, 15 and 20 respectively, has therefore been investigated. It should also be noted that the employment of this algorithm allows an extension of the maximum link reach by 500 km, which corresponds to 5 spans.

In Fig. 6 we assess the influence of the laser linewidth on the TE performance. A back-to-back case with a fixed OSNR of 25 dB is considered. Both transmitter and local oscillator are simulated with the same linewidth value. Fig. 6 shows that the system with TE performs better than the one without and that the performance difference increases with the linewidth value.

We can conclude that TE is effective for single channel uncompensated transmission regardless of the length of the considered link and the linewidth of both transmitter and local oscillator lasers.

V. EXPERIMENT UNCOMPENSATED TRANSMISSION

A. Setup

The setup for the PDM 16 QAM coherent optical (CO) uncompensated transmission system is illustrated in Fig. 7. At the transmitter side four sets of random generated data, corresponding to the 4 bits per symbol, are created in MATLAB and encoded with a CC. Three different rates are considered $R = \frac{1}{2}, \frac{2}{3}, \frac{3}{4}$. A 16, 32 and 64 states trellis is employed at the

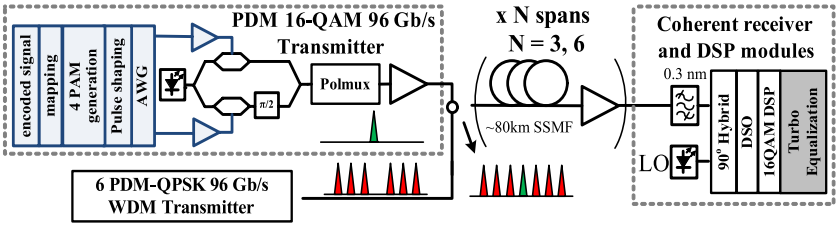

Fig. 7. Experiment setup for uncompensated link transmission in a WDM scenario. AWG: arbitrary waveform generator.

transmitter side respectively for CC with $R = \frac{1}{2}, \frac{2}{3}, \frac{3}{4}$. The resulting coded bits are interleaved to avoid block errors, and employed to generate two independent Gray mapped 4-PAM signal with a 24 Gbit/s Arbitrary Waveform Generator. The central optical channel, on which the BER performance will be assessed, is therefore a 12 Gbaud PDM 16-QAM, generated by driving a MZM with the two decorrelated 4-PAM electrical data signals. Polarization-division multiplexing is emulated by multiplexing the signal with its delayed copy in the orthogonal polarization to obtain a total bit rate of 96 Gbit/s.

Six 24 Gbaud PDM QPSK channels, three on each side, are combined with the PDM 16 QAM channel resulting in a 7 channel system on 100 GHz grid. Each of the QPSK signal has a bit rate of 96 Gbit/s, as the central 16-QAM carrier. Fiber transmission is realized over 3 and 6 SSMF spans, each approximately 80 km, for a total length of 251 and 497 km, without dispersion compensation and amplified using a double-stage EDFAs. At the receiver side an ECL with 100 kHz linewidth is employed as local oscillator (LO). The received signal is sampled by a DSO with 40 GS/s sampling rate and 13 GHz bandwidth. The offline DSP based receiver includes digital filter, CD compensation, MMA, polarization demultiplexing, carrier and phase recovery. The SISO TE structure is then applied. A SOVA binary decoder, with 64, 128, and 256 states depth is applied respectively for CC with $R = \frac{1}{2}, \frac{2}{3}, \frac{3}{4}$.

B. Results

Here, we study the impact of the rate of the employed CC and of multiple iterations on the performance of the 16-QAM using TE. First, we assess the performance of TE for back-to-back (B2B) case when a $R = \frac{1}{2}$ CC with a 16 states trellis is employed at the transmitter side. In Fig. 8 (a), we study the performance of the TE for the central 16-QAM signal of the considered WDM scheme. The results are shown in terms of BER as a function of the measured OSNR in dB. Performance obtained without TE, with one iteration and with two iterations is presented. Moreover the theoretical curve for 12 GBaud PDM 16-QAM is reported. Fig. 8 (a) shows that the system after one TE performs better than when no TE is applied for all the considered OSNR values. A gain higher than one order of magnitude in terms of BER is accomplished. Additional gain can be obtained incrementing the iterations number of the studied scheme, as the results obtained with a second iteration confirm. Thanks to the TE routine the gap between experimental results and the theoretical curve is also reduced.

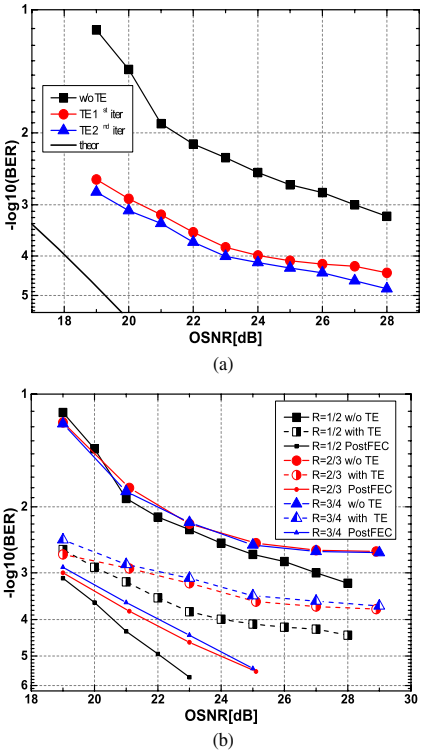

Fig. 8. (a) BER as a function of OSNR for back-to-back measurements for $R = \frac{1}{2}$ CC. (b) Comparison of BER as a function of OSNR for $R = \frac{1}{2}, \frac{2}{3}$, and $\frac{3}{4}$.

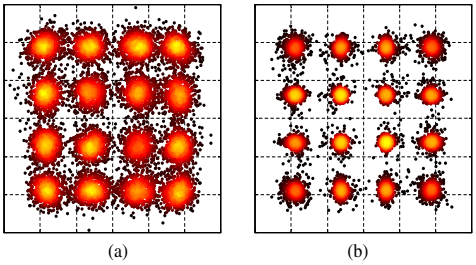

Fig. 9. Constellation of the demodulated 96 Gbit/s PDM 16-QAM signal (a) without TE and (b) after 1 iteration.

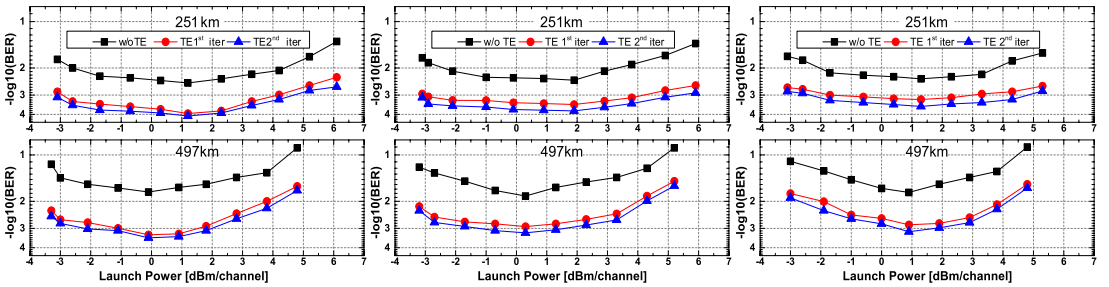

Fig. 10. BER as a function of link input power for 251 and 497 km uncompensated link transmission for (a) $R = \frac{1}{2}$ CC (b) $R = \frac{2}{3}$ CC (c) $R = \frac{3}{4}$ CC.

The dependence from the rate of the chosen code is assessed through validation of the TE effect for three different CCs. The performance of TE for three CC with rate $R = \frac{1}{2}, \frac{2}{3}$ and $\frac{3}{4}$ is illustrated in Fig. 8(b). PostFEC values obtained with soft decision BER accomplished by the second error counter in Fig. 2 are also reported. It is to be noted that TE performance and gain slightly degrade when the rate value of the CC increases. This results are in cohesion with the PostFEC values reported.

The constellation diagrams of demodulated 16-QAM signal without and after one TE iteration are illustrated in Fig. 9. It is observed a visible reduction of the clusters' spread already after one iteration. The considered OSNR is 21 dB for the $R = \frac{1}{2}$ CC case and the accomplished BER are 1.2×10^{-2} without TE and 6.76×10^{-4} after one TE iteration.

In Fig. 10, we evaluate the performance of uncompensated link transmission for the above mentioned three CC with different rates. Two transmission distances are considered, 251 and 497 km, corresponding to 3 and 6 spans respectively. The results are shown in terms of BER as a function of the link input power. The system after one TE performs better than when no TE is applied for the same link input power. In terms of BER performance the TE approach guarantee a gain of about one order of magnitude at the best operational point and similar values for all the considered link input power values. A maximum of 5 dB gain is provided by the presence of our chosen CC in the loop. The total benefit is therefore obtained due to the employment of the complete TE iteration. The validity of the proposed scheme are assessed through validation of its performance for the three different CC. In cohesion with what observed for the PosFEC values and the B2B case, the performance slightly degrade when the rate of the CC is increasing. Nevertheless, gains of one order of magnitude in terms of BER are obtained for all the considered rates. Furthermore additional gain is accomplished by the use of an additional iteration. The second iteration provides similar performance for all the considered cases.

In Fig. 11, we extend our study to multiple TE iterations. The results are shown in terms of BER as a function of the iteration number. When the iteration number is 0, the performance corresponds to the results obtained without TE. A transmission link of 497 km with a $R = \frac{1}{2}$ CC is considered. Performance obtained for three different values of launch power, 3.0 dBm, 0.1 dBm

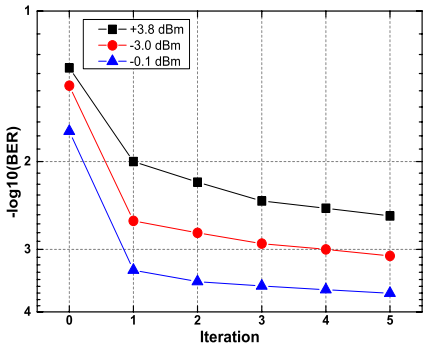

Fig. 11. BER as a function of iteration number for three different launch power values for 497 km and $R = \frac{1}{2}$ CC.

and $+3.8$ dBm are presented. According to the results accomplished, similar performance is expected also for rate $R = \frac{2}{3}$ and $\frac{3}{4}$. It should also be noted that the first and second iterations have the highest gains, the BER keeps decreasing with the iteration number, for the 3.0 dBm and 0.1 dBm link input power case. In the case of $+3.8$ dBm, when the signal is affected by non-linearities, the first 3 iteration give substantial gain, while the consecutive iterations give moderate gains, because of the improve quality signal. The employment of additional iterations guarantees an improvement in performance. If we consider as an example the link input power $+3.8$ dBm, the black squared curve. The first iteration provides an improvement of $\frac{1}{2}$ order of magnitude in terms of BER. If we now compare the performance obtain for iteration 5 with the performance obtained for iteration 0 (when no TE scheme is applied), we have an improvement of 1 order of magnitude in terms of BER.

We can conclude that TE is effective for a WDM uncompensated transmission scheme regardless of the OSNR value in a back-to-back case and length of the considered link. Multiple iterations are proven to allow additional gain. Furthermore the performance and gain of TE are dependent from the rate of the CC considered. Both overhead and achievable TE gain need to be taken into account when designing the FEC to be used in the routine.

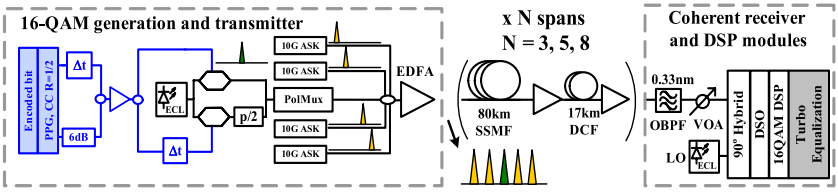

Fig. 12. Experiment setup for dispersion managed link transmission with legacy channels. PPG: pulse pattern generator, CC: convolutional code, ECL: external cavity laser, EDFA: erbium-doped fiber amplifier, OBPF: optical bandpass filter, VOA: variable optical attenuator.

VI. Dispersion Managed System With Legacy Channels

A. Setup

The setup for the PDM 16 QAM coherent optical (CO) dispersion managed transmission system is illustrated in Fig. 12. It is composed of three main blocks: 16-QAM generation and transmitter, link transmission, coherent receiver and DSP modules. A 1000 bits data frame is encoded offline by a CC and loaded into the memory of a programmable pulse pattern generator (PPG). The data outputs at 10 Gbaud are delayed to guarantee decorrelation, subsequently combined to create a 4 level electrical signal, amplified, and split into two branches to be fed to an I/Q optical modulator. An external cavity laser (ECL) with a linewidth of 100 kHz is employed at the transmitter. The optical 16-QAM signal is then sent to a polarization multiplexing stage to generate the PDM 16-QAM signals.

Four 10 G transponders are then multiplexed with the 16-QAM signal to emulate the interfering channels which have been placed symmetrically around the central signal. The spacing is varied between 200, 100 and 50 GHz.

An EDFA is applied to adjust the launch power to the link, including a pre-compensation of the dispersion equivalent to 40 km of SSMF. The transmission link block consists of spans of SSMF of 80 km length and dispersion compensated fiber of 17 km length. EDFA amplification is used for span loss compensation. Three link lengths 240, 400 and 640 km, corresponding to a number of spans equal to 3, 5 and 8 respectively, are evaluated. The input power to the link, measured at point A, is varied between -4 dBm and 4 dBm with a granularity of 1 dB. At the receiver side, we apply coherent detection and DSP modules. We employ an ECL with 100 kHz linewidth as local oscillator (LO) and a variable optical attenuator at the signal input to maintain a constant ratio between the signal received and the local oscillator. A 40 GSa/s sampling rate Digital Signal Oscilloscope (DSO) with 13 GHz bandwidth is employed to sample the received signals and then off-line signal processing is performed. The DSP module includes digital filter, RDE, polarization demultiplexing, frequency and carrier phase recovery followed by the SISO TE structure.

B. Results

Here we study the impact of TE in a dispersion managed transmission system with and without legacy channels. A dispersion managed transmission link consisting of spans of SSMF of 80 km length is considered. A $R = \frac{1}{2}$ CC is employed at the transmitter side. According to the results presented in Section V, similar performance is expected also for rate $R = \frac{2}{3}$ and $\frac{3}{4}$.

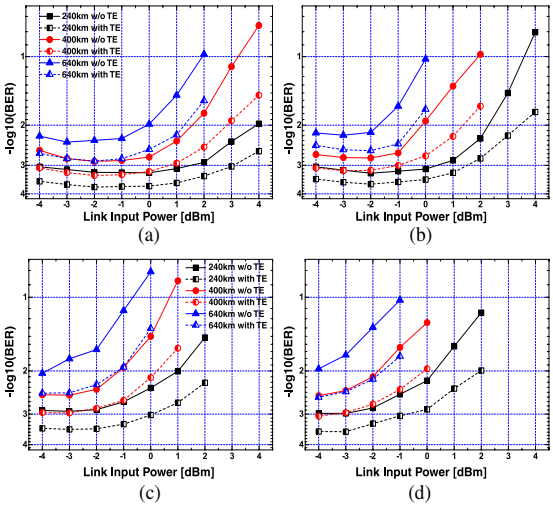

Fig. 13. Performance of single channel. BER as a function of link input power to the transmission span with and without TE for 240, 400 and 640 km compensated link for (a) single channel (b) with legacy channels spaced 200 GHz (c) with legacy channels spaced 100 GHz (d) with legacy channels spaced 50 GHz.

1) Performance of Single Channel: In Fig. 13 (a), we evaluate the performance of a single channel transmission. Three transmission distances are considered, 240, 400, and 640 km, corresponding to 3, 5 and 8 spans respectively. The results are shown in terms of BER as a function of the link input power. The system after one TE performs better than when no TE is applied for the same link input power. In terms of BER performance the TE approach guarantees a gain of about half order of magnitude at the best operational point and similar values for all the considered link input power values. It is to be noted that when the link input power is increasing, and therefore the performance degradation becomes also dominated by non-linear effects, moderate higher gain are achievable after only one TE iteration.

2) Performance With Interfering Channels: In Fig. 13 (b)–(d), we extend our study and we asses the validity of TE in dispersion managed transmission with legacy channels. A 200, 100, and 50 GHz spacing is illustrated in Fig. 13 (b),(c), and (d) respectively. The results are also in this case shown in terms of

BER as a function of the link input power. We note that also in this cases the system after one TE performs better than when no TE is applied for the same link input power. In terms of BER performance the TE approach guarantees a gain of about one order of magnitude at the best operational point and similar values for all the considered link input power values. Even though the total performance is affected by the presence of the ASK interfering channels, which cause a penalty of 3 dB in terms of input power, similar gain and performance are accomplished also in the presence of closed spaced legacy channels.

VII. Conclusion

In this paper, we assessed the effect of the use of TE in high order modulation coherent optical transmission. The concept has been proved by simulation and experimental validation. We first studied the impact of TE on system performance by simulations and showed that high gain in terms of BER can be obtained. We further showed that the use of TE enhances the performance regardless of the length of the considered link and of the lasers' linewidth. We then assessed the impact of TE in an experimental validation of uncompensated link transmission in a WDM scenario. TE is proven effective regardless of the OSNR value in a back-to-back case and length of the link. We further show that multiple iterations allow additional gain regardless of the considered link input power. Furthermore the performance and gain of TE are also shown to be dependent from the rate of the CC considered. Investigations based on simulated data and experimental verification are also in good agreement. Finally, we reported on the impact of TE in a dispersion managed transmission system with and without legacy channels. We show that similar performance is accomplished for all the reported cases, without and with co-propagating legacy channels. Effort in this topic should be devoted to further improve the benefit of the TE routine by means of more complex code employment and adoption of high gain FEC outer code. Moreover the reachable benefit in higher order modulation, such as 64-QAM, are of interest.

References

[1] P. J. Winzer, "High-spectral-efficiency optical modulation formats," *J. Lightw. Technol.*, vol. 30, no. 24, pp. 3824–3835, Dec. 15, 2012.

[2] M. Selmi, C. Gosset, M. Noelle, P. Ciblat, and Y. Jaouën, "Block-wise digital signal processing for polmux qam/psk optical coherent systems," *J. Lightw. Technol.*, vol. 29, no. 20, pp. 3070–3082, 2011.

[3] S. J. Savory, "Digital coherent optical receivers: Algorithms and subsystems," *IEEE J. Sel. Topics Quantum Electron.*, vol. 16, no. 5, pp. 1164–1179, Sep./Oct. 2010.

[4] T. Mizuochi, T. Sugihara, Y. Miyata, K. Kubo, K. Onohara, S. Hirano, H. Yoshida, T. Yoshida, and T. Ichikawa, "Evolution and status of forward error correction," presented at the Optical Fiber Communication Conference. Washington, DC, USA2012.

[5] A. Bononi, N. Rossi, and P. Serena, "Transmission limitations due to fiber nonlinearity," in *Optical Fiber Communication Conference.*, Washington, DC, USA, 2011, pp. 1–3.

[6] C. Xie, "Impact of nonlinear and polarization effects on coherent systems," presented at the European Conference and Exposition on Optical Communications. Washington, DCUSA, 2011.

[7] E. Ip and J. Kahn, "Compensation of dispersion and nonlinear impairments using digital backpropagation," *J. Lightw. Technol.*, vol. 26, no. 20, pp. 3416–3425, Oct. 15,, 2008.

[8] A. P. T. Lau, J. M. Kahn *et al.*, "Signal design and detection in presence of nonlinear phase noise," *J. Lightw. Technol.*, vol. 25, no. 10, pp. 3008–3016, 2007.

[9] N. Stojanovic, Y. Huang, F. N. Hauske, Y. Fang, M. Chen, C. Xie, and Q. Xiong, "MLSE-based nonlinearity mitigation for wdm 112 Gbit/s PDM-QPSK transmissions with digital coherent receiver," in *Opt. Fiber Commun.Conf.*, 2011, pp. 1–3.

[10] Z. Tao, L. Dou, W. Yan, L. Li, T. Hoshida, and J. C. Rasmussen, "Multiplier-free intrachannel nonlinearity compensating algorithm operating at symbol rate," *J. Lightw. Technol.*, vol. 29, no. 17, pp. 2570–2576, 2011.

[11] D. Zibar, O. Winther, N. Franceschi, R. Borkowski, A. Caballero, V. Arlunno, M. N. Schmidt, N. G. Gonzales, B. Mao, Y. Ye, K. J. Larsen, and I. T. Monroy, "Nonlinear impairment compensation using expectation maximization for dispersion managed and unmanaged pdm 16-qam transmission," *Opt. Exp.*, vol. 20, no. 26, pp. B181–B196, 2012.

[12] T. Sugihara, T. Yoshida, and T. Mizuochi, "Collaborative signal processing with fec in digital coherent systems," presented at the Optical Fiber Communication Conference. Washington, DC, USA 2013.

[13] C. Douillard, M. Jézéquel, C. Berrou, A. Picart, P. Didier, and A. Glavieux, "Iterative correction of intersymbol interference: Turbo-equalization," *Eur. Trans. Telecommun.*, vol. 6, no. 5, pp. 507–511, 1995.

[14] M. Jäger, T. Rankl, J. Speidel, H. Bülow, and F. Buchali, "Performance of turbo equalizers for optical pmd channels," *J. Lightw. Technol.*, vol. 24, no. 3, p. 1226, 2006.

[15] H. F. Haunstein, T. Schorr, A. Zottmann, W. Sauer-Greff, and R. Urbansky, "Performance comparison of MLSE and iterative equalization in FEC systems for PMD channels with respect to implementation complexity," *J. Lightw. Technol.*, vol. 24, no. 11, pp. 4047–4054, 2006.

[16] T. Schorr, W. Sauer-Greff, R. Urbansky, and H. Haunstein, "Design and performance of high-rate irregular ldpc codes for turbo equalization of pmd channels," in *Proc. Opt. Fiber Commun. Nat. Fiber Opt. Eng. Conf.*, 2007, pp. 1–3.

[17] W. Sauer-Greff and R. Urbansky, "Iterative equalization and FEC decoding in optical communication systems: Concepts and performance," presented at the Optical Fiber Communication Conf. Washington, DCUSA, 2008.

[18] I. B. Djordjevic, H. G. Batshon, M. Cvijetic, L. Xu, and T. Wang, "PMD compensation by LDPC-coded turbo equalization," *IEEE Photon. Technol. Lett.*, vol. 19, no. 15, pp. 1163–1165, Aug. 2007.

[19] I. B. Djordjevic, L. L. Minkov, L. Xu, and T. Wang, "Suppression of fiber nonlinearities and pmd in coded-modulation schemes with coherent detection by using turbo equalization," *J. Opt. Commun. Network.*, vol. 1, no. 6, pp. 555–564, 2009.

[20] L. Xu, I. Djordjevic, and T. Wang, "Turbo equalization for mitigation of linear and nonlinear impairments in high-speed optical transmission systems," in *Proc. IEEE Photon. Conf.*, 2011, pp. 825–826.

[21] I. Djordjevic, L. Minkov, and H. Batshon, "Mitigation of linear and nonlinear impairments in high-speed optical networks by using ldpc-coded turbo equalization," *IEEE J. Sel. Areas Commun.*, vol. 26, no. 6, pp. 73–83, Aug. 2008.

[22] L. Minkov, I. Djordjevic, L. Xu, and T. Wang, "Pmd compensation in polarization-multiplexed multilevel modulations by turbo equalization," *IEEE Photon. Technol. Lett.*, vol. 21, no. 23, pp. 1773–1775, Dec. 2009.

[23] S. Zhang, Y. Zhang, M.-F. Huang, F. Yaman, E. Mateo, D. Qian, L. Xu, Y. Shao, and I. Djordjevic, "Transoceanic transmission of 40 117.6 gb/s pdm-ofdm-16qam over hybrid large-core/ultralow-loss fiber," *J. Lightw. Technol.*, vol. 31, no. 4, pp. 498–505, 2013.

[24] M. Sakib, V. Mahalingam, W. Gross, and O. Liboiron-Ladouceur, "Optical front-end for soft-decision LDPC codes in optical communication systems," *J. Opt. Commun. Network.*, vol. 3, no. 6, pp. 533–541, 2011.

[25] V. Arlunno, A. Caballero, R. Borkowski, S. Saldaña Cercós, D. Zibar, K. J. Larsen, and I. Tafur Monroy, "Turbo equalization techniques towards robust PDM-16-QAM optical fiber transmission," *J. Opt. Commun. Netw.*, 2013, to be published.

[26] V. Arlunno, A. Caballero, R. Borkowski, D. Zibar, K. J. Larsen, and I. Tafur Monroy, "Counteracting 16-qam optical fibre transmission impairments with iterative turbo equalization," *IEEE Photon. Technol. Lett.*, vol. 25, no. 21, pp. 2097–2100, Nov. 2013.

[27] T. Wuth, E. Agrell, M. Karlsson, and M. Sköld, "Fiber communications using convolutional coding and bandwidth-efficient modulation," *Opt. Exp.*, vol. 14, no. 2, pp. 542–555, 2006.

[28] J. Benesty, H. Rey, L. R. Vega, and S. Tressens, "A nonparametric VSS NLMS algorithm," *IEEE Signal Process. Lett.*, vol. 13, no. 10, pp. 581–584, Oct. 2006.

[29] F. Tosato and P. Bisaglia, "Simplified soft-output demapper for binary interleaved cofdm with application to hiperlan/2," in *Proc. IEEE Int. Conf. Commun.*, 2002, vol. 2, pp. 664–668.

Valeria Arlunno was born in 1984 in Gattinara, Italy. She received the B.Sc. and M.Sc. degree in telecommunications engineering from Politecnico di Torino, Torino, Italy, respectively, in 2006 and 2009. In 2009, she joined the Optcom Group, Politecnico di Torino as a Research Assistant. She is currently working toward the Ph.D. degree in optical communications engineering at DTU Fotonik, Technical University of Denmark, with the Metro-Access and Short Range Systems Research Group of the Department of Photonics Engineering. Her research interests include the areas of coherent optical communications and digital signal processing.

Antonio Caballero was born in 1985 in Zaragoza, Spain. He received the B.Sc. and M.Sc. degrees in Telecommunications Engineering from Centro Politécnico Superior, Zaragoza, Spain, in 2008. He received his Ph.D. in Optical Communications Engineering at DTU Fotonik, Technical University of Denmark, in September 2011, with a thesis on high-capacity radio-over-?ber links. He was a Visiting Researcher at The Photonics and Networking Research Laboratory at Stanford University from February to June 2010, under supervision of Prof. Leonid G. Kazovsky. He is currently a postdoctoral researcher at DTU Fotonik. His research interests are in the area of coherent optical communications as well as radio-over-fiber links.

Robert Borkowski was born in Lodz, Poland, in 1987. He received the M.Sc. degree in telecommunications from the Technical University of Denmark in 2011 and the M.Sc. degree in electronics and telecommunications from the Technical University of Lodz in 2012. He is now working towards his Ph.D. degree in the field of optical communications in the Metro-Access and Short Range Systems group at DTU Fotonik, Department of Photonics Engineering, Technical University of Denmark. He is involved in the EU FP7 project CHRON (Cognitive Heterogeneous Reconfigurable Optical Networks). His research interests are in the areas of optical performance monitoring, coherent transmission systems and digital signal processing for fiber-optic communications.

Darko Zibar was born on December 9th, 1978, in Belgrade former Yugoslavia. He received the M.Sc. degree in Telecommunication in 2004 from the Technical University of Denmark and the Ph.D. degree in 2007 from the Department of Communications, Optics and Materials, COM•DTU within the field of optical communications. He was a Visiting Researcher with Optoelectronic Research Group led by Prof. John E. Bowers, at the University of California, Santa Barbara (UCSB) from January 2006 to August 2006, and January 2008 working on coherent receivers for phase-modulated analog optical links. From February 2009 until July 2009, he was Visiting Researcher with Nokia-Siemens Networks working on digital clock recovery for 112 Gb/s polarization multiplexed systems. Currently, he is employed at DTU Fotonik, Technical University of Denmark as the Assistant Professor. His research interests are in the area of coherent optical communication, with the emphasis on digital demodulation and compensation techniques. Darko Zibar is a recipient of the Best Student Paper Award at the IEEE Microwave Photonics Conference (MWP) 2006, for his work on novel optical phase demodulator based on a sampling phase-locked loop as well as Villum Kann Rasmussen postdoctoral research grant in 2007.

Knud J. Larsen received th M.S.E.E. and Ph.D. degrees from the Technical University of Denmark, Kgs. Lyngby, Denmark. He was at Ericsson Signal Systems as a Senior Engineer and Project Manager involved in design and implementation of communication systems and traffic control systems. Since 1986, he has been a Professor at the Technical University of Denmark (previously the Institute of Telecommunication, now the Department of Photonics), teaching and doing research in communication theory and coding. He has worked extensively on studies of error correction for the European Space Agency and is now involved in projects related to optical transmission. Together with four colleagues he received the 1991 Information Theory Society Paper Award for a paper on algebraic geometry codes.

Idelfonso Tafur Monroy received the M.Sc. degree in multichannel telecommunications from the Bonch-Bruevitch Institute of Communications, St. Petersburg, Russia, in 1992, the Technology Licenciate degree in telecommunications theory from the Royal Institute of Technology, Stockholm, Sweden, in 1996, and the Ph.D. degree from the Eindhoven University of Technology, Eindhoven, The Netherlands, in 1999. He is currently a Professor and the Head of the Metro-Access and Short Range Communications Group, Department of Photonics Engineering, Technical University of Denmark, Lyngby, Denmark. In 1996, he joined the Department of Electrical Engineering, Eindhoven University of Technology, where he was an Assistant Professor until 2006. He has participated in several European research framework projects in photonic technologies and their applications to communication systems and networks. He is currently involved in the ICT European projects GigaWaM and EURO-FOS and is the Technical Coordinator of the ICT-CHRON project. His research interests include hybrid optical-wireless communication systems, high-capacity optical fiber communications, digital signal processing for optical transceivers for baseband and radio-over-fiber links, application of nanophotonic technologies in the metropolitan and access segments of optical networks as well as in short-range optical-wireless communication links.

Paper 4: Digital non-linear equalization for flexible capacity ultradense WDM channels for metro core networking

V. Arlunno, X. Zhang, K. J. Larsen, D. Zibar and I. Tafur Monroy, "Digital non-linear equalization for flexible capacity ultradense WDM channels for metro core networking," in *Optics Express*, Vol. 19, No. 26, December 2011.

Digital non-linear equalization for flexible capacity ultradense WDM channels for metro core networking

Valeria Arlunno,* Xu Zhang, Knud J. Larsen, Darko Zibar, and Idelfonso Tafur Monroy

DTU Fotonik, Department of Photonics Engineering, Technical University of Denmark, DK-2800 Kgs. Lygnby, Denmark

**vaar@fotonik.dtu.dk*

Abstract: An experimental demonstration of Ultradense WDM with advanced digital signal processing is presented. The scheme proposed allows the use of independent tunable DFB lasers spaced at 12.5 GHz for ultradense WDM PM-QPSK flexible capacity channels for metro core networking. To allocate extremely closed carriers, we demonstrate that a digital non-linear equalization allow to mitigate inter-channel interference and improve overall system performance in terms of OSNR. Evaluation of the algorithm and comparison with an ultradense WDM system with coherent carriers generated from a single laser are also reported.

OCIS codes: (060.1660) Coherent communications; (060.4510) Optical communications.

References and links

1. M. Jinno, B. Kozicki, H. Takara, A. Watanabe, Y. Sone, T. Tanaka, and A. Hirano, "Distance-Adaptive Spectrum Resource Allocation in Spectrum-Sliced Elastic Optical Path Network," IEEE Commun. Mag. **48**(8), 138–145 (2010).
2. N. Amaya, G. S. Zervas, M. Irfan, Y. R. Zhou, A. Lord, and D. Simeonidou, "Experimental demonstration of gridless spectrum and time optical switching," Opt. Express **19**(12), 11182–11188 (2011).
3. N. Amaya, M. Irfan, G. Zervas, K. Banias, M. Garrich, I. Henning, D. Simeonidou, Y. R. Zhou, A. Lord, K. Smith, V. J. F. Rancano, S. Liu, P. Petropoulos, and D. J. Richardson, "Gridless Optical Networking Field Trial: Flexible Spectrum Switching, Defragmentation and Transport of 10G/40G/100G/555G over 620-km Field Fiber," in *European Conf. Opt. Commun.*, OSA Technical Digest (CD) (Optical Society of America, 2011), paper Th.13.K.1.
4. D. J. Geisler, R. Proietti, Y. Yin, R. P. Scott, X. Cai, N. K. Fontaine, L. Paraschis, O. Gerstel, and S. J. B. Yoo, "The First Testbed Demonstration of a Flexible Bandwidth Network with a Real-Time Adaptive Control Plane," in *European Conf. Opt. Commun.*, OSA Technical Digest (CD) (Optical Society of America, 2011), paper Th.13.K.2.
5. A. Patel, P. Ji, J. Jue, and T. Wang, "Survivable Transparent Flexible Optical WDM (FWDM) Networks," *Optical Fiber Communication Conference*, OSA Technical Digest (CD) (Optical Society of America, 2011), paper OTuI2.
6. A. Patel, P. Ji, J. Jue, and T. Wang, "Defragmentation of Transparent Flexible Optical WDM (FWDM) Networks," in Optical Fiber Communication Conference, OSA Technical Digest (CD) (Optical Society of America, 2011), paper OTuI8.
7. P. N. Ji, A. Patel, D. Qian, J. Jue, J. Hu, Y. Aono, and T. Wang, "Optical Layer Traffic Grooming in Flexible Optical WDM (FWDM) Networks," in *European Conf. Opt. Commun.*, OSA Technical Digest (CD) (Optical Society of America, 2011), paper We.10.P1.102.
8. J. Berthold, "Toward 100G Networking and Beyond", in *European Conf. Opt. Commun.*, OSA Technical Digest (CD) (Optical Society of America, 2011), paper Tu.3.K.1.
9. M. Wu and W. Way, "Fiber Nonlinearity Limitations in Ultra-Dense WDM systems," J. Lightwave Technol. **22**(6), 1483–1498 (2004).
10. J. Kurzweil, *An Introduction to Digital Communications* (John Wiley & Sons, Inc., 1999), Chap. 10.
11. D. Zibar, R. Sambaraju, A. Caballero, J. Herrera, and I. Tafur Monroy, "Carrier Recovery and Equalization for Photonic-Wireless Links with Capacities up to 40 Gb/s in 75-110 GHz Band," in *Optical Fiber Communication Conference*, OSA Technical Digest (CD) (Optical Society of America, 2011), paper OThJ4.

#155730 - $15.00 USD
Received 30 Sep 2011; accepted 1 Nov 2011; published 18 Nov 2011

1. Introduction

Rigid and coarse granularity of wavelength-division-multiplexing (WDM) systems leads to inefficient capacity utilization, which partly results from the lost spectrum due to the difference between the real spectral occupancy of the signal and the ITU-T grid. A promising way would be to introduce the concept of a frequency slot instead of the current frequency grid [1], moving toward flexible grid and grid-less solutions [2–4]. In flexible optical WDM (FWDM), spectral resources are allocated in a flexible and dynamic way; channel spacing and center wavelength are not fixed on the ITU-T grid, resulting in higher spectral efficiency [5,6]. Standardization towards more flexible scenario specifying frequency slots of variable width rather than a fixed frequency grid is currently ongoing in ITU-T SG.15, Q.6. Even in this higher-efficient bandwidth allocation scenario, the bandwidth is non optimally utilized as large guard bands are still employed, as shown in Fig. 1 [7]. Ultra-dense (UD) WDM with a channel spacing of less than 25 GHz, may provide an evolutionary path from conventional infrastructures towards more scalable and spectrally efficient networks. This trend, supported by the increased demand for more capacity, flexibility and upgradeability of transmission technique while keeping some legacy ones will require a comprehensive reexamination of the way metro-core networks are designed and built [8].

Increasing the number of wavelengths within a fixed optical bandwidth (e.g., C band), by decreasing the spacing between neighboring channels, allows an increase in the system capacity without requiring of high-speed electronics (e.g., >40 Gb/s), while keeping compatibility with the 10 Gb/s SONET/SDH equipment. UDWDM systems with no aliasing condition (i.e. with channel spacing higher than the double the baud rate) have been studied, with particular attention to limitations introduced by fiber nonlinearity effects such as Four-Wave Mixing (FWM), Cross-Phase Modulation (XPM), fiber chromatic dispersion-induced symbol intersymbol interference (ISI) [9]. However, to cope with the required bandwidth efficiency, future UDWDM schemes will need to use extremely close channel spacing; this implies taking measures to mitigate the resultant detrimental effects from crosstalk and neighboring channels interferences.

In this paper we experimentally demonstrate that an upgraded digital signal processing (DSP) allows for closer channel spacing, up to 12.5 GHz, using conventional independent DFB light sources for a 40 Gb/s ultradense 3 channel WDM PM-QPSK system with coherent detection. The employment of a digital nonlinear equalizer, such as a Decision Feedback Equalizer (DFE), can mitigate inter-channel interference and improve overall system performance in terms of OSNR. Our proof of principle experiment demonstrates that in a 50GHz bandwidth (in accordance to the ITU-T grid) up to 4 channels can be transmitted, improving the total bit rate from 40 Gb/s to 160 Gb/s per slot, with a minor upgrade in the electronic equipment.

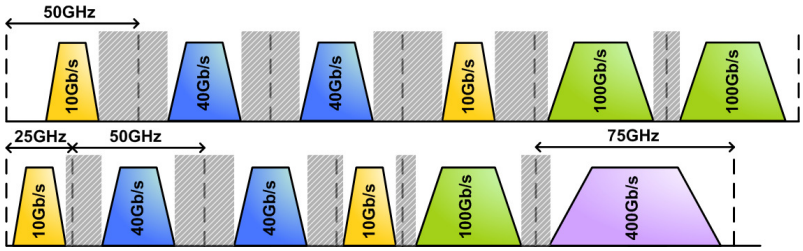

Fig. 1. Moving from fix to flex grid scenario. Large guard bands are still employed in both schemes.

#155730 - $15.00 USD
Received 30 Sep 2011; accepted 1 Nov 2011; published 18 Nov 2011

2. System setup

The general outline of the experimental setup for the UDWDM polarization multiplexing (PM) QPSK coherent optical (CO) system is shown in Fig. 2. At the transmitter side three carriers are generated employing three independent tunable distributed feedback lasers (DFB) with 10 MHz linewidth; one of them is fixed at a central wavelength (λ_c) of 1550.511 nm. Different channel spacing values $\Delta\lambda$ (20, 18, 16, 14, 13, 12, 11 and 10 GHz) between the 3 carriers have been realized by changing the wavelength of the right (λ_r) and left (λ_l) DFB lasers as to have the desired spectral separation. A 40 GHz bandwidth photodiode and an Electrical Spectrum Analyzer are used to verify correct spacing between the three channels. A polarization beam splitter divides the signal into two orthogonal polarization which are then fed into two optical I/Q modulator (nested Mach-Zehnder modulator). A 10 Gb/s pattern generator (PPG) generates the pseudo random binary sequence (PRBS), with 2^{15}-1 bit length, that drives the two QPSK modulators. Two uncorrelated branches of polarization orthogonal QPSK signals are then combined with a polarization beam combiner (PBC) to generate the PM QPSK signals, at 10 Gbaud. An 80 km span of standard single mode fiber (SMF) is used as optical transmission link. At the receiver side an optical tunable band-pass filter (0.33 nm or 37.5 GHz full width at half maximum, FWHM, at 1550 nm) is employed before the optical pre-amplifier; a second band-pass filter (0.5 nm or 62.5 GHz FWHM at 1550 nm) rejects the out of band ASE noise. An external cavity laser (ECL) with 100 kHz linewidth is used as local oscillator (LO). The PM coherent receiver consists of two 90° hybrids and balanced photodetectors. The photodetected inphase and quadrature outputs are sampled at 40 GS/s for offline demodulation. Digital signal processing (DSP) algorithms implement digital filtering, PM QPSK constant modulus algorithm (CMA) equalization, QPSK carrier phase recovery and bit error decision. As the channel distortion or the ISI of a transmission system is too severe for a linear equalizer to mitigate the channel impairments, non-linear equalizer has been used. A DFE is a non-linear structure that uses previous detector decision to eliminate the ISI on pulses currently demodulated. The basic idea is that if the values of the symbols previously detected are known, then ISI contributed by these symbols can be canceled out exactly at the output of the forward filter by subtracting past symbol values with appropriate weighting. The DFE equalizer will not amplify the noise, cause according to its structure, the equalization process is done through the feedback, noiseless, data applying symbol-by-symbol detection

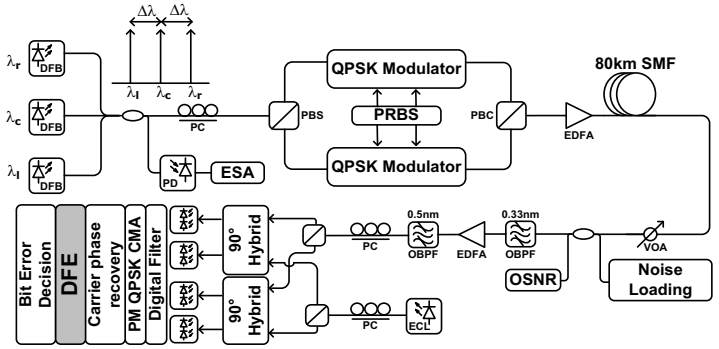

Fig. 2. Experiment setup of UDWDM PM QPSK system; DFB: Distributed feedback laser; PD: 40G photodiode; ESA: Electrical Spectrum Analyzer; PC: polarization controller; PBS: polarization beam splitter; PBC: polarization beam combiner; EDFA: erbium-doped fiber amplifier; VOA: variable optical attenuator; OBPF: optical band-pass filter; ECL: external cavity laser.

#155730 - $15.00 USD Received 30 Sep 2011; accepted 1 Nov 2011; published 18 Nov 2011

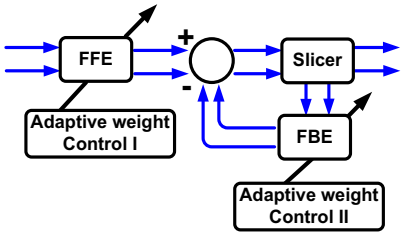

Fig. 3. Non-linear Decision Feedback Equalizer (DFE) structure.

with successive cancellation of the interference caused by the detected symbols [10]. A nonlinear DFE, shown in Fig. 3, consisting of a feed-forward filter (FFE) and a feed-back filter (FBE) is used in our DSP receiver, after the carrier phase recovery block, to improve the system performances [11]. The taps of the two equalizers are adjusted using a least mean square (LMS) stochastic algorithm.

3. Results

After optimize the PM CMA algorithm structure, we have investigated the impact of a nonlinear decision feedback equalizer on the system performances (this structure is indicated as DFE in the graphs); the best configuration is composed of a 1 tap feedforward filter (FFE) and a 7 or 9 taps feedback filter (FBE). The digital filter is then re-optimized to improve further the BER curves. The measured BER performances of the UDWDM PM QPSK for back-to-back (B2B) system are shown in Fig. 4. Figure 4(a) shows the BER experimental performances as a function of the measured OSNR for a spacing of 14 GHz without nonlinear equalization, with the nonlinear equalization structure DFE and with further optimization of the digital filter. It can be observed that the non-linear equalization and the optimization of the digital filter afterward, can improve the system performances up to 4.5 dB in terms of OSNR. The BER versus carrier spacing for two fixed value of OSNR is shown in Fig. 4(b); the results show that the DSP implementation can improve the experimental BER results for all the different spacing. For a fix spacing the algorithm can improve the BER result, while for a fix BER value the use of DSP, it allows closer channel. Of particular importance is 12.5 GHz of spacing which, thanks to the nonlinear equalization, shows performances better then the UFEC limit for both the chosen OSNR.

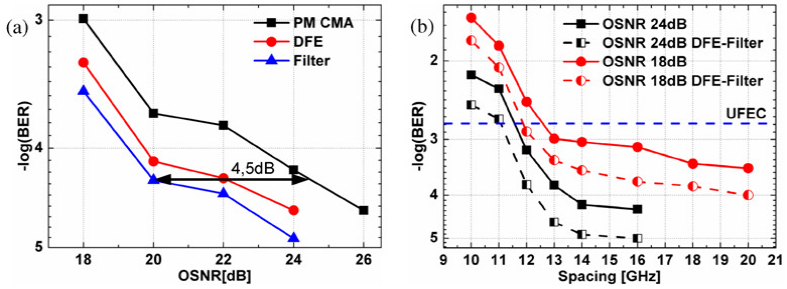

Fig. 4. (a) BER as a function of OSNR for a spacing of 14GHz without nonlinear equalization, with DFE and with optimization of the digital filter. (b) BER as a function of the spacing for two fixed values of OSNR with and without nonlinear equalization.

#155730 - $15.00 USD
(C) 2011 OSA
Received 30 Sep 2011; accepted 1 Nov 2011; published 18 Nov 2011
12 December 2011 / Vol. 19, No. 26 / OPTICS EXPRESS B273

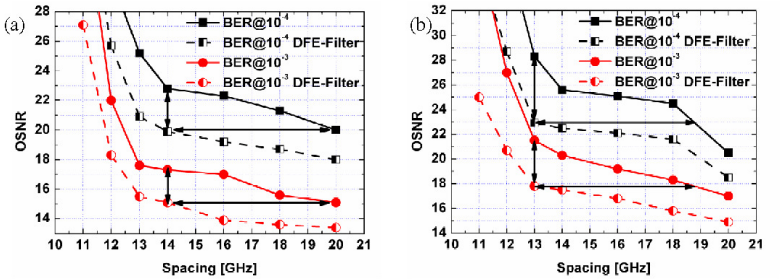

Fig. 5. (a) OSNR as a function of the spacing for two fixed values of BER with and without nonlinear equalization for Back-to-Back. (b) OSNR as a function of the spacing for two fixed values of BER with and without nonlinear equalization for 80Km of SMF.

Figure 5 shows OSNR performance as a function of the spacing with and without nonlinear equalization for Back-to-Back and 80 km of SMF optical transmission are presented. The BER is fixed 10^{-4} and 10^{-3}, both below the UFEC level. The improvement enabled by the DSP implementation on both BER and spacing values is substantial. As shown in Fig. 5(a) the proposed algorithm can improve up to 3 dB of OSNR with the same spacing value between the carriers; on the other hand for a fix OSNR the carriers can be generated 6 GHz closer, moving from 20 GHz of spacing, case where we have no aliasing, to 14 GHz of spacing. The same behavior is observed for 80 km of optical transmission. It can be observed in Fig. 5(b) that with the same spacing value between the carriers, the improvement in terms of OSNR is 3 dB for BER 10^{-3} and 5dB for BER 10^{-4}; for the same OSNR then the carriers can be 6 GHz closer, moving to 19 GHz to 13 GHz. It should be noticed that the length of the FBE is 7 or 9 taps compared to 1 tap for the FFE, indicating that the signal is affected by non-linearities.

To prove the efficiency of the algorithm used, we have evaluated its performances in a system with 3 coherent carriers. Figure 6 shows the transmitter side of the two configuration under study, the UDWDM with different lasers previously presented, called from now on DFB, and the new scheme. A single tunable DFB with 10MHz linewidth is employed to drive a Mach-Zehnder modulator (MZM), to generate three coherent carriers. The different channel spacing $\Delta\lambda$ (20, 18, 16, 14, 13, 12, 11 and 10 GHz) between the 3 carriers has now been realized by operating the synthesizer, the input source to the MZM, as to have the desired spectral separation. From now on we will refer to the scheme as MZM.

After optimize the PM CMA algorithm structure, we have investigated the impact of the same nonlinear decision feedback equalizer of the UDWDM DFB case on the system performances; also in this case the digital filter is then re-optimized to improve further the BER curves. The BER versus carrier spacing for a fixed OSNR value is shown if Fig. 7(a); the

#155730 - $15.00 USD Received 30 Sep 2011; accepted 1 Nov 2011; published 18 Nov 2011

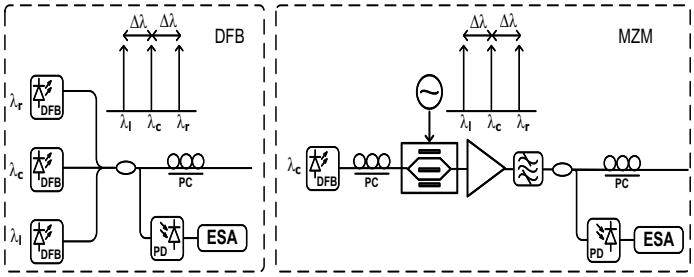

Fig. 6. Experiment setup of transmitter side for UDWDM with DFB scheme and MZM scheme.

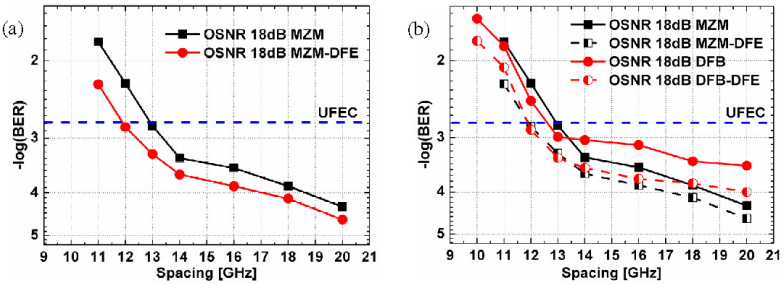

Fig. 7. (a) BER as a function of the spacing for a fixed value of OSNR with and without nonlinear equalization for UDWDM MZM case. (b) BER as a function of the spacing for a fixed value of OSNR for UDWDM DFB and MZM case.

results show that the DSP implementation can improve the experimental BER results for all the different spacing. In this case, the results show higher improvement for smaller frequency spacing between the 3 carriers. The employment of our suggested non-linear equalization 12.5 GHz of spacing shows performances better then the UFEC limit also for the UDWDM MZM case. No results are displayed for a frequency separation equals to 10 GHz, because in this case with this configuration, we will not have an UDWDM scheme, but an OFDM. Figure 7(b) shows the BER versus carrier spacing for the same fixed OSNR value for both cases under study. In both cases is appreciable the benefit introduced by non-linear equalization. For frequency separation between the 3 carriers higher than 14 GHz, the BER performances are better in the MZM case, but in the DFB case the DFE algorithm provides higher improvement. For frequency separation smaller than 14 GHz, in particular for the 12.5 GHz case, the BER performances of the schemes are comparable.

The results obtained suggest more efficient and flexible utilization of the available bandwidth. In case of ITU-T grid with 50 GHz spacing, one single 40 Gb/s signal can be transmitted per slot. Using the proposed UDWDM DFB with DSP non linear equalization, up to 4 channels (12.5 GHz of spacing) per slot can be transmitted with a total bit-rate of 160 Gb/s, with a minor upgrade in the electronic equipment and higher flexibility. Better results per slot could also be obtained with a single carrier higher data rate signal (100 Gb/s), but this would imply higher speed electronics and no compatibility anymore with the existing 10 Gb/s SONET/SDH equipment.

#155730 - $15.00 USD
(C) 2011 OSA
Received 30 Sep 2011; accepted 1 Nov 2011; published 18 Nov 2011
12 December 2011 / Vol. 19, No. 26 / OPTICS EXPRESS B275

4. Conclusion

We have experimentally demonstrated a flexible ultradense WDM QPSK system with upgrading DSP algorithms. The DFE nonlinear equalizer structure proposed allows for extremely closed spacing (up to 12.5 GHz), where bit error rate performances below the UFEC limit are obtained. In a 50 GHz ITU-T grid, the structure presented in this paper allows to quadruple the number of users in a flexible way, moving from a total bit rate of 40 Gb/s per slot to 160 Gb/s. We believe that the upgradable and flexible structure proposed well suit in the trend towards next generation flex-grid and grid-less scenarios.

Acknowledgments

The research leading to these results has received funding from the European Community's Seventh Framework Programme [FP7/2007-2013] under grant agreement n° 258644, CHRON project. The authors thank Teraxion for the technical expertise provided.

#155730 - $15.00 USD Received 30 Sep 2011; accepted 1 Nov 2011; published 18 Nov 2011

Paper 5: 1.2 Tb/s Ultredense WDM Long Reach and Spectral Efficiency Access Link with Digital Detection

X. Zhang, V. Arlunno, J. Bevensee Jensen, I. Tafur Monroy, D. Zibar, R. Younce "1.2 Tb/s Ultredense WDM Long Reach and Spectral Efficiency Access Link with Digital Detection," in *Photonics Conference (PHO), 2011 IEEE*, Arlington, USA, 2011, paper ThBB5.

ThBB5 (Contributed Oral)
4:45 PM – 5:00 PM

1.2 Tb/s Ultredense WDM Long Reach and Spectral Efficiency Access Link with Digital Detection

Xu Zhang[(1)], Valeria Arlunno[(1)], J. Bevensee Jensen[(1)], I. Tafur Monroy[(1)], Darko Zibar[(1)], Richard Younce[(2)]
(1) Department of Photonic Engineering, Technical University of Denmark, Ørsteds Plads DK2800, Kgs, Lyngby, Denmark
(2) Tellabs, 1415 West Diehl Road, Naperville, IL 60563 USA.
xuzhn@fotonik.dtu.dk

Abstract— **We experimentally demonstrate an ultradense WDM system with sub-channel spacing at the baud rate, achieving 4.0 b/s/Hz spectral efficiency and aggregate capacity of 1.2 Tb/s data transmission over 80-km SMF, for long reach access networking.**

I. Introduction

With the rapid growth of capacity requirements of optical transmission networks, there is a strong need to realize high bit rate and highly spectral efficient (SE) optical transmission technologies. Next-generation optical access networks will therefore consider supporting aggregate capacities beyond 40 Gb/s and in the longer term capacities approaching 1 Tb/s. The challenges for Tb/s access networks are related to efficient spectral usage, to benefit from well-established and mature components and technologies at the C and L bands; and to reduce complexity, particularly at the end-user side; and where possible in the whole system. Therefore, since digital coherent transmission technology is becoming preferable for next generation optical transport links, it is interesting to evaluate its performance and feasibility and derive requirements for its application in long reach metro-access links. Recent research experiments have demonstrated dense wavelength division multiplexing (DWDM) systems with advanced modulation formats, such as quadrature phase shift keying (QPSK) and orthogonal frequency division multiplexing (OFDM), achieving capacity of 1 Tb/s mainly for long haul application [1-3]. A dual polarization (DP) QPSK DWDM system with 10 sub-channels, employing 10 continuous-wave (CW) lasers achieving 3.0 b/s/Hz of SE has been demonstrated [1]. An optical OFDM WDM experiment based on single sideband modulation achieved 3.3 b/s/Hz of SE [2]. To best of our knowledge, the closest sub-channel spacing for conventional (non-OFDM) DWDM system achieved 1.1 times of baud rate with 3.6 b/s/Hz of SE [3].

In this paper, we report on an experimental implementation of a long reach ultradense WDM system based on a single distributed feed back (DFB) laser to generate 30 sub-channels with DP QPSK modulation. The sub-channel spacing is equal to the baud-rate, achieving 4.0 b/s/Hz of SE and 1.2 Tb/s of aggregate capacity over 80 km SMF for metro-access networking. To avoid the employment of arrayed waveguide grating, a coherent receiver with local oscillator (LO) laser is used to select the sub-channel. We have developed digital signal processing (DSP) algorithms to compensate for optical transmission impairments including chromatic dispersion (CD). A decision feed back equalizer (DFE) algorithm has also been implemented in the DSP to mitigate the effects of inter-channel interference (ICI) in the ultradense WDM system. The employment of non-linear DFE equalizer guarantees system bit error rate (BER) back to back performance below the FEC threshold for all 30 sub-channels.

II. Experiment setup

The ultradense WDM structure is realized using recirculated single side band modulation (SSB) [3]. Figure 1 shows the schematic of our experimental setup. A single DFB laser operating at 1549.53 nm (193.47 THz) with 10 MHz line-width is used source to generate the sub-channels. A nested Mach-Zehneder modulator operates as single side band modulator. An external synthesizer drives the single side band modulator to control the sub-channel generation loop, which is also called the comb generator [3]. Comb generator shifts the first input channel by a frequency spacing determined by the external synthesizer clock output. In the experiment, frequency spacing is set equal to 10 GHz. As a result, each round generates one more sub-channel. A tunable optical band-pass filter with full width at half maximum (FWHM) of 5 nm (625 GHz) is used to control the bandwidth of the comb generator. After the comb generator, the sub-channels are separated into two orthogonal polarizations by a polarization beam splitter (PBS). The polarized sub-channels are then fed into two identical QPSK modulators. A non-return-zero (NRZ) pseudo random binary sequence (PRBS) with 2^{15}-1 bit length provides the electrical data source. After the QPSK modulator, two uncorrelated branches of orthogonally polarized QPSK signals are combined by a polarization beam combiner (PBC) to generate the DP QPSK signals. Differently from [2] and [3], we first generate sub-channels and then QPSK modulate each polarization branch individually. This schematic provides the possibility of using a different modulation format for each polarization branch. Meanwhile, a polarization controller (PC) inside the comb generator is used to control polarization rotation during one round. If polarization maintaining fiber is used throughout the comb generator, the PC can be omitted. A pre-amplified receiver structure is then implemented. A tunable optical band-pass filter (0.5 nm/62.5 GHz FWHM) is used after the pre-amplifier in order to remove ASE noise from the EDFA. The local oscillator (LO) is a wavelength tunable external cavity laser (ECL) with 100 kHz line-width. In the coherent receiver structure, tuning LO wavelength enables channel selection due to optical heterodyning at the photodiode. The coherent receiver consists of two 90° hybrids and balanced detectors. 40 Gb/s digital sampling oscilloscope

at the coherent receiver is used to sample the inphase and quadrature components. In our experiment, we employed DSP algorithms to compensate for chromatic dispersion (CD), instead of using dispersion compensation fiber (DCF) after 80 km single mode fiber (SMF) transmission. A constant modulus algorithm (CMA) enables polarization rotation compensation; DSP algorithms implement frequency and phase off set removal, QPSK demodulation and bit error detection. Since the sub-channels are spaced at a frequency corresponding to the baud rate, crosstalk and overlap from sub-channels severely affects the BER performance. Therefore we develop a DFE algorithm in DSP to reduce the detrimental effect of ICI.

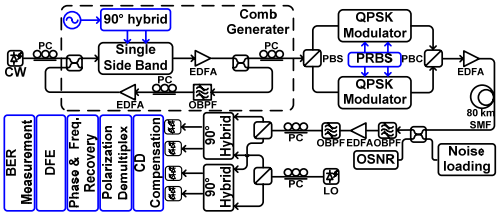

Figure 1. Experiment setup: OBPF, optical band-pass filter; PC, polarization controller; ECL, external cavity laser; PBS, polarization beam splitter; PBC, polarization beam combiner; OSNR, optical SNR monitor.

III. RESULTS AND DISCUSSION

Figure 2 shows the sub-channels signal spectra, Figure 2 (a) shows the signal spectrum after sub-channel generation and Figure 2 (b) shows the signal spectrum after modulation and transmission. To avoid performance degradation, we select sub-channels with tone to noise ratio (TNR) more than 25 dB. The TNR differences between different sub-channels are induced by the loop accumulated ASE noise from EDFA [2]. From Figure 2, we can verify the generation of more than 30 sub-channels in 5 nm (625 GHz) bandwidth from 1545.10 nm to 1550.10 nm; we can generate even more sub-channels with a low noise EDFA to further improve system transmission bit rate. For 25 dB TNR and above, we successfully detect the sub-channels with bit error rate (BER) below the 7% overhead FEC threshold as shown in the Figure 3.

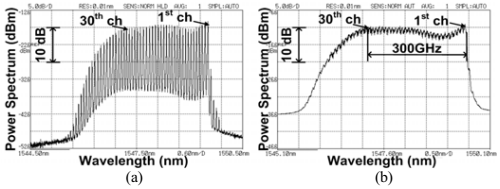

Figure 2. Ultradense WDM signal spectrum for 30 sub-channels. (a) after Comb generator (b) after transmission.

Figure 3 shows the BER performance of the ultradense WDM system with back to back and 80 km SMF transmission using DSP dispersion compensation algorithms. Figure 3 (a) shows the BER performance for back to back of 30 sub-channels. Figure 3 (a) shows the BER performance for all of 30 sub-channels is below the 7% overhead FEC threshold. Variations observed in BER performance across sub-channels are due to differences in the TNR of the different sub-channels. Figure 3 (b) shows the BER performance for 10th sub-channel back to back and 80 km SMF transmission with DSP compensation algorithms. We select one sub-channel (10th sub-channel) from the ultradense WDM signal and measure the ICI penalty. For reference, we show the single channel 40 Gb/s DP QPSK back to back and 80 km SMF transmission BER performance. Figure 3 (b) indicates that after 80 km SMF transmission, DSP compensation algorithms are able to compensate for CD. The BER performance of back to back and 80 km transmission measurement penalty is lower than 0.5 dB. Figure 3 (b) shows the 10th sub-channel BER performance comparison between scenarios with and without DFE after 80km SMF transmission. Since the ultradense WDM sub-channels are spaced exactly at the baud rate, we implement the DFE algorithm to reduce ICI. As a result, from Figure 3 (b), DFE algorithm improves the BER performance by about 2.7 dB.

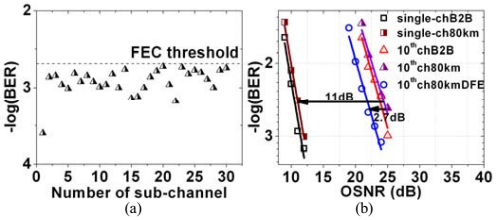

Figure 3. Ultradense WDM signal BER performance for 30 sub-channels. (a) back to back BER performances for 30 sub-channels. (b) ultradense WDM 10th sub-channels BER performance with back to back and 80 km SMF transmission compared with the BER performance of single channel 40 Gb/s DP QPSK system, and ultradense WDM 10th sub-channels transmission BER performance with DFE.

IV. CONCLUSION

We experimentally demonstrate a WDM 30×40 Gb/s DP QPSK achieving 1.2 Tb/s transmission over 80 km SMF for long reach metro-access networking on a bandwidth of 300 GHz. The ultradense WDM sub-channel spacing at exactly the baud rate achieves 4.0 b/s/Hz of SE; DSP algorithms compensate for CD and ICI effects. Our results show that ultradense WDM systems can be realized with higher SE and higher capacity than conventional WDM and are suitable for potential applications in metro-access networking.

REFERENCES

[1] Chongjin Xie and etc, "Hybrid 224-Gb/s and 112-Gb/s DP-QPSK Transmission at 50-GHz Channel Spacing over 1200-km Dispersion-Managed LEAF Spans and 3 ROADMs" OFC 2011 PDPD2.

[2] Yiran Ma and etc, "1-Tb/s Single-Channel Coherent Optical OFDM Transmission With Orthogonal-Band Multiplexing and Subwavelength Bandwidth Access" JLT Vol.28, No.4, February 15, 2010.

[3] Giancarlo Gavioli and etc, "Ultra-Narrow-Spacing 10-Channel 1.12 Tb/s D-WDM Long-Haul Transmission Over Uncompensated SMF and NZDSF" IEEE PTL Vol. 22, No. 19, October 1, 2010.

Paper 6: Radio Over Fiber Link With Adaptive Order n-QAM Optical Phase Modulated OFDM And Digital Coherent Detection

V. Arlunno, R. Borkowski, N. Guerrero Gonzalez, A. Caballero, K. Prince, J. Bevensee Jensen, D. Zibar, K. J. Larsen and I. Tafur Monroy, "Radio Over Fiber Link With Adaptive Order n-QAM Optical Phase Modulated OFDM And Digital Coherent Detection," in *Microwave and Optical Technology Letters*, Vol. 53, No. 10, October 2011

tuning varactor for USPCS/WCDMA/m-WiMAX/WLAN, IEEE Trans Antennas Propag 58 (2010), 2404–2411.
4. T.H. Hsieh and J.S. Row, A reconfigurable design for bandwidth enhancement of circularly polarized slot antennas, Microwave Opt Technol Lett 52 (2010), 1377–1380.
5. R. Raj, B. Poussot, J.-M. Laheurte, and O. Vendier, Pattern reconfiguration of microstrip antenna using flip-chip mounted packaged MEMS, Microwave Opt Technol Lett 52 (2010), 574–577.
6. J.L. Araque Quijano and G. Vecchi, Optimization of an innovative type of compact frequency-reconfigurable antenna, IEEE Trans Antennas Propag 57 (2009), 9–18.
7. U.L. Rohde and D.P. Newkirk, RF/Microwave circuits design for wireless applications, Wiley, New York, 2000.

RADIO OVER FIBER LINK WITH ADAPTIVE ORDER n-QAM OPTICAL PHASE MODULATED OFDM AND DIGITAL COHERENT DETECTION

Valeria Arlunno, Robert Borkowski, Neil Guerrero Gonzalez, Antonio Caballero, Kamau Price, Jesper Bevensee Jensen, Darko Zibar, Knud J. Larsen, and Idelfonso Tafur Monroy
DTU Fotonik, Department of Photonics Engineering, Technical University of Denmark, DK-2800 Kgs. Lygnby, Denmark;
Corresponding author: vaar@fotonik.dtu.dk

Received 21 December 2010

ABSTRACT: *Successful digital coherent demodulation of asynchronous optical phase-modulated adaptive order QAM (4, 16, and 64) orthogonal frequency division multiplexing signals is achieved by a single reconfigurable digital receiver after 78 km of optical deployed fiber transmission.* © 2011 Wiley Periodicals, Inc. Microwave Opt Technol Lett 53:2245–2247, 2011; View this article online at wileyonlinelibrary.com. DOI 10.1002/mop.26274

Key words: *radio over fiber; phase modulation; coherent detection; OFDM*

1. INTRODUCTION

Orthogonal frequency division multiplexing (OFDM) is a promising modulation format for optical communications, as it provides large immunity to chromatic dispersion (CD) and polarization mode dispersion effects and also provides high spectral efficiency [1–3]. This is because OFDM implements a large number of orthogonal radio frequency (RF) subcarriers, each of them having lower symbol rate than the bit rate of the message source [1, 2]. Recently, coherent detection optical OFDM (CO-OFDM) using digital signal processing (DSP) has been proposed as a promising alternative to maximize the spectral/power efficiency by exploiting the advantages of DSP such as linear and nonlinear fiber impairments compensation in the digital domain and software reconfigurability [2, 3].

So far, optical intensity modulation for CO-OFDM has been dominantly used due to its simplicity; however, it suffers from higher sensitivity to fiber nonlinearities due to the relative large peak-to-average power ratio [1]. Optical phase modulation (PM) has the potential to improve robustness to fiber nonlinearities by encoding the information in the optical phase and thus maintaining a constant optical power. Furthermore, optically phase-modulated links can also potentially enable large dynamic range, high capacity, and higher spectral efficiency for transmission of microwave RF signals over optical fiber links [3–6].

In this article, we report on the use of optical PM for CO-OFDM transmission links supported by a reconfigurable DSP receiver that allows for adaptation of the modulation order of the transmitted signal. We demonstrate performance using QAM constellations having 4, 16, and 64 points. We report on experiments using 78 km of single mode fiber (SMF) deployed fiber and 40 km of SMF. For all reported experiments, a bit error rate (BER) value better than 10^{-3} was achieved for all used OFDM subcarriers, complying with the forward error correction limit. Our results demonstrate the transmission robustness of phase-modulated OFDM links and their potential for use in scenarios with need for flexible modulation format assignment to subcarriers.

2. EXPERIMENTAL SETUP

The general outline of the experimental setup for the adaptive order 4-QAM, 16-QAM, and 64-QAM phase-modulated (PM) coherent optical (CO)-OFDM link is shown in Figure 1. The PM CO-4QAM-OFDM signal was transmitted over 78 km of field-deployed fiber, whereas a standard SMF was used for optical transmission of the PM CO-16QAM-OFDM signal.

The baseband adaptive order n-QAM OFDM signal was obtained from a pseudorandom binary sequence of length $2^{15}-1$ bits. In all cases, 256 subcarriers without oversampling were used with 26 samples (10%) cyclic prefix per OFDM symbol. OFDM frame is composed of two Schmidl training symbols [7], followed by eight data symbols. The use of these two training symbols makes receiver independent of transmitter synchronization and allows us to avoid a clock reference for synchronizing

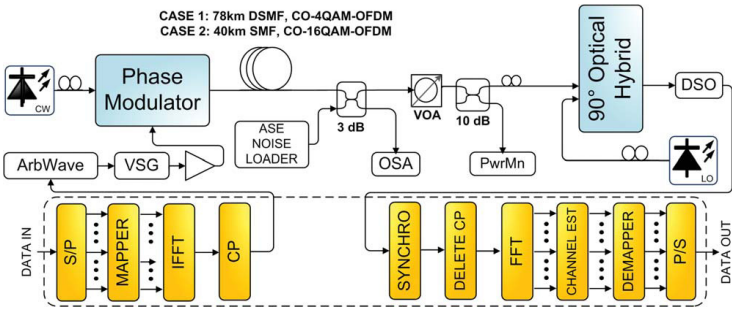

Figure 1 Experiment layout; ArbWave: arbitrary waveform; VSG: vector signal generator; OSA: optical Spectrum Analyzer; PwrMn: power measurement point; DSO: digital sampling oscilloscope. [Color figure can be viewed in the online issue, which is available at wileyonlinelibrary.com]

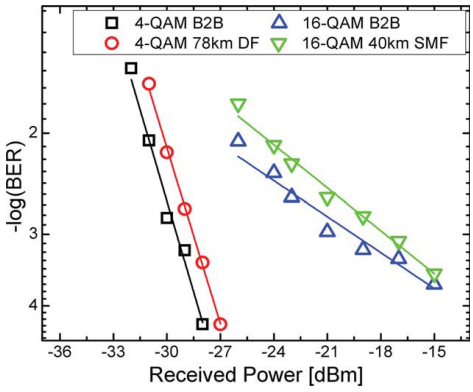

Figure 2 OFDM BER as a function of the Received Optical Power (dBm) for Back to Back and optical transmission; DF: deployed fiber

the arbitrary waveform generator (AWG) and digital storage oscilloscope in our experimental setup.

The software-generated OFDM baseband signal was upsampled by a factor of 5 and fed to a 1.25 GSa/s AWG. Resultant electrical OFDM signal with a bit rate of 0.5 Gb/s for 4-QAM and 1 Gb/s for 16-QAM was upconverted to a carrier frequency of 5 and a 6 GHz, respectively, by using a free-running vector signal generator (VSG). The output power of the VSG was fixed at −25 dBm. Output of the VSG was then amplified to 2 dBm and used to drive an optical phase modulator (PM) supplied with a continuous laser (CW) laser at 1553.78 nm. At the receiver, a 90° optical hybrid was used to mix the received optical data signal with the tunable external cavity local oscillator laser. Samples taken from the sampling scope with a sample rate of 40 GSa/s were processed offline. First, carrier-recovery digital PLL and linear demodulation was performed without any dispersion compensation algorithm. The signal was downconverted to baseband and timing offset estimated using a smoothed Schmidl timing metric followed by a carrier frequency offset estimation algorithm [7]. In contrast to [3], the system presented here is fully asynchronous PM CO-OFDM transmission link, whose receiver and transmitter are not triggered by a common clock signal. The phase offset and amplitude for every channel is corrected by using the training sequence as an equalization reference. A structure typical for an OFDM receiver is then used.

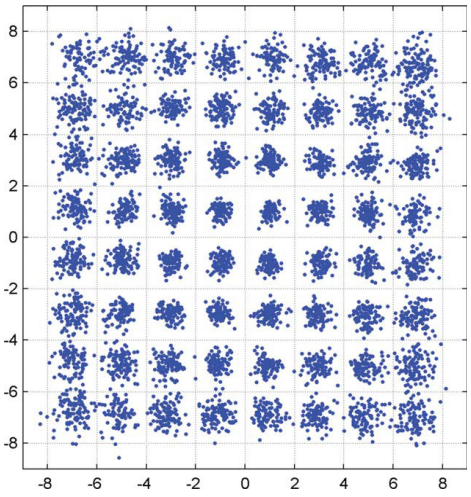

Figure 4 Received OFDM constellation diagrams for all 64-QAM subcarriers superimposed. [Color figure can be viewed in the online issue, which is available at wileyonlinelibrary.com]

In the case of CO adaptive n-QAM OFDM, the generating software has been modified as to support four different modulation formats. Namely, 4-QAM modulation is used on the first subcarrier of every OFDM symbol, 16-QAM on the second, QPSK on the third, and 8-QAM on the fourth; this arrangement is then repeated as to fill all 256 subcarriers in use.

3. EXPERIMENTAL RESULTS

The measured BER performances of the 4-QAM and 16-QAM OFDM signal for the back-to-back (B2B) system and optical

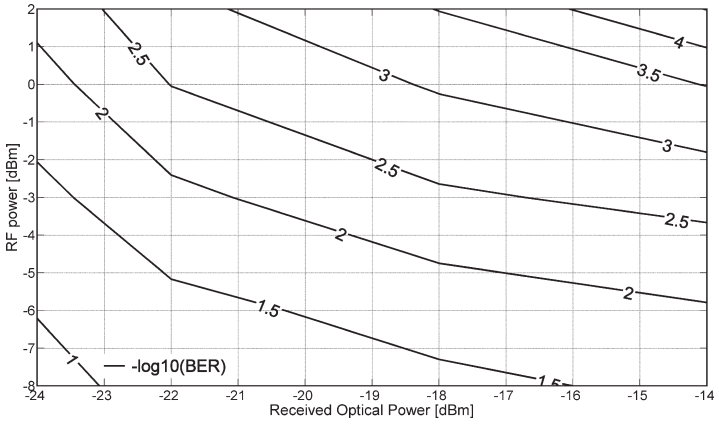

Figure 3 Contour plot RF optical power versus Received Optical Power for 16-QAM OFDM

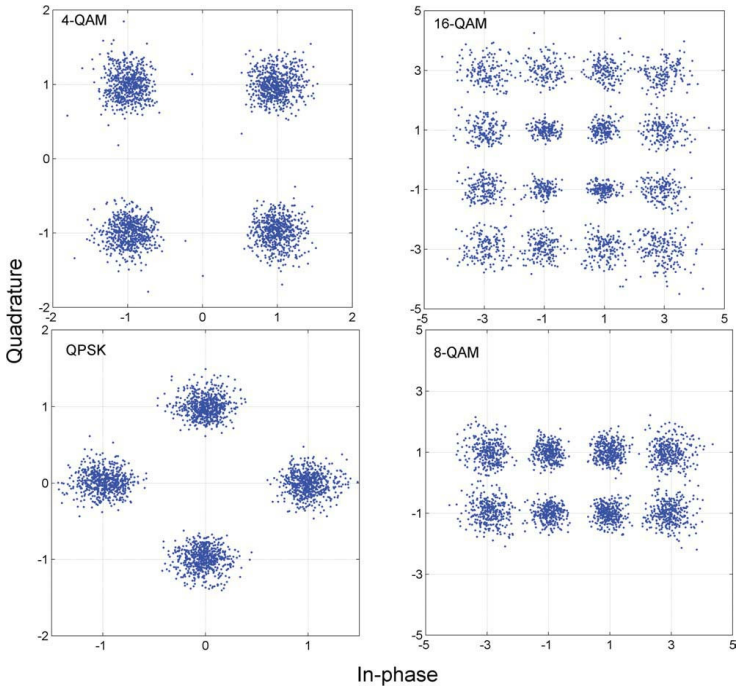

Figure 5 Received OFDM constellation diagrams for the first-fourth subcarriers of the adaptive n-QAM. [Color figure can be viewed in the online issue, which is available at wileyonlinelibrary.com]

link transmission are shown in Figure 2; in the first case, the signal has been transmitted over 78 km of deployed SMF while in the second over 40 km of SMF. As insets, the received constellation diagram of the 250 Mbaud 4-QAM and 16-QAM PM CO-OFDM signal at 10^{-4} BER in B2B configuration are shown; the constellation points look clear and well separated.

Figure 3 is a contour plot showing the relation between the RF output power measured at the output of the VSG and the optical received power at the input of the coherent receiver to obtain specific BER values for B2B CO-16QAM-OFDM. For instance, a BER value at 10^{-4} is measured by setting VSG output power anywhere in the range between 1 and 2 dBm and the optical received power (via a variable optical attenuator) between -16 and -14 dBm. For 16QAM-OFDM [Fig. 2(a)], the RF power was fixed at 2 dBm, corresponding to a modulation index value of 0.36 rad.

Figure 4 shows the constellation diagram for the initial CO-64QAM-OFDM trial with a BER value of 10^{-3}, whereas Figure 5 shows constellation diagrams used for the initial m-QAM CO-OFDM trial with a BER value of 10^{-3}. In the second case, the reported results are obtained for an RF power equal to 2 dBm.

4. CONCLUSIONS

Successful signal demodulation of phase-modulated (PM) coherent optical (CO) 4-QAM and 16-QAM OFDM signals after fiber transmission (78 km of field deployed fiber for 4-QAM and 40 km of SMF for 16-QAM) have been experimentally demonstrated by using a single reconfigurable digital receiver. We also have demonstrated the easy reconfigurability of the implemented digital receiver capable of achieving BER values at 10^{-3} for back-to-back PM CO-64QAM-OFDM and CO adaptive n-QAM OFDM without hardware changes in the experimental setup. Phase-modulated coherent optical OFDM systems are a promising solution for applications in converged wireless/wireline service delivery in optical networking scenarios with reconfigurable digital coherent receivers.

REFERENCES

1. B. Djordjevic and B. Vasic, Orthogonal frequency division multiplexing for high-speed optical transmission, Opt Express 14 (2006).
2. W. Shieh and C. Athaudage, Coherent optical orthogonal frequency division multiplexing, Electron Lett 42, May 2006.
3. Z. Wu, H. Wen, X. Zheng, H. Zhang, and Y. Guo, Phase modulated coherent optical OFDM by phase restoration of optical field, Proc. MWP 2010, TH4–15.
4. T.R. Clark and M.L. Dennis, Coherent optical phase-modulated link, IEEE Photon Technol Lett 19, August 15, 2009.
5. D. Zibar, I. Tafur Monroy, C. Peucheret, L.A. Johansson, J.E. Bowers, and P. Jeppesen, DSP based coherent receiver for phase-modulated radio-over-fibre optical links, Proc. OFC 2008, OThH3.
6. D. Zibar, X. Yu, C. Peucheret, P. Jeppesen, and I. Tafur Monroy, Digital coherent receiver for phase-modulated radio-over-fiber optical links, IEEE Photon Technol Lett 21, February 1, 2009.
7. T.M. Schmidl and D.C. Cox, Robust Frequency and timing synchronization for OFDM, IEEE Transactions on communications, vol. 45, no. 12, December 1997.

Paper 7: Single- and Multiband OFDM Photonic Wireless Links in the 75-110 GHz Band Employing Optical Combs

M. Beltran, L. Deng, X. Pang, X. Zhang, V. Arlunno, Y. Zhao, X. Yu, R. Llorente, D. Liu, and I. Tafur Monroy "Single- and Multiband OFDM Photonic Wireless Links in the 75-110 GHz Band Employing Optical Combs," in *IEEE Photonics journal*, Volume 4, Number 5, October 2012

IEEE Photonics Journal
An IEEE Photonics Society Publication

Open Access

Single- and Multiband OFDM Photonic Wireless Links in the 75–110 GHz Band Employing Optical Combs

Volume 4, Number 5, October 2012

M. Beltrán, Member, IEEE
L. Deng, Student Member, IEEE
X. Pang
X. Zhang
V. Arlunno
Y. Zhao
X. Yu, Member, IEEE
R. Llorente, Member, IEEE
D. Liu
I. Tafur Monroy, Member, IEEE

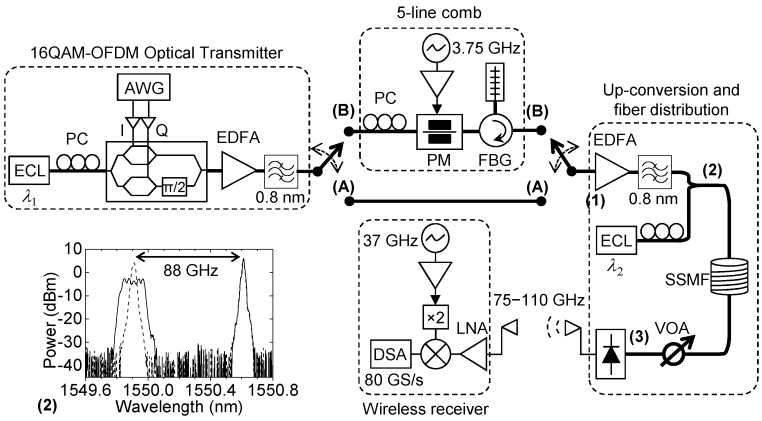

DOI: 10.1109/JPHOT.2012.2223205
1943-0655/$31.00 ©2012 IEEE

Single- and Multiband OFDM Photonic Wireless Links in the 75−110 GHz Band Employing Optical Combs

M. Beltrán,[1] *Member, IEEE*, L. Deng,[2] *Student Member, IEEE*, X. Pang,[3] X. Zhang,[3] V. Arlunno,[3] Y. Zhao,[3] X. Yu,[3] *Member, IEEE*, R. Llorente,[1] *Member, IEEE*, D. Liu,[2] and I. Tafur Monroy,[3] *Member, IEEE*

[1]Valencia Nanophotonics Technology Center, Universidad Politécnica de Valencia, 46022 Valencia, Spain
[2]College of Optoelectronics Science and Engineering, HuaZhong University of Science and Technology, Wuhan 430074, China
[3]DTU Fotonik, Department of Photonics Engineering, Technical University of Denmark, 2800 Kgs. Lyngby, Denmark

DOI: 10.1109/JPHOT.2012.2223205
1943-0655/$31.00 ©2012 IEEE

Manuscript received September 28, 2012; accepted October 3, 2012. Date of publication October 9, 2012; Date of current version October 18, 2012. This work was supported in part by the European Commission through the Seventh Framework Program (FP7) ICT-249142 FIVER Project, by the Spain Plan Nacional I+D+I project TEC2009-14250 ULTRADEF, by the National 863 Program of China under Grant 2009AA01A347, by Tektronix, Agilent Technologies, Radiometer Physics GmbH, Rohde&Schwarz, and u^{2}t Photonics, and by the Danish Project OPSCODER. Corresponding author: M. Beltrán (e-mail: mbeltran@ntc.upv.es).

Abstract: The photonic generation of electrical orthogonal frequency-division multiplexing (OFDM) modulated wireless signals in the 75−110 GHz band is experimentally demonstrated employing in-phase/quadrature electrooptical modulation and optical heterodyn upconversion. The wireless transmission of 16-quadrature-amplitude-modulation OFDM signals is demonstrated with a bit error rate performance within the forward error correction limits. Signals of 19.1 Gb/s in 6.3-GHz bandwidth are transmitted over up to 1.3-m wireless distance. Optical comb generation is further employed to support different channels, allowing the cost and energy efficiency of the system to be increased and supporting different users in the system. Four channels at 9.6 Gb/s/ch in 14.4-GHz bandwidth are generated and transmitted over up to 1.3-m wireless distance. The transmission of a 9.6-Gb/s single-channel signal occupying 3.2-GHz bandwidth over 22.8 km of standard single-mode fiber and 0.6 m of wireless distance is also demonstrated in the multiband system.

Index Terms: Microwave photonics signal processing, frequency combs, heterodyning, fiber optics systems, orthogonal frequency division multiplexing.

1. Introduction

Wireless communication links supporting very high capacity are required to provide access network services such as 10-gigabit Ethernet (10 Gb/s), Super Hi-Vision (SHV)/Ultra High Definition (UHD) TV data (> 24 Gb/s), OC-768/STM-256 data (43 Gb/s), and 100-gigabit Ethernet (100 Gb/s), and also for close-proximity bulk data transfer [1]. Millimeter-wave wireless systems at around 60 GHz and higher frequencies can provide bandwidth enough to easily support multi-Gb/s communications, being a potential solution for future seamless integrated optical/wireless access, as well as for mobile backhauling [2]. The 60-GHz band has been widely studied as a wide bandwidth has been regulated in many countries for unlicensed use with a high equivalent isotropic radiated power

TABLE 1

Photonic Wireless Systems in the 75−110 GHz Band (MLL: Mode-locked laser, NBUTC-PD: Near-ballistic uni-travelling-carrier photodiode, IQ: In-phase/quadrature electrooptical modulator, DP-QPSK: Dual-polarization QPSK modulator, MZM: Mach–Zehnder modulator)

Mod. format	Data rate (Gb/s)	Frequency range (GHz)	Fiber length (km)	Wireless distance (m)	Technology		Ref.
					Transmitter	Receiver	
OOK	20 BER<10^{-12}	85.5–100.5	25	0.2	MLL+NBUTC-PD	Power detector	[10]
Optical QPSK-OFDM	40 BER<10^{-2}	70–95	–	–	MZM comb+IQ+ECL heterodyning	Optical detection	[13]
16-QAM	40 BER<$2{\cdot}10^{-3}$	82.5–102.5	–	0.03	Two-tone optical generator+DP-QPSK +UTC-PD	Electrical heterodyne	[11]
16-QAM PolMux	100 BER<$2{\cdot}10^{-3}$	75–100	–	1.2	IQ+ECL heterodyning	Electrical heterodyne	[12]
Three-band QPSK-OFDM	8.3 /ch BER<$2{\cdot}10^{-3}$	79.25–94.25	22.8 0.01	0.5 2	MZM comb+IQ+ECL heterodyning	Electrical heterodyne	[22]
Three-band 16-QAM-OFDM	15.1 /ch BER<$2{\cdot}10^{-3}$	78.5–93.5	0.01	0.6	IQ+MZM comb+ECL heterodyning	Electrical heterodyne	[23]
16-QAM-OFDM	19.1 BER<$2{\cdot}10^{-3}$	77.4–83.8	0.01	1.3	IQ+ECL heterodyning	Electrical heterodyne	This work
Four-band 16-QAM-OFDM	9.6 /ch BER<$2{\cdot}10^{-3}$	78.9–93.3	0.01	1.3	IQ+PM comb+ECL heterodyning	Electrical heterodyne	This work

(EIRP) of higher than 40 dBm allowed [3]. A number of standards in the 60-GHz band have recently been proposed, including WirelessHD, ECMA-387, IEEE 802.15.3c, and WiGig. These technologies target to provide up to 7-Gb/s data rates at short-range indoor wireless distances of up to 10 m. Standard devices of 60 GHz are also available for wireless display connectivity, for HD audio/video streaming from the consumer electronics, personal computing, and portable devices to HDTVs. In addition, other higher frequency millimeter-wave bands can potentially offer larger bandwidths to support higher capacities, as well as lower atmospheric loss to extend wireless transmission distances as compared to the 60-GHz band [4]. Of particular interest, the 71−76/81−86 GHz paired band has been allocated for commercial use in the United States, Europe, and other countries, and permits point-to-point communications over distances of several kilometers. Commercial equipment is easily available in the 71−76/81−86 GHz band supporting 1.25-Gb/s Gigabit Ethernet connectivity. Electronic-based millimeter-wave wireless links at frequencies higher than 100 GHz have also been demonstrated providing up to 20 Gb/s with polarization multiplexing (PolMux) over the kilometer distance [5].

Radio-over-fiber technology combined with millimeter-wave wireless systems is seen as a fast deployable and cost-effective solution for providing seamless integrated optical/wireless access at $>$ 10 Gb/s [2]. Radio-over-fiber systems operating within 7-GHz bandwidth in the 60-GHz band have been reported to provide capacities higher than 10 Gb/s when spectrally efficient electrical orthogonal frequency-division multiplexing (OFDM) modulation based on quadrature amplitude modulation (QAM) and electrooptical modulation for upconversion are employed, such as 27 Gb/s for 2.5-m wireless distance employing 16-QAM-OFDM [6], 21 Gb/s for 500-m standard single-mode fiber (SSMF) transmission and 10-m (or 2.5 m in bidirectional system) wireless transmission employing 8-QAM-OFDM [7], 26.5 Gb/s for 100-km SSMF and 3-m wireless distance employing adaptive-level QAM-OFDM in amplified long-reach networks [8], and 50 Gb/s for 4-m wireless distance employing 16-QAM-OFDM and multiple-input multiple-output (MIMO) spatial multiplexing [9]. In addition, radio-over-fiber systems in the 75−110 GHz band (W-band) are recently attracting increasing interest to deliver 40 Gb/s and beyond. A number of photonic wireless transmission systems in the 75−110 GHz band have been demonstrated, as summarized in Table 1. A system providing error-free 20 Gb/s with on–off keying (OOK) modulation and simple RF power detection has

been demonstrated including 25 km of fiber transmission [10]. Spectral efficient modulation formats have also been employed, at 20 Gb/s and 40 Gb/s based on quadrature phase-shift keying (QPSK) and 16-QAM formats, respectively [11], and up to 100 Gb/s based on 16-QAM with PolMux [12]. A system based on optical OFDM with optical detection has also been demonstrated [13]. For fixed wireless access over the kilometer distance, photonic wireless links in the 75−110 GHz band have been reported at $<$ 10 Gb/s employing differential phase-shift keying modulation [14]. Finally, millimeter-wave systems operating at frequencies higher than 110 GHz based on photonic generation have been demonstrated to provide error-free $>$ 20 Gb/s at 300 GHz with OOK modulation [5].

Photonic millimeter-wave wireless links have been reported using the wide RF bandwidth in a single channel. A different approach is to allocate multiple channels of lower data rate signals to serve different users in the system. The multiband approach also enables flexible bandwidth allocation by aggregating channels, thus relaxing the power and bandwidth requirements of electrooptical equipment such as digital-to-analog/analog-to-digital converters (DAC/ADC) for energy-efficient and cost-effective systems. Combined optical access and wireless transmission of multiband OFDM-based signals in the 60-GHz band has been demonstrated based on subcarrier multiplexing (SCM) [3]. Wavelength division multiplexing (WDM) architectures can also be employed, where multiple wavelengths produced by an optical frequency comb or by a continuous-wave laser array support the different channels [15].

A number of approaches have been demonstrated for optical comb generation. Mode-locked lasers provide stable and sharp spectral components over a wide bandwidth with low noise qualities. In addition, optical frequency combs based on electrooptic modulators driven by large-amplitude sinusoidal signals permit arbitrary wavelength spacing by adjusting the frequency of the sinusoidal signals [16]–[18]. Although this technique can provide a relatively flat optical comb, it can be limited by the insertion loss of the modulator together with the modulation efficiency. Finally, gain-switched pulsed lasers can be employed for simple and cost-efficient multicarrier generation [19]. Additionally, the number of comb wavelengths can be increased without influencing optical bandwidth by applying an adequate time-domain periodic multiphase modulation on the laser pulse train [20].

In this paper, we experimentally demonstrate the optical generation, wireless transmission, and electrical heterodyn detection of multiband OFDM-based wireless signals in the 75−110 GHz band. The proposed system has the following advantages: 1) Electrical OFDM modulation with a high number of subcarriers has been widely used in optical and wireless communications systems to benefit from its high spectral efficiency, flexibility, and robustness against fiber dispersion impairments and wireless multipath fading [3], [21]. 2) Seamless allocation of multiple channels in the wide RF bandwidth is demonstrated enabled by optical comb generation [22]. 3) Optical heterodyn mixing enables seamless optical frequency upconversion, highly scalable in RF frequency [13]. The phase and frequency drift originated from the wireless signal generation, and detection is compensated by baseband digital signal processing (DSP) at the receiver, thus avoiding the need for phase-locking techniques. Based on this approach, we have demonstrated the combined SSMF and wireless transmission of a three-channel QPSK-OFDM signal at 8.3 Gb/s/ch with a bandwidth of 5 GHz/ch (15-GHz total RF bandwidth) [22], as summarized in Table 1. The wireless transmission of three-channel signals has also been demonstrated employing 16-QAM-OFDM [23], as summarized in Table 1. In this paper, the wireless transmission of four-channel 16-QAM-OFDM signals [24] is compared with that of the signal generated in a single-band system, with a bit error rate (BER) performance within the standard forward error correction (FEC) limit of $2 \cdot 10^{-3}$, as summarized in Table 1. After removing the 7% overhead for FEC, the effective data rates are 17.8 Gb/s and 8.9 Gb/s/ch with a spectral efficiency of 2.8 b/s/Hz and 2.8 b/s/Hz/ch, respectively.

2. Theoretical Description

Considering the line-of-sight (LOS) case in the wireless link, the signal-to-noise ratio (SNR) at the receiver side can be calculated in dB using the link power budget equation [25]

$$\mathrm{SNR} = P_T + G_T + G_R - L_{FS} - L_I - (N_o + 10\log(B) + NF) \tag{1}$$

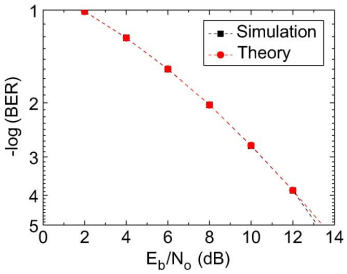

Fig. 1. Bit error probability curve for 16-QAM-OFDM in AWGN.

where P_T is the transmitter power, G_T and G_R are the transmitter and receiver antenna gain, respectively, I_L is the implementation loss of the link, N_0 is the thermal noise in 1 Hz of bandwidth, B is the system bandwidth, and NF is the noise figure of the receiver. L_{FS} represents the free space loss as given by $L_{FS} = 20\log(4\pi fd/c)$, where c is the light speed, f is the signal frequency, and d is the wireless distance in the far field.

For link budget analysis, the most important aspect of a given modulation technique is the SNR necessary for a receiver to achieve a specified level of reliability in terms of BER. BER is a function of the energy per bit relative to the noise power E_b/N_o. In the additive white Gaussian noise (AWGN) channel, single carrier and OFDM have approximately the same performance in terms of E_b/N_o, and the theoretical BER of 16-QAM-OFDM is shown in Fig. 1 [25]. The corresponding curve simulated for the 16-QAM-OFDM signal employed in the experimental work exhibits slight differences with the theoretical curve, as shown in Fig. 1. Note that E_b/N_o is independent of the system data rate R_b. SNR and E_b/N_o can be related by

$$\text{SNR} = (E_b/N_o) \cdot (R_b/B). \tag{2}$$

In addition, considering the resistance load and the responsivity of the photodetector employed in the experimental work, P_T can be related to the received optical power P_{opt} by

$$P_T(\text{dBm}) = 2P_{\text{opt}}(\text{dBm}) - 22. \tag{3}$$

3. Experimental Setup

Fig. 2 shows the schematic of the experimental setup. At the optical OFDM transmitter, a baseband OFDM signal is generated employing a two-channel arbitrary waveform generator (Tektronix AWG7122C) and in-phase/quadrature (IQ) electrooptical modulation. The OFDM signal comprises a data stream consisting of a pseudorandom bit sequence (PRBS) of length $2^{15} - 1$ mapped onto 72 16-QAM subcarriers, which, together with eight pilot subcarriers, one zero power dc subcarrier, and 47 zero-power edge subcarriers, are converted to the time domain via an inverse fast Fourier transform (IFFT) of size 128. A cyclic prefix of length 13 samples is employed, resulting in an OFDM symbol size of 141. To facilitate OFDM frame synchronization and channel estimation, ten training symbols are inserted at the beginning of each OFDM frame that contains 150 data symbols. The real and imaginary parts of the complex OFDM signal are clipped and converted to analog signals at the outputs of the AWG. The two filtered signals are amplified and applied to an IQ modulator connected to an external-cavity laser (ECL) at $\lambda_1 = 1549.9$ nm with 100-kHz linewidth. The IQ modulator reduces to half the bandwidth requirement of the DAC, although it introduces high transmission loss as it is biased at the minimum transmission point. In this way, an optical OFDM signal is generated, which is amplified by an erbium-doped fiber amplifier (EDFA). An optical bandpass filter with 0.8-nm bandwidth is employed to filter noise.

The optical OFDM signal is expanded by optical comb generation based on an electrooptic phase modulator (PM) [16] to form five OFDM channels. The output from the comb is further filtered by a

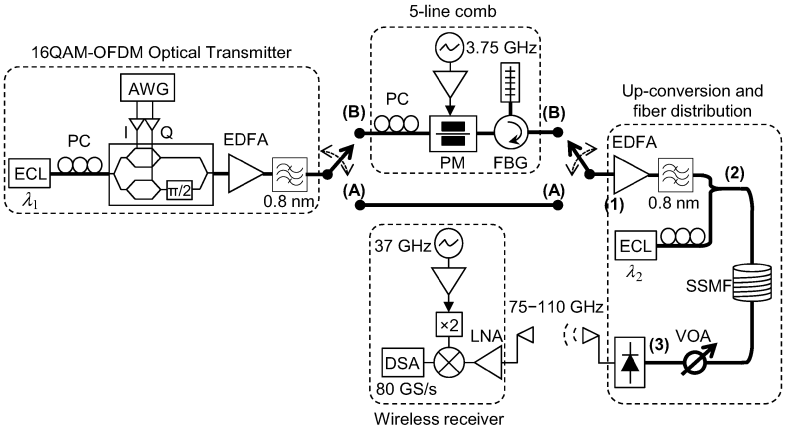

Fig. 2. Experimental setup of an OFDM photonic wireless system in the 75–110 GHz band. Configuration (A): single-band system. Configuration (B): multiband system employing optical comb generation. PC: Polarization controller, VOA: Variable optical attenuator.

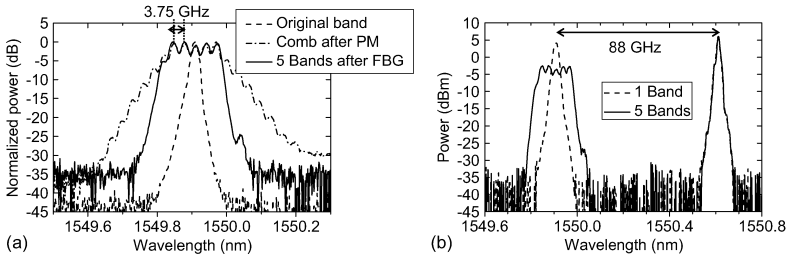

Fig. 3. (a) Optical spectra measured at various points in Fig. 2. (b) Optical spectra measured at point (2) in Fig. 2. (Resolution bandwidth: 0.01 nm).

fiber Bragg grating (FBG) with 25-GHz bandwidth operating in reflection to reduce crosstalk penalty from the edge comb lines, as shown in Fig. 3(a). The comb wavelength spacing is set to 3.75 GHz to minimize crosstalk penalty while maximizing spectral efficiency. It should be noted that the optical comb repeats the same OFDM signal. The effect of crosstalk when independent data bit streams are coded for each OFDM channel should be further investigated for the application in reality. This could be done by using different optical carriers and modulate each of them in a different I/Q modulator by each OFDM data signal. The modulated optical carriers would then be optically combined to generate an optical multiband OFDM signal, as shown in [15]. Decorrelation of adjacent channels at least has usually been considered for emulation of a real system, e.g., by employing frequency shifting and optical delay [21] or two modulators for odd and even channels [15].

To perform optical frequency upconversion, the optical OFDM signal at point (1) in Fig. 2 is amplified and combined with an unmodulated continuous-wave optical carrier from an ECL with 100-kHz linewidth at λ_2 located at the desired RF carrier apart. Fig. 3(b) shows the spectrum of the combined signal at point (2) in Fig. 2. The combined signal is transmitted over fiber to a remote antenna site where the optical ODFM signal and the unmodulated carrier are heterodyn mixed in a 100-GHz photodetector (u^2t Photonics, XPDV4120R). The photodetected signal is an OFDM signal

at the desired RF carrier in the 75−110 GHz band, which is fed to a rectangular horn antenna in the 75−110 GHz band with 24-dBi gain.

After wireless transmission, the RF OFDM signal is received by a similar antenna with 25-dBi gain and amplified by a low-noise amplifier (LNA; Radiometer Physics, 75−105 GHz) with 25-dB gain. An electrical mixer (75−110 GHz RF and 1−36 GHz IF) driven by a local oscillator (LO) signal at 74 GHz is employed for frequency downconversion. The LO signal is generated by frequency doubling a 37-GHz signal from a signal generator (Rohde&Schwarz, SMF100A). The downconverted signal is digitized by a digital signal analyzer at 80 GS/s with 32-GHz real-time bandwidth (Agilent, DSAX93204A) and demodulated by offline DSP.

In the receiver DSP, each OFDM channel is demodulated individually after frequency downconversion and low-pass filtering (LPF). For each baseband OFDM channel, time synchronization, frequency and channel estimation, pilot-assisted phase estimation, data recovery by symbol mapping and serialization, and BER test are performed. To mitigate the dispersion and nonlinearity effects induced by fiber and wireless transmission, one-tap equalizer and an effective algorithm combining intrasymbol frequency-domain averaging [26] and digital phase-locked loop are employed for channel estimation. The effect of the algorithm can be observed in the constellation diagrams in [23]. The pilot-assisted phase estimation consists of estimating the common phase error due to the laser phase noise, as described in [27]. BER is evaluated by counting the number of errors considering 42 912 bits. Note that the frequency/phase estimation algorithm (frequency and channel estimation and pilot-assisted phase estimation) can track the frequency jitter of the ECL lasers provided that a maximum frequency offset is not exceeded; otherwise, advanced algorithms may be employed [13].

4. Transmission Performance

The feasibility of the photonic generation and wireless transmission of 16-QAM-OFDM signals in the 75–110 GHz band has been evaluated. The performance of single-band signals generated by IQ modulation and optical heterodyn upconversion, configuration (A) in Fig. 2 is first evaluated. Wireless transmission performance is further evaluated when the RF bandwidth is used in multiple channels employing optical comb generation, configuration (B) in Fig. 2. The performance of the single-channel signal in the multiband system when the RF signal driving the PM in Fig. 2 is off is also evaluated.

4.1. Single-Band System

In the single-band system, configuration (A) in Fig. 2, the AWG operates at 10 GS/s, resulting in an optical OFDM signal at 19.14 Gb/s $(10\ \text{GS/s} \cdot \log_2(16) \cdot 72/141 \cdot 150/160)$ with a bandwidth of 6.328 GHz $(10\ \text{GS/s} \cdot 81/128)$. Two antialiasing LPF with 3.4-GHz bandwidth are employed at the AWG outputs. The RF carrier frequency is set at 80.6 GHz by tuning λ_2 in Fig. 2.

Fig. 4(a) shows the BER performance of the 19.14-Gb/s single-band 16-QAM-OFDM signal as a function of the received optical power at point (3) in Fig. 2 for different wireless transmission distances compared with the theoretical slope for 16-QAM-OFDM in AWGN. The receiver sensitivities at the FEC limit of $2 \cdot 10^{-3}$ are −2.1 dBm, −0.7 dBm, and 1.7 dBm for 0.5 m, 0.75 m, and 1.3 m of wireless distance, respectively. Fig. 4(b) shows received constellations confirming the BER performance shown in Fig. 4(a). The electrical spectrum of the 19.14-Gb/s signal after digitization at the receiver is shown in Fig. 4(c).

The difference in the receiver sensitivity at 0.5 m and 0.75 m or at 0.75 m and 1.3 m is near the theoretical values of 1.75 dB or 2.4 dB, respectively. From (1) and (3), the difference in the received optical power P_{opt} required for a given BER at different wireless distance due to the increased free space loss L_{FS} is given by $\Delta P_{\text{opt}} = \Delta L_{FS}/2$. In addition, the signal does not exhibit an apparent BER floor, and it is not expected to be significantly limited by the residual phase error after pilot-assisted phase estimation considering an estimated phase error variance of 0.0179 rad^2 for a combined laser linewidth of 200 kHz and a symbol rate of 70.2 MSymbol/s [28].

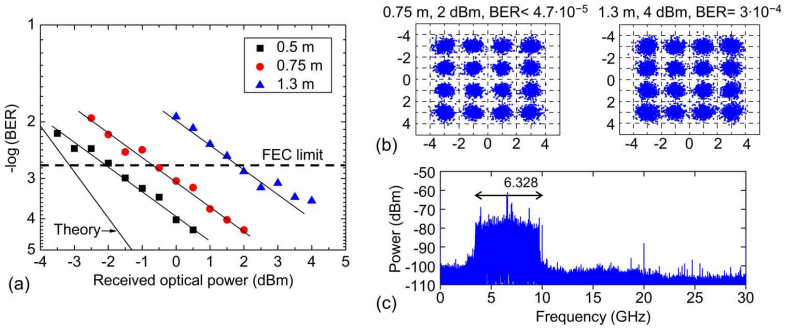

Fig. 4. (a) BER performance of the 19.14 Gb/s single-band system, configuration (A) in Fig. 2, as a function of the received optical power and wireless distance. (b) Constellation diagrams. (c) Electrical spectrum after digitization at the receiver at 2 dBm received optical power and 0.75 m wireless distance.

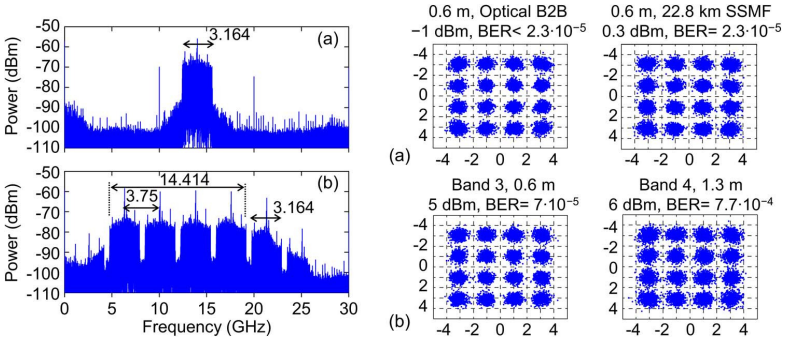

Fig. 5. Electrical spectra after digitization at the receiver at 4.5 dBm received optical power for optical B2B and 0.6 m wireless distance, and constellation diagrams, for configuration (B) in Fig. 2. (a) 9.57 Gb/s single-band OFDM signal. (b) 9.57 Gb/s/ch four-band OFDM signal.

4.2. Multiband System

In the multiband system, configuration (B) in Fig. 2, the AWG operates at 5 GS/s, resulting in an optical OFDM signal at 9.57 Gb/s $(5\ \text{GS/s} \cdot \log_2(16) \cdot 72/141 \cdot 150/160)$ with a bandwidth of 3.164 GHz $(5\ \text{GS/s} \cdot 81/128)$. Two antialiasing LPF with 2.5-GHz bandwidth are employed at the AWG outputs. The RF carrier frequency is set at 88 GHz by tuning λ_2 in Fig. 2.

Up to four RF OFDM bands out of the five optical OFDM bands can be demodulated within the FEC limits due to the frequency response of the photodetector. BER performance of the four OFDM channels at 9.57 Gb/s/ch has been evaluated and compared with the performance of the 9.57-Gb/s single-band OFDM signal. The performance of the single-band OFDM signal is evaluated when the RF signal driving the PM in Fig. 2 is off. Fig. 5 shows the electrical spectra of the single- and four-band OFDM signals after digitization at the receiver. Received constellations are also shown in Fig. 5, confirming the BER performance shown in Fig. 6. Fig. 6 shows the measured BER as a function of the received optical power at point (3) in Fig. 2. Fig. 6(a) shows BER performance of the 9.57-Gb/s single-band 16-QAM-OFDM signal for combined optical and wireless transmission compared with the theoretical slope for 16-QAM-OFDM in AWGN. The receiver sensitivity at the FEC limit of $2 \cdot 10^{-3}$ is -4.2 dBm and -0.6 dBm for optical back-to-back (B2B) and 0.6 m and 1.3 m

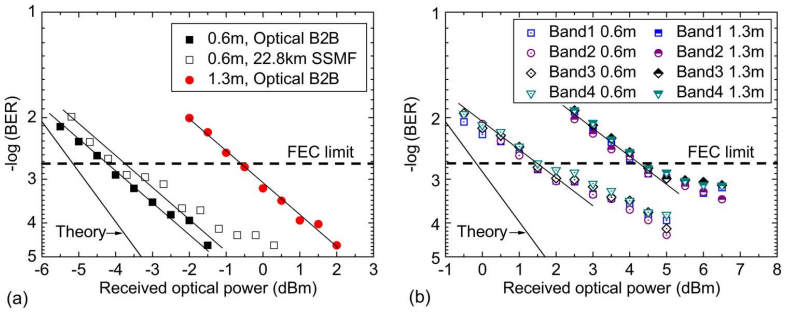

Fig. 6. BER performance of the multiband system, configuration (B) in Fig. 2, as a function of received optical power. (a) 9.57 Gb/s single-band OFDM signal as a function of optical and wireless transmission distance. (b) 9.57 Gb/s/ch four-band OFDM signal as a function of wireless distance for optical B2B.

of wireless distance, respectively. As compared with the 9.57-Gb/s single-band OFDM signal in Fig. 6(a), the 19.14-Gb/s single-band OFDM signal in Fig. 4(a) exhibits 2.7-dB and 2.3-dB penalty in receiver sensitivity, respectively. Theoretically, it is expected that the single-band OFDM signal in Fig. 4(a) at twice the data rate and bandwidth have a near 1.5-dB receiver sensitivity penalty compared with the single-band OFDM signal in Fig. 6(a), as given by $10\log(2)/2$ from (1), (2), and (3). The difference between theory and experiment may be mainly ascribed to the higher optical SNR penalty due to residual laser phase noise, which is expected for the lower symbol rate signal in Fig. 6(a) with an estimated phase error variance of 0.0358 rad^2 [28]. The BER curves in Figs. 4(a) and 6(a) have similar slopes. In addition, optical transmission over 22.8 km of SSMF induces 0.4-dB receiver sensitivity penalty for 0.6-m wireless distance. BER is degraded for received optical power higher than 0.3 dBm due to fiber nonlinearity, corresponding to an optical power of 5.8 dBm at the input of the fiber. The fiber nonlinearity is the reason that the BER is not below the FEC limit for combined 22.8-km SSMF and 1.3-m wireless distance.

Fig. 6(b) shows the wireless transmission performance of the four OFDM bands for optical B2B compared with the theoretical slope for 16-QAM-OFDM in AWGN. There is negligible power penalty among the different OFDM bands when one OFDM subcarrier in the second band is removed during BER evaluation. The receiver sensitivity at the FEC limit of $2 \cdot 10^{-3}$ is 1.5 dBm and 4.3 dBm for 0.6 m and 1.3 m of wireless distance, respectively. The optical comb reduces the optical SNR; the maximum power spectral density decreases by 6.6−7.6 dB, as shown in Fig. 3(b), thus inducing a receiver sensitivity penalty of 5.7 dB and 4.9 dB for 0.6 m and 1.3 m of wireless distance, respectively. The four-band BER in Fig. 6(b) slope more gradually with received optical power than the single-band BER in Fig. 6(a) due to the increased optical noise. Although the SNR is dominated by electrical noise, decreasing the received optical power increases the BER, the optical noise affects performance. Reducing the channel spacing would increase the optical noise, thus reducing the slope, as shown in [23]. Furthermore, BER is degraded for received optical power higher than 5 dBm and 6 dBm due to receiver saturation. In addition, although it is expected that BER is degraded due to fiber nonlinearity from a higher received optical power for the multiband OFDM signal compared with the single-band OFDM signal [23], the BER is not below the FEC limit for combined 22.8-km SSMF and 0.6- or 1.3-m wireless distance.

Fig. 6 also indicates that the required received optical power to achieve BER $< 2 \cdot 10^{-3}$ is up to 5 dBm, corresponding to a maximum transmitter power of −12 dBm and a maximum EIRP of 12 dBm. The received RF power is approximately −36 dBm and −36.5 dBm for 2-dBm and 5-dBm received optical power at 0.6 m and 1.3 m of wireless distance, respectively. The wireless distance could be extended by employing a W-band high-power amplifier at the transmitter and a higher gain LNA at the receiver side.

As expected, the difference in the receiver sensitivity at 0.6 m and 1.3 m in Fig. 6(a) and in Fig. 6(b) is near 3.4 dB, as given by $\Delta P_{\text{opt}} = \Delta L_{FS}/2$.

The herein demonstrated system supports four channels in 14.4-GHz total bandwidth with 4.3-dBm receiver optical sensitivity for 1.3-m wireless distance as compared with three channels in 11.2-GHz or 9.4-GHz total bandwidth with 2.8 dBm or 3.2 dBm, respectively [23].

The demonstrated single-band transmission could be suitable for delivering 10-Gigabit Ethernet signals [see Fig. 6(a)] or UHDTV signals [see Fig. 4(a)] to a single user. Although with higher complexity and lower performance, the multiband system [see Fig. 6(b)] could be suitable for providing multiuser or higher capacity access, e.g., up to four 10-Gigabit Ethernet users and up to two UHDTV users or one OC-768/STM-256 user by aggregating channels.

5. Conclusion

The photonic generation and wireless transmission of electrical 16-QAM-OFDM signals in the 75−110 GHz band has been experimentally demonstrated using a single RF band and when the RF bandwidth is used in multiple channels. A single-band system at 17.8-Gb/s effective data rate in 6.3-GHz bandwidth has been demonstrated up to 1.3 m of wireless distance. This signal exhibits up to 2.7-dB penalty in receiver optical sensitivity as compared with a single band at 8.9 Gb/s effective data rate in 3.2-GHz bandwidth in a system supporting multiband generation. The transmission of the 8.9-Gb/s signal over combined 22.8-km SSMF and 0.6-m wireless distance has also been demonstrated. The transmission of up to four channels at an effective data rate of 8.9 Gb/s/ch in 14.4-GHz bandwidth has been demonstrated up to 1.3 m of wireless distance employing an optical comb. The proposed multiband radio-over-fiber approach can provide a cost- and power-efficient solution for high-capacity hybrid wireless/optical links supporting multiple users with flexible bandwidth allocation.

References

[1] T. Nagatsuma, T. Takada, H.-J. Song, K. Ajito, N. Kukutsu, and Y. Kado, "Millimeter- and THz-wave photonics towards 100-Gb/s wireless transmission," in *Proc. IEEE 23rd Annu. Meet. Photon. Soc.*, 2010, pp. 385–386.

[2] A. Stöhr, "10 Gb/s wireless transmission using millimeter-wave over optical fiber systems," presented at the Proc. Opt. Fiber Commun. Conf., Los Angeles, CA, 2011, Paper OTuO3.

[3] M. Beltrán, J. B. Jensen, X. Yu, R. Llorente, R. Rodes, M. Ortsiefer, C. Neumeyr, and I. Tafur Monroy, "Performance of a 60-GHz DCM-OFDM and BPSK-impulse ultra-wideband system with radio-over-fiber and wireless transmission employing a directly-modulated VCSEL," *IEEE J. Sel. Areas Commun.*, vol. 29, no. 6, pp. 1295–1303, Jun. 2011.

[4] J. Wells, "Faster than fiber: The future of multi-Gb/s wireless," *IEEE Microw. Mag.*, vol. 10, no. 3, pp. 104–112, May 2009.

[5] T. Nagatsuma, "Photonic generation of millimeter waves and its applications," presented at the Proc. Opt. Fiber Commun. Conf., Los Angeles, CA, 2012, Paper OM2B.7.

[6] M. Weiss, A. Stöhr, F. Lecoche, and B. Charbonnier, "27 Gb/s photonic wireless 60 GHz transmission system using 16-QAM OFDM," *Proc. Int. Top. Meet. Microw. Photon.*, pp. 1–3, 2009.

[7] P.-T. Shih, A. Ngoma, C.-T. Lin, F. Annunziata, J. Chen, J. George, M. Sauer, and S. Chi, "2 × 21 Gbps symmetrical full-duplex transmission of OFDM wireless signals over a bidirectional IMDD radio-over-fiber system at 60 GHz," presented at the Proc. Eur. Conf. Opt. Commun., Torino, Italy, 2010, Paper Th.9.B.4.

[8] C. Wei, C. Lin, M. Chao, W. Jiang, and C. Ho, "Long-reach 26.54-Gbps OFDM RoF system at 60 GHz over 100-km fiber and 3-m wireless transmission employing phase noise compensation and bit-loading algorithms," presented at the Proc. Eur. Conf. Opt. Commun., Geneva, Switzerland, 2011, Paper We.7.C.5.

[9] C.-H. Ho, R. Sambaraju, W.-J. Jiang, T. H. Lu, C.-Y. Wang, H. Yang, W.-Y. Lee, C.-T. Lin, C.-C. Wei, S. Chi, and A. Ng'oma, "50-Gb/s radio-over-fiber system employing MIMO and OFDM modulation at 60 GHz," presented at the Proc. Opt. Fiber Commun. Conf., Los Angeles, CA, 2012, Paper OM2B.3.

[10] F.-M. Kuo, C.-B. Huang, J.-W. Shi, N.-W. Chen, H.-P. Chuang, J. Bowers, and C.-L. Pan, "Remotely up-converted 20-Gb/s error-free wireless on–off-keying data transmission at W-band using an ultrawideband photonic transmitter-mixer," *IEEE Photon. J.*, vol. 3, no. 2, pp. 209–219, Apr. 2011.

[11] A. Kanno, K. Inagaki, I. Morohashi, T. Sakamoto, T. Kuri, I. Hosako, T. Kawanishi, Y. Yoshida, and K. Kitayama, "40 Gb/s W-band (75–110 GHz) 16-QAM radio-over-fiber signal generation and its wireless transmission," *Opt. Exp.*, vol. 19, no. 26, pp. B56–B63, Dec. 2011.

[12] X. Pang, A. Caballero, A. Dogadaev, V. Arlunno, R. Borkowski, J. S. Pedersen, L. Deng, F. Karinou, F. Roubeau, D. Zibar, X. Yu, and I. Tafur Monroy, "100 Gb/s hybrid optical fiber-wireless link in the W-band (75–110 GHz)," *Opt. Exp.*, vol. 19, no. 25, pp. 24944–24949, Dec. 2011.

[13] D. Zibar, R. Sambaraju, A. Caballero, J. Herrera, U. Westergren, A. Walber, J. B. Jensen, J. Marti, and I. Tafur Monroy, "High-capacity wireless signal generation and demodulation in 75- to 110-GHz band employing all-optical OFDM," *IEEE Photon. Technol. Lett.*, vol. 23, no. 12, pp. 810–812, Jun. 2011.

[14] R.-W. Ridgway, D.-W. Nippa, and S. Yen, "Data transmission using differential phase-shift keying on a 92 GHz carrier," *IEEE Trans. Microw. Theory Tech.*, vol. 58, no. 11, pp. 3117–3126, Nov. 2010.

[15] R. Freund, G. Bosco, L. Oxenlwe, M. Winter, A. D. Ellis, M. Nölle, C. Schmidt-Langhorst, R. Ludwig, C. Schubert, A. Carena, P. Poggiolini, M. Galili, H. C. H. Mulvad, D. Hillerkuss, R. Schmogrow, W. Freude, J. Leuthold, F. C. G. Gunning, J. Zhao, P. Frascella, S. K. Ibrahim, and N. M. Suibhne, "Single- and multi-carrier techniques to build up Tb/s per channel transmission systems," presented at the Proc. Int. Conf. Transparent Opt. Netw., Munich, Germany, 2010, Paper Tu.D1.4.
[16] Z. Jiang, D. E. Leaird, and A. M. Weiner, "Optical processing based on spectral line-by-line pulse shaping on a phase-modulated CW laser," *IEEE J. Quantum Electron.*, vol. 42, no. 7, pp. 657–665, Jul. 2006.
[17] I. Morohashi, T. Sakamoto, H. Sotobayashi, T. Kawanishi, and I. Hosako, "Broadband wavelength-tunable ultrashort pulse source using a Mach–Zehnder modulator and dispersion-flattened dispersion-decreasing fiber," *Opt. Lett.*, vol. 34, no. 15, pp. 2297–2299, Aug. 2009.
[18] J. Yu, Z. Dong, and N. Chi, "Generation, transmission and coherent detection of 11.2 Tb/s (112 $\times$ 100Gb/s) single source optical OFDM superchannel," presented at the Proc. Opt. Fiber Commun. Conf., Los Angeles, CA, 2011, Paper PDPA6.
[19] P. M. Anandarajah, R. Maher, Y. Q. Xu, S. Latkowski, J. O'Carroll, S. G. Murdoch, R. Phelan, J. O'Gorman, and L. P. Barry, "Generation of coherent multicarrier signals by gain switching of discrete mode lasers," *IEEE Photon. J.*, vol. 3, no. 1, pp. 112–122, Feb. 2011.
[20] M. Beltrán, J. Caraquitena, R. Llorente, and J. Marti, "Reconfigurable multiwavelength source based on electrooptic phase modulation of a pulsed laser," *IEEE Photon. Technol. Lett.*, vol. 23, no. 16, pp. 1175–1177, Aug. 2011.
[21] X. Liu, S. Chandrasekhar, B. Zhu, P. J. Winzer, A. H. Gnauck, and D. W. Peckham, "Transmission of a 448-Gb/s reduced-guard-interval CO-OFDM signal with a 60-GHz optical bandwidth over 2000 km of ULAF and five 80-GHz-grid ROADMs," presented at the Proc. Opt. Fiber Commun. Conf., San Diego, CA, 2010, Paper PDPC2.
[22] L. Deng, M. Beltrán, X. Pang, X. Zhang, V. Arlunno, Y. Zhao, A. Caballero, A. Dogadaev, X. Yu, R. Llorente, D. Liu, and I. Tafur Monroy, "Fiber wireless transmission of 8.3-Gb/s/ch QPSK-OFDM signals in 75-110-GHz band," *IEEE Photon. Technol. Lett.*, vol. 24, no. 5, pp. 383–385, Mar. 2012.
[23] L. Deng, D. Liu, X. Pang, X. Zhang, V. Arlunno, Y. Zhao, A. Caballero, A. K. Dogadaev, X. Yu, I. T. Monroy, M. Beltrán, and R. Llorente, "42.13 Gb/s 16QAM-OFDM photonics-wireless transmission in 75-110 GHz band," *Progr. Electromagn. Res.*, vol. 126, pp. 449–461, Mar. 2012.
[24] M. Beltrán, L. Deng, X. Pang, X. Zhang, V. Arlunno, Y. Zhao, X. Yu, R. Llorente, D. Liu, and I. Tafur Monroy, "38.2-Gb/s optical-wireless transmission in 75–110 GHz based on electrical OFDM with optical comb expansion," presented at the Proc. Opt. Fiber Commun. Conf., Los Angeles, CA, 2012, Paper OM2B.2.
[25] J. G. Proakis, *Digital Communications*, 4th ed. New York: McGraw-Hill, 2001.
[26] X. Liu and F. Buchali, "Intra-symbol frequency-domain averaging based channel estimation for coherent optical OFDM," *Opt. Exp.*, vol. 16, no. 26, pp. 21944–21957, Dec. 2008.
[27] W. Shieh and I. Djordjevic, *OFDM for Optical Communications*. San Diego, CA: Academic, 2010.
[28] X. Yi, W. Shieh, and Y. Ma, "Phase noise effects on high spectral efficiency coherent optical OFDM transmission," *J. Lightw. Technol.*, vol. 26, no. 10, pp. 1309–1316, May 2008.

Paper 8: Reconfigurable Digital Coherent Receiver for Metro-Access Networks Supporting Mixed Modulation Formats and Bit-rates

A. Caballero, N. Guerrero Gonzalez, V. Arlunno, R. Borkowski, T. T. Pham, R. Rodes, X. Zhang, M. B. Othman, K. Prince, X. Yu, J. B. Jensen, D. Zibar, and I. Tafur Monroy, "Reconfigurable Digital Coherent Receiver for Metro-Access Networks Supporting Mixed Modulation Formats and Bit-rates," in *Optical Fiber Technology Journal*, Vol. 19, No. 6, December 2013.

Optical Fiber Technology 19 (2013) 638–642

Contents lists available at ScienceDirect

Optical Fiber Technology

www.elsevier.com/locate/yofte

Reconfigurable digital coherent receiver for metro-access networks supporting mixed modulation formats and bit-rates

Antonio Caballero *, Neil Guerrero Gonzalez, Valeria Arlunno, Robert Borkowski, Tien Thang Pham, Roberto Rodes, Xu Zhang, Maisara Binti Othman, Kamau Prince, Xianbin Yu, Jesper Bevensee Jensen, Darko Zibar, Idelfonso Tafur Monroy

DTU Fotonik, Department of Photonics Engineering, Technical University of Denmark, Kgs. Lyngby, Denmark

ARTICLE INFO

Article history:
Received 6 June 2013
Revised 26 August 2013
Available online 28 October 2013

Keywords:
Coherent communications
Phase modulation
Radio-over-fiber systems
Digital coherent receivers

ABSTRACT

A single, reconfigurable, digital coherent receiver is proposed and experimentally demonstrated for converged wireless and optical fiber transport. The capacity of reconstructing the full transmitted optical field allows for the demodulation of mixed modulation formats and bit-rates. We performed experimental validation of different modulation formats, including VCSEL based OOK, baseband QPSK, RoF OFDM and wireless IR-UWB over a 78 km deployed fiber link.

1. Introduction

Next generation metro-access networks will need to support diverse broadband services including converged wireless and wireline optical access over a unified fiber platform, satisfying bandwidth requirements [1] as well as fulfilling stringent power budget and chromatic dispersion constrains [2]. Future metro-access networks will also require agile re-configurability to seamlessly accommodate for emerging new services and increased bandwidth requirements [1]. The introduction of different modulation formats and bitrates into the metro-access networking scenario is creating a highly heterogeneous environment that represents a new challenge to tackle in the near future. Approaches looking for solutions to one or more of the above issues are radio-over-fiber systems for integrating baseband and wireless service delivery over optical fiber access networks [3]. The combination of high bitrate baseband has been proposed for the transport of wireless signal in the digital domain [4]. Most of these approaches focus on methods for generating the wireless signals carrying orthogonal frequency division multiplexing (OFDM) [5]; however, the detection is usually performed with independent receivers, increasing the complexity of these architectures.

A promising approach recently proposed to increase the capacity of passive optical networks (PON) is wavelength-division multiplexing (WDM) combined with coherent detection. Compared to direct-detection (DD), coherent detection allows for closely spaced channels with increased receiver sensitivity to cope with the required large number of users and to extend the reach of metro-access networks [6,7]; also, coherent receivers does not require an arrayed waveguide grating (AWG) at the receiver to filter the undesired wavelengths [7], making this technology compatible with the passive optical splitting of legacy PONs. Digital coherent detection also allows for the detection of wireless signals [8] providing the required high linearity and high capacity of next generation wireless networks.

Although experimental demonstrations of converged service delivery have been reported in the literature [2,3] they use a dedicated receiver for each modulation or bit-rate. The approach of separate receivers is shown in Fig. 1, where different receivers are used to detect baseband signals, intensity-modulated (IM) or phase-modulated (PM), and analog signals, from a typical radio-over-fiber (RoF) such as WIFI or WIMAX to an ultra-wide band (UWB). The use of coherent detection allows reconfiguring the digital signal processing (DSP) software in the demodulator for each modulation format, thus there is only one receiver needed. Furthermore, it allows longer reach and avoids the use of an AWG to separate the different channels.

In this paper we present and experimentally demonstrate a single, reconfigurable, digital receiver supporting mixed modulation formats, baseband and wireless-over-fiber, with reconfiguration in the digital signal processing domain. We provide a detail description of the architecture and building blocks of the architecture.

* Corresponding author. Address: DTU Fotonik, B. 358 R. 105, 2800 Kgs. Lyngby, Denmark.
E-mail address: acaj@fotonik.dtu.dk (A. Caballero).

1068-5200/$ - see front matter © 2013 Elsevier Inc. All rights reserved.
http://dx.doi.org/10.1016/j.yofte.2013.10.004

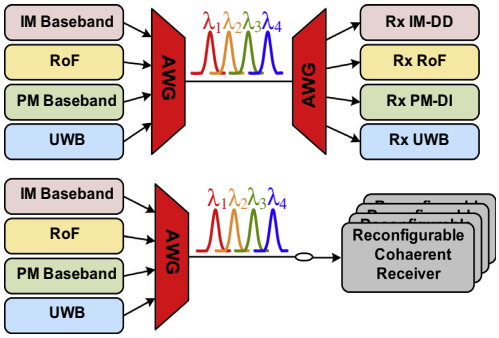

Fig. 1. Architecture of a WDM-PON with dedicated receivers (top) and with a single reconfigurable digital receiver (bottom).

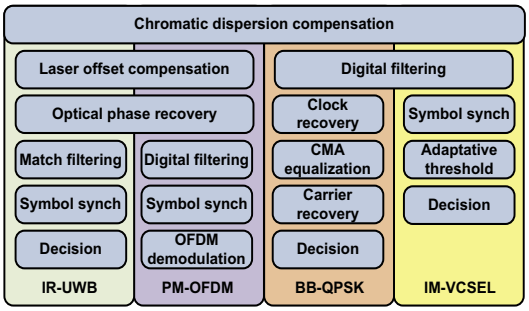

Fig. 2. Schematic diagram of the reconfigurable digital receiver.

Furthermore we detail the experimental demonstration first presented in [9] for 20 Gb/s non-return-to-zero quadrature phase-shift keying (NRZ-QPSK), optically phase-modulated 5 GHz OFDM RoF and 2 Gb/s impulse radio UWB (IR-UWB), and 5 Gb/s directly modulated vertical cavity surface emitting laser (VCSEL) after 78 km of deployed fiber link.

2. Single reconfigurable receiver

Recent advances in high-speed DSP and analog-to-digital (A/D) conversion (ADC) have enabled the integration of digital receiver into optical communication systems [8,10]. The main advantages digital receivers can offer over traditional signal demodulation schemes include the following:

- Cost effectiveness and compactness.
- Possibilities to adaptively compensate for channel impairments in the electronic domain (such as chromatic dispersion, polarization mode dispersion, etc.) using signal processing techniques.
- Design versatility and robust operation by enabling reception of different formats using the same receiver hardware based on the channel condition.
- Enhance performance, arising from the full recovery of the optical field information: digital coherent receivers enhanced OSNR tolerance, better compatibility with advanced modulation formats, and enhanced electronic equalization of linear and nonlinear effects in the transmission link [11].

The first experimental demonstration of converge wired and wireless over deployed fiber [2] employed dedicated receivers for each signal. The baseband DQPSK signal was demodulated using a delay interferometer (DI); the RoF was detected using a photodiode (PD) and RF low-noise amplifier and for the UWB, also a PD was used. For the RoF using phase-modulation, a digital coherent receiver was used.

A single reconfigurable receiver in the uplink transmission, as proposed in this paper, has the benefit of demodulating different types of optical signals, with variable modulation formats and bitrates. The use of coherent detection also benefits from improved sensitivity.

A schematic diagram of the employed single digital receiver is shown in Fig. 2. The single digital receiver first compensates for the chromatic dispersion of the link, which is a common impairment for all the modulation formats. For the analog detection (IR-UWB and PM-OFDM), the DSP first performs a recovery of the optical phase using a combination of optical carrier-recovery digital phase-locked loop (PLL), to compensate for the lasers frequency offset, followed by linear signal demodulation [8], which extracts the phase of the optical field. Then, the IR-UWB is demodulated by match filter with the transmitted pulse-shape [11], whereas the PM-OFDM is demodulated using standard OFDM demodulation based on Schmidl training symbols [12]. For the baseband QPSK (BB-QPSK) a standard receiver is used, based on clock-recovery, constant-modulus algorithm (CMA) and carrier recovery [8,13]. The intensity modulated (IM) VCSEL is demodulated using match filter. An adaptive threshold is used afterwards to compensate for the absence of VCSEL temperature control and decision gating [14]. The reconfiguration for each modulation format was performed by digitally switching between the four signal demodulation DSP blocks. In our developed software, we first perform a switch from the 4 possible signals, loading their individual bitrates and modulation formats, the DSP modules needed for demodulation and their initialization parameters. As the possible modulation formats are finite, these initialization values can be stored in a modulation format database. In future, the identification of the modulation format could be automatized.

3. Experimental demonstration

Fig. 3 shows a block diagram of the heterogeneous optical network and setup used in the experiment. The field-deployed fiber connects the Kgs. Lyngby campus of the Technical University of Denmark (DTU) and the Taastrup suburb of Copenhagen. The fiber is a G.652 standard single-mode fiber (SMF) type (16.5 ps/nm/km chromatic dispersion, 0.20 dB/km attenuation). The total length of the fiber was 78 km, exceeding current standards but suitable for future longer reach PON. The total link loss was 27 dB. ITU standard operating wavelengths were used for all channels at 200 GHz separation due to equipment availability. The total launch power into the deployed fiber was kept to +4 dBm, with an equal launch power per carrier of −2 dBm. Due to the bitrates of this experiment and previous work in RoF [11] and baseband coherent [16], we would expect low penalty from closer WDM spacing, such as 50 GHz.

The optical spectrum each of the four different signals is shown in Fig. 4. At the receiver side, emulating the central office, an erbium doped fiber amplifier (EDFA) was used as preamplifier followed by an optical bandpass filter to reduced ASE noise. The optical power level to the coherent receiver was set to −11 dBm. A tunable external cavity laser (ECL), with a linewidth of 100 kHz, was used as local oscillator (LO) for all the received signal types. The in-phase and quadrature signals after the 90° optical hybrid were detected with two pairs of balanced photodiodes, having full-width at half-maximum bandwidth of 7.5 GHz. The detected photocurrents were digitized using a sampling oscilloscope at

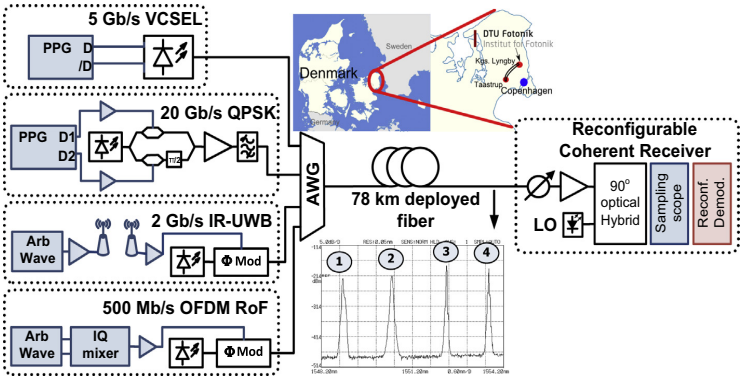

Fig. 3. Experiment layout of the heterogeneous optical network investigated in the experiment. Route of installed optical fiber is also shown. Reconfigurable receiver construction allows local oscillator (LO) tuning for channel selection. PPG: pulse pattern generator; Arb Wave: arbitrary waveform.

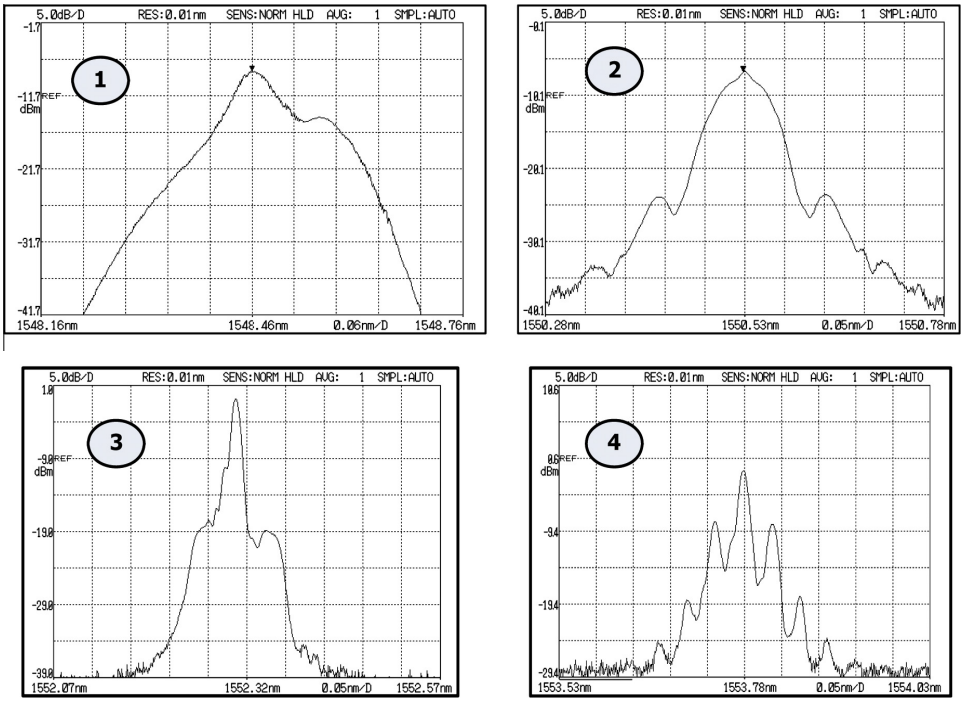

Fig. 4. Optical spectrums of the four different optical signals at the input of the fiber.

40 GSa/s for offline processing, with the receiver structure described in Fig. 2.

3.1. 5 Gb/s intensity-modulated and coherently detected VCSEL

A pulse pattern generator (PPG) at 5 Gb/s directly modulated a 1548.5 nm single-mode VCSEL. Single drive configuration was used for the VCSEL with a driving peak-peak voltage of 1 V. A pseudo random binary sequence (PRBS) with a length of 2^{15}-1 was used for this experiment. The bias current of the VCSEL was used to tune the wavelength to the assigned AWG channel. Bias current was set to 14 mA. The output power of the VCSEL was measured to be 0.5 dBm.

3.2. 20 Gb/s NRZ-QPSK

The transmitter of the baseband QPSK subsystem consisted on a nested Mach–Zehnder modulator (MZM) driven by two independent electrical signals at 10 Gb/s with PRBS 2^{15}-1. The laser source was a DFB centered at 1550.5 nm and with a value of the linewidth of 2 MHz.

3.3. 2 Gb/s phase-modulated IR-UWB

An Arbitrary Waveform Generator (AWG) with 24 GSa/s sampling rate was utilized to program a 5th order derivative Gaussian pulse, with good compliance with FCC mask [11]. A bipolar

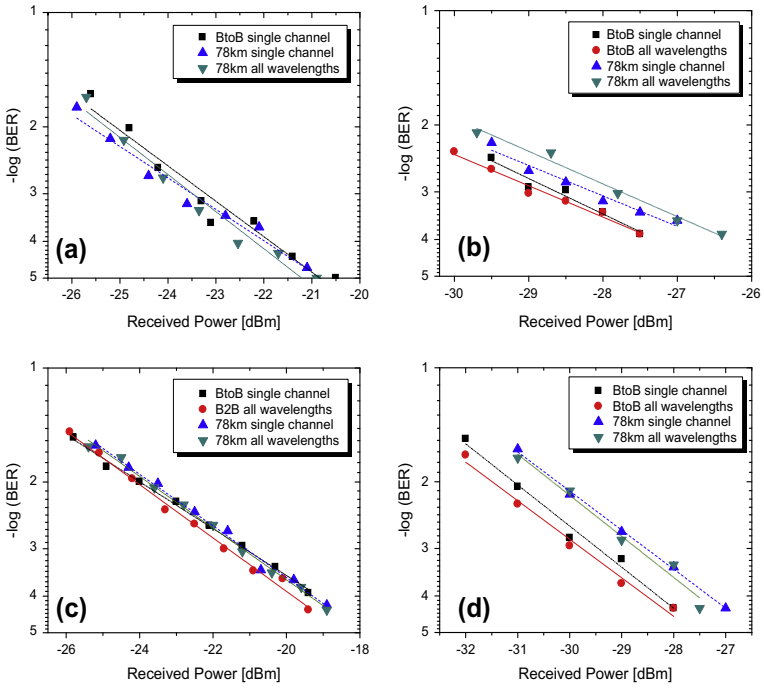

Fig. 5. Measured BER performances for (a) 5 Gb/s intensity-modulated VCSEL, (b) 20 Gb/s QPSK baseband, (c) 2 Gb/s phase-modulated IR-UWB, and (d) 5 GHz OFDM RoF.

modulation at a bit rate of 2 Gb/s was applied to the generated pulses with a PRBS 2^{11}-1. The UWB signal was transmitted using an omni-directional antenna with 0 dBi gain and received after 1 m wireless transmission by a directive antenna with up to 12 dBi gain within the UWB frequency range. The received wireless signal was amplified by an electrical low noise amplifier, filtered and then amplified again to drive the optical phase modulator. The DFB laser source of this channel was set at 1552.3 nm.

3.4. 5 GHz OFDM RoF

The OFDM baseband signal was generated in software using a 2^{15}-1 PRBS as input data stream. 256 4-QAM subcarriers were used with 26 samples cyclic prefix per OFDM symbol. The OFDM frame was composed of two Schmidl training symbols [13,15] followed by eight data symbols. The in-phase and quadrature signals were fed to an AWG with a 1.25 GSa/s rate, for a total bit rate of 500 Mb/s. The signal was then upconverted to a frequency of 5 GHz using a Vector Signal Generator (VSG), driving an optical phase modulator supplied with a DFB laser at 1553.78 nm.

4. Results

To demonstrate the performance of our reconfigurable digital coherent receiver, we measured bit error rate (BER) curves for back-to-back (B2B) and after 78 km of deployed fiber transmission (considering both single and all simultaneous channel performance) as a function of the received optical power. The results for each channel are shown in Fig. 5. For all four subsystems, a BER value below 10^{-3} (FEC threshold) is achieved for all considered scenarios. The worst receiver sensitivity achieved was −23 dBm, resulting in 21 dB link budget for +4 dBm total launch power.

4.1. 5 Gb/s coherently detected, intensity-modulated VCSEL

As we can see in Fig. 5a, the VCSEL coherently detected subsystem achieves a sensitivity of −24 dBm at 10^{-3} for both B2B and 78 km deployed fiber. As the chromatic dispersion and chirp were completely compensated by DSP no penalty was appreciated compared with the B2B case.

4.2. 20 Gb/s QPSK baseband

Fig. 5b shows that fiber transmission incurred in 1 dB power penalty difference at 10^{-3} BER. In the simultaneous presence of the other three channels, there was an observable *minor* 0.5 dB penalty both for back to back and after transmission. We attribute this penalty to the presence of the IM-VCSEL neighbour channel inducing cross-phase modulation. The receiver sensitivity was −28 dBm for the WDM transmission.

4.3. 2 Gb/s phase-modulated IR-UWB

As shown in Fig. 5c the measured BER performances of the UWB subsystem were consistent for all cases. The BER performance is below the FEC limit when the received optical power was higher than −23 dBm, including 1 m of wireless transmission.

4.4. 5 GHz OFDM RoF

Fig. 5d shows that for the case of four simultaneously integrated channels, OFDM suffered 0.5 dB of power penalty, for both B2B and 78 km fiber transmission compared to single OFDM channel transmission. This yielded receiver sensitivity at a BER of $10^{-3}$of −29.5 dBm for the B2B system, and −28.5 dBm for the 78 km optical transmission link, respectively.

5. Conclusion

A single reconfigurable DSP enabled coherent receiver is proposed for long reach converged PON for uplink transmission. We experimentally demonstrated its performance for mixed modulation formats and bit rates over a deployed fiber link. In our reported experiment, four different types of wireline and wireless services including 20 Gb/s QPSK baseband, 5 Gb/s OOK, 5 GHz OFDM RoF and 2 Gb/s IR-UWB are successfully demodulated after transmission over 78 km deployed fiber link. The demonstrated links exceeds current access lengths and due to the low launch power and high sensitivity, we expect that minor penalty will be induced for closer WDM spacing. The receiver used the same optical front-end, is able to switch among baseband and wireless types of signals by DSP reconfiguring to baseband only. This demonstrated digital reconfigurable coherent receiver has potential to enable unified support for signal detection on highly heterogeneous next generation metro-access networks.

Acknowledgments

The authors thank Tektronix Denmark for the loan of the AWG7000 and Globalconnect Denmark for access to the deployed fiber. This work was partly supported by Danish Research Council under Grant OPSCODER and by the European Union FP7 Information Communication Technology (ICT)-ALPHA.

References

[1] K. Sato, H. Hasegawa, Optical networking technologies that will create future bandwidth abundant networks, J. Opt. Comm. Network. 1 (2009) 81–83.
[2] K. Prince, J.B. Jensen, A. Caballero, X. Yu, T.B. Gibbon, D. Zibar, N. Guerrero, A.V. Osadchiy, I. Tafur Monroy, Converged wireline and wireless access over a 78-km deployed fiber long-reach WDM PON, Photon. Technol. Lett. 21 (2009) 1274–1276.
[3] M. Popov, The convergence of wired and wireless services delivery in access and home networks, in: Proc. of OFC, 2010 (paper OWQ6).
[4] A. Nirmalathas, P.A. Gamage, C. Lim, D. Novak, R. Waterhouse, Digitized Radio-Over-Fiber technologies for converged optical wireless access network, J. Lightw. Technol. 28 (2010) 2366–2375.
[5] H. Yu-Ting, A novel lightwave centralized bidirectional hybrid access network: seamless integration of RoF with WDM-OFDM-PON, Photon. Technol. Lett. 23 (2011) 1085–1087.
[6] H. Rohde, S. Smolorz, E. Gottwald, K. Kloppe, Next generation optical access: 1 Gbit/s for everyone, in: ECOC 2009, 10.5.5.
[7] D. Lavery, M. Ionescu, S. Makovejs, E. Torrengo, S.J. Savory, A long-reach ultra-dense 10 Gbit/s WDM-PON using a digital coherent receiver, Opt. Express 18 (2010) 25855–25860.
[8] A. Caballero, D. Zibar, I. Tafur Monroy, Performance evaluation of digital coherent receivers for phase-modulated Radio-Over-Fiber links, J. Lightw. Technol. 29 (2011) 3282–3292.
[9] N.G. Gonzalez, A. Caballero, R. Borkowski, V. Arlunno, T.T. Pham, R. Rodes, X. Zhang, M.B. Othman, K. Prince, X. Yu, J.B. Jensen, D. Zibar, I.T. Monroy, Reconfigurable digital coherent receiver for metro-access networks supporting mixed modulation formats and bit-rates, in: OFC 2011, OMW7.
[10] L. Kazovsky, W.-T. Shaw, D. Gutierrez, N. Cheng, S.-W. Wong, Next-generation optical access networks, J. Lightw. Technol. 25 (2007) 3428–3442.
[11] T.T. Pham, N. Guerrero Gonzalez, X. Yu, D. Zibar, L. Dittmann, I. Tafur Monroy, Robust BPSK impulse radio UWB-over-Fiber systems using optical phase modulation, in: OFC 2011, OTuF6.
[12] V. Arlunno, R. Borkowski, N. Guerrero Gonzalez, A. Caballero, K. Prince, J.B. Jensen, D. Zibar, K.J. Larsen, I. Tafur Monroy, Radio over fiber link with adaptive order n-QAM optical phase modulated OFDM and digital coherent detection, Microw. Opt. Technol. Lett. 53 (2011) 2245–2247.
[13] T. Pfau, S. Hoffmann, R. Noé, Hardware-efficient coherent digital receiver concept with feedforward carrier recovery for M-QAM constellations, J. Lightw. Technol 27 (2009) 989–999.
[14] J.B. Jensen, R. Rodes Lopez, D. Zibar, I. Tafur Monroy, Coherent detection for 1550 nm, 5 Gbit/s VCSEL based 40 km bidirectional PON transmission, in: OFC 2011, OTuB2.
[15] T. Schmidt, D. Cox, Robust frequency and timing synchronization for OFDM, Trans. Commun. 45 (1997) 1613–1621.
[16] M. Alfiad, M. Kuschnerov, T. Wuth, T.J. Xia, G. Wellbrock, E. Schmidt, D. van den Borne, B. Spinnler, C.J. Weiske, E. de Man, A. Napoli, M. Finkenzeller, S. Spaelter, M. Rehman, J. Behel, M. Chbat, J. Stachowiak, D. Peterson, W. Lee, M. Pollock, B. Basch, D. Chen, M. Freiberger, B. Lankl, H. de Waardt, 111-Gb/s transmission over 1040-km field-deployed fiber with 10G/40G neighbors, Photon. Technol. Lett. 21 (2010) 615–617.

Bibliography

[1] CISCO, "Cisco visual networking index: Forecast and methodlogy, 2012–2017," CISCO, Tech. Rep., 2013.

[2] E. Ip, P. Ji, E. Mateo, Y.-K. Huang, L. Xu, D. Qian, N. Bai, and T. Wang, "100G and beyond transmission technologies for evolving optical networks and relevant physical-layer issues," *Proceedings of the IEEE*, vol. 100, no. 5, pp. 1065–1078, 2012.

[3] P. J. Winzer, "High-spectral-efficiency optical modulation formats," *IEEE/OSA J. Lightw. Technol.*, vol. 30, no. 24, pp. 3824 –3835, dec.15, 2012.

[4] R.-J. Essiambre, G. Kramer, P. J. Winzer, G. J. Foschini, and B. Goebel, "Capacity limits of optical fiber networks," *IEEE/OSA J. Lightw. Technol.*, vol. 28, no. 4, pp. 662–701, 2010.

[5] T. Zami, "Comparison of elastic implementations for wdm networks," in *European Conference and Exposition on Optical Communications*. Optical Society of America, 2011.

[6] I. Recommendation, "Spectral grids for WDM applications: DWDM frequency grid," 2012.

[7] J. Armstrong, "OFDM for optical communications," *IEEE/OSA J. Lightw. Technol.*, vol. 27, no. 3, pp. 189–204, Feb.1, 2009.

[8] S. J. Savory, "Digital coherent optical receivers: algorithms and subsystems," *Selected Topics in Quantum Electronics, IEEE Journal of*, vol. 16, no. 5, pp. 1164–1179, 2010.

[9] H. Song and M. Brandt-Pearce, "Range of influence and impact of physical impairments in long-haul DWDM systems," *IEEE/OSA J. Lightw. Technol.*, vol. 31, no. 6, pp. 846–854, 2013.

[10] C. E. Shannon, "A mathematical theory of communication," *Bell Syst. Tech. J.*, vol. 27, p. 379–423 and 623–656, 1948.

[11] P. Winzer, "Beyond 100g ethernet," *IEEE Commun. Mag.*, vol. 48, no. 7, pp. 26–30, 2010.

[12] R. Essiambre and R. W. Tkach, "Capacity trends and limits of optical communication networks," *Proceedings of the IEEE*, vol. 100, no. 5, pp. 1035–1055, 2012.

[13] D. Wulich, "Definition of efficient papr in ofdm," *Communications Letters, IEEE*, vol. 9, no. 9, pp. 832–834, 2005.

[14] N. Benvenuto, R. Dinis, D. Falconer, and S. Tomasin, "Single carrier modulation with nonlinear frequency domain equalization: an idea whose time has come—again," *Proceedings of the IEEE*, vol. 98, no. 1, pp. 69–96, 2010.

[15] C. Douillard, M. Jézéquel, C. Berrou, A. Picart, P. Didier, A. Glavieux *et al.*, "Iterative correction of intersymbol interference: Turbo-equalization," *European Transactions on Telecommunications*, vol. 6, no. 5, pp. 507–511, 1995.

[16] S. Savory, A. Stewart, S. Wood, G. Gavioli, M. Taylor, R. Killey, and P. Bayvel, "Digital equalisation of 40Gbit/s per wavelength transmission over 2480km of standard fibre without optical dispersion compensation," in *Optical Communications, 2006. ECOC 2006. European Conference on*. IEEE, 2006, pp. 1–2.

[17] C. A. Belfiore and J. H. Park Jr, "Decision feedback equalization," *Proceedings of the IEEE*, vol. 67, no. 8, pp. 1143–1156, 1979.

[18] D. Zibar, R. Sambaraju, A. Caballero, J. Herrera, and I. Tafur Monroy, "Carrier recovery and equalization for photonic-wireless links with capacities up to 40 gb/s in 75-110 ghz band," in *Optical Fiber Communication Conference*. Optical Society of America, 2011.

[19] P. Winzer, A. Gnauck, C. Doerr, M. Magarini, and L. Buhl, "Spectrally efficient long-haul optical networking using 112-Gb/s polarization-multiplexed 16-QAM," *IEEE/OSA J. Lightw. Technol.*, vol. 28, no. 4, pp. 547 –556, feb.15, 2010.

[20] M. S. Alfiad, M. Kuschnerov, S. L. Jansen, T. Wuth, D. van den Borne, and H. de Waardt, "11x224-Gb/s POLMUX-RZ-16 QAM transmission over 670 km of SSMF with 50-GHz channel spacing," *IEEE Photon. Technol. Lett.*, vol. 22, no. 15, pp. 1150–1152, 2010.

[21] H. Zhang, J.-X. Cai, H. Batshon, C. Davidson, Y. Sun, M. Mazurczyk, D. Foursa, A. Pilipetskii, G. Mohs, and N. S. Bergano, "16qam transmission with 5.2 bits/s/hz spectral efficiency over transoceanic distance," *Opt. Express*, vol. 20, no. 11, pp. 11 688–11 693, 2012.

[22] Y. Gao, J. Ke, K. Zhong, J. Cartledge, and S. Yam, "Assessment of intrachannel nonlinear compensation for 112 gb/s dual-polarization 16qam systems," *IEEE/OSA J. Lightw. Technol.*, vol. 30, no. 24, pp. 3902–3910, 2012.

[23] E. Tipsuwannakul, J. Li, M. Karlsson, and P. A. Andrekson, "Performance comparisons of DP-16QAM and duobinary-shaped DP-QPSK for optical systems with 4.1 Bit/s/Hz spectral efficiency," *IEEE/OSA J. Lightw. Technol.*, vol. 30, no. 14, pp. 2307–2314, 2012.

[24] J. Yu, Z. Dong, H.-C. Chien, Z. Jia, X. Li, D. Huo, M. Gunkel, P. Wagner, H. Mayer, and A. Schippel, "Transmission of 200 g pdm-csrz-qpsk and pdm-16 qam with a se of 4 b/s/hz," *IEEE/OSA J. Lightw. Technol.*, vol. 31, no. 4, pp. 515–522, 2013.

[25] X. Zhou, J. Yu, M.-F. Huang, Y. Shao, T. Wang, L. Nelson, P. Magill, M. Birk, P. I. Borel, D. W. Peckham *et al.*, "64-tb/s, 8 b/s/hz, pdm-36qam transmission over 320 km using both pre-and post-transmission digital signal processing," *IEEE/OSA J. Lightw. Technol.*, vol. 29, no. 4, pp. 571–577, 2011.

[26] A. H. Gnauck, P. J. Winzer, A. Konczykowska, F. Jorge, J.-Y. Dupuy, M. Riet, G. Charlet, B. Zhu, and D. W. Peckham, "Generation and transmission of 21.4-Gbaud PDM 64-QAM using a novel high-power DAC driving a single I/Q modulator," *IEEE/OSA J. Lightw. Technol.*, vol. 30, no. 4, pp. 532–536, 2012.

[27] D. Qian, M.-F. Huang, E. Ip, Y.-K. Huang, Y. Shao, J. Hu, and T. Wang, "High capacity/spectral efficiency 101.7-Tb/s WDM transmission using PDM-128QAM-OFDM over 165-km SSMF within C- and L-bands," *IEEE/OSA J. Lightw. Technol.*, vol. 30, no. 10, pp. 1540–1548, 2012.

[28] J. X. Cai, Y. Cai, C. Davidson, D. Foursa, A. Lucero, O. Sinkin, W. Patterson, A. Pilipetskii, G. Mohs, and N. S. Bergano, "Transmission of 96x100G pre-filtered PDM-RZ-QPSK channels with 300% spectral efficiency over 10,608km and 400% spectral efficiency over 4,368km," *Optical Fiber Communication Conference*, pp. 1–3, 2010.

[29] J. Wang, X. He, K. Gao, L. Myers, C. Xie, and Z. Pan, "8x400-gbit/s pdm-qpsk with 100 ghz channel spacing over 2000km transmission using map detection," in *CLEO: Science and Innovations*. Optical Society of America, 2011.

[30] J.-X. Cai, C. R. Davidson, A. Lucero, H. Zhang, D. G. Foursa, O. V. Sinkin, W. W. Patterson, A. N. Pilipetskii, G. Mohs, and N. S. Bergano, "20 Tbit/s transmission over 6860 km with sub-nyquist channel spacing," *IEEE/OSA J. Lightw. Technol.*, vol. 30, no. 4, pp. 651–657, 2012.

[31] J. Cai, "100G transoceanic length transmission with high spectral efficiency using bandwidth constrained PDM-QPSK," in *Optical Fiber Communication Conference*. Optical Society of America, 2011.

[32] H. F. Haunstein, W. Sauer-Greff, A. Dittrich, K. Sticht, and R. Urbansky, "Principles for electronic equalization of polarization-mode dispersion," *IEEE/OSA J. Lightw. Technol.*, vol. 22, no. 4, pp. 1169–1182, 2004.

[33] Y. Mori, K. Igarashi, K. Katoh, and K. Kikuchi, "Decision-feedback carrier-phase estimation for digital coherent optical receivers," in *Joint conference of the Opto-Electronics and Communications Conference, 2008 and the 2008 Australian Conference on Optical Fibre Technology. OECC/ACOFT 2008.* IEEE, 2008, pp. 1–2.

[34] M. Alfiad, D. van den Borne, M. Kuschnerov, B. Spinnler, T. Wuth, A. Napoli, S. Jansen, and H. de Waardt, "FFE, DFE and MLSE equalizers in phase modulated transmission systems," in *LEOS Annual Meeting Conference Proceedings, 2009. LEOS'09. IEEE.* IEEE, 2009, pp. 193–194.

[35] D. Zibar, R. Sambaraju, A. Caballero, J. Herrera, U. Westergren, A. Walber, J. B. Jensen, J. Marti, and I. T. Monroy, "High-capacity wireless signal generation and demodulation in 75-to 110-ghz band

employing all-optical ofdm," *IEEE Photon. Technol. Lett.*, vol. 23, no. 12, pp. 810–812, 2011.

[36] A. Caballero, D. Zibar, R. Sambaraju, J. Martí, and I. T. Monroy, "High-capacity 60 GHz and 75–110 GHz band links employing all-optical OFDM generation and digital coherent detection," *IEEE/OSA J. Lightw. Technol.*, vol. 30, no. 1, pp. 147–155, 2012.

[37] X. Zhang, X. Pang, L. Deng, D. Zibar, I. T. Monroy, and R. Younce, "High phase noise tolerant pilot-tone-aided dp-qpsk optical communication systems," *Opt. Express*, vol. 20, no. 18, pp. 19 990–19 995, 2012.

[38] J. Fickers, A. Ghazisaeidi, M. Salsi, G. Charlet, P. Emplit, and F. Horlin, "Decision-feedback equalization of bandwidth-constrained N-WDM coherent optical communication systems," *IEEE/OSA J. Lightw. Technol.*, vol. 31, no. 10, pp. 1529–1537, 2013.

[39] D. Zeolla, A. Antonino, G. Bosco, and R. Gaudino, "DFE versus MLSE electronic equalization for Gigabit/s SI-POF transmission systems," *IEEE Photon. Technol. Lett.*, vol. 23, no. 8, pp. 510–512, 2011.

[40] W. Shieh, X. Yi, Y. Ma, and Y. Tang, "Theoretical and experimental study on PMD-supported transmission using polarization diversity in coherent optical OFDM systems," *Opt. Express*, vol. 15, no. 16, pp. 9936–9947, 2007.

[41] L. Tomba, "On the effect of wiener phase noise in OFDM systems," *IEEE Trans. Commun.*, vol. 46, no. 5, pp. 580–583, 1998.

[42] F. Z. Merli and G. M. Vitetta, "A factor graph approach to the iterative detection of OFDM signals in the presence of carrier frequency offset and phase noise," *Wireless Communications, IEEE Transactions on*, vol. 7, no. 3, pp. 868–877, 2008.

[43] S. L. Jansen, I. Morita, T. C. Schenk, N. Takeda, and H. Tanaka, "Coherent optical 25.8-gb/s ofdm transmission over 4160-km ssmf," *IEEE/OSA J. Lightw. Technol.*, vol. 26, no. 1, pp. 6–15, 2008.

[44] D. Qian, M.-F. Huang, E. Ip, Y.-K. Huang, Y. Shao, J. Hu, and T. Wang, "101.7-tb/s (370× 294-gb/s) pdm-128qam-ofdm transmission over 3× 55-km ssmf using pilot-based phase noise mitigation," in

Optical Fiber Communication Conference. Optical Society of America, 2011.

[45] Y. Chen, S. Adhikari, N. Hanik, and S. L. Jansen, "Pilot-aided sampling frequency offset compensation for coherent optical ofdm," in *Optical Fiber Communication Conference*. IEEE, 2012, pp. 1–3.

[46] A. Barbieri, G. Colavolpe, T. Foggi, E. Forestieri, and G. Prati, "OFDM versus single-carrier transmission for 100 Gbps optical communication," *IEEE/OSA J. Lightw. Technol.*, vol. 28, no. 17, pp. 2537–2551, 2010.

[47] T. M. Schmidl and D. C. Cox, "Robust frequency and timing synchronization for OFDM," *IEEE Trans. Commun.*, vol. 45, no. 12, pp. 1613–1621, 1997.

[48] H. Minn, M. Zeng, and V. K. Bhargava, "On timing offset estimation for OFDM systems," *Communications Letters, IEEE*, vol. 4, no. 7, pp. 242–244, 2000.

[49] B. Park, H. Cheon, C. Kang, and D. Hong, "A novel timing estimation method for OFDM systems," *Communications Letters, IEEE*, vol. 7, no. 5, pp. 239–241, 2003.

[50] A. B. Awoseyila, C. Kasparis, and B. G. Evans, "Improved preamble-aided timing estimation for OFDM systems," *Communications Letters, IEEE*, vol. 12, no. 11, pp. 825–827, 2008.

[51] A. Awoseyila, C. Kasparis, and B. Evans, "Robust time-domain timing and frequency synchronization for OFDM systems," *Consumer Electronics, IEEE Transactions on*, vol. 55, no. 2, pp. 391–399, 2009.

[52] H. Abdzadeh-Ziabari and M. G. Shayesteh, "Robust timing and frequency synchronization for OFDM systems," *Vehicular Technology, IEEE Transactions on*, vol. 60, no. 8, pp. 3646–3656, 2011.

[53] D. Plant, Q. Zhuge, M. Morsy-Osman, M. Chagnon, X. Xu, and M. Qiu, "Flexible transceivers using adaptive digital signal processing for single carrier and OFDM," in *Optical Fiber Communication Conference*. Optical Society of America, 2013.

[54] R. Schmogrow, R. Bouziane, M. Meyer, P. Milder, P. Schindler, R. Killey, P. Bayvel, C. Koos, W. Freude, and J. Leuthold, "Real-time OFDM or nyquist pulse generation–which performs better with

limited resources?" *Opt. Express*, vol. 20, no. 26, pp. B543–B551, 2012.

[55] G. Bosco, V. Curri, A. Carena, P. Poggiolini, and F. Forghieri, "On the performance of nyquist-WDM terabit superchannels based on PM-BPSK, PM-QPSK, PM-8QAM or PM-16QAM subcarriers," *IEEE/OSA J. Lightw. Technol.*, vol. 29, no. 1, pp. 53–61, 2011.

[56] J. Wang, Z. Pan *et al.*, "Generation of spectrally efficient nyquist-wdm qpsk signals using digital fir or fde filters at transmitters," *IEEE/OSA J. Lightw. Technol.*, 2012.

[57] C. Liu, W. Jian, H.-C. Chien, A. Chowdhury, and G.-K. Chang, "Experimental analyses and optimization of equalization techniques for 60-GHz OFDM radio-over-fiber system," in *Optical Fiber Communication Conference*. IEEE, 2010, pp. 1–3.

[58] W.-J. Jiang, C.-T. Lin, A. Ng'oma, P.-T. Shih, J. Chen, M. Sauer, F. Annunziata, and S. Chi, "Simple 14-Gb/s short-range radio-over-fiber system employing a single-electrode MZM for 60-GHz wireless applications," *IEEE/OSA J. Lightw. Technol.*, vol. 28, no. 16, pp. 2238–2246, 2010.

[59] A. Ng'oma, C.-T. Lin, L.-Y. W. He, W.-J. Jiang, F. Annunziata, J. Chen, P.-T. Shih, J. George, and S. Chi, "31 Gbps RoF system employing adaptive bit-loading OFDM modulation at 60 GHz," in *Optical Fiber Communication Conference*. IEEE, 2011, pp. 1–3.

[60] F. Li, J. Yu, Z. Cao, J. Xiao, H. Chen, and L. Chen, "Reducing the peak-to-average power ratio with companding transform coding in 60 GHz OFDM-ROF systems," *IEEE/OSA J. Opt. Commun. Netw.*, vol. 4, no. 3, pp. 202–209, 2012.

[61] P. Lombard, Y. Le Guennec, G. Maury, E. Novakov, and B. Cabon, "Optical distribution and upconversion of MB-OFDM in ultrawideband-over-fiber systems," *IEEE/OSA J. Lightw. Technol.*, vol. 27, no. 9, pp. 1072–1078, 2009.

[62] D. Wake, A. Nkansah, and N. J. Gomes, "Radio over fiber link design for next generation wireless systems," *IEEE/OSA J. Lightw. Technol.*, vol. 28, no. 16, pp. 2456–2464, 2010.

[63] T. Inoue, K. Tanizawa, and S. Namiki, "Experimental study on parametric tunable dispersion compensation for WDM channels with mixed OOK and QPSK formats," *Electronics Letters*, vol. 49, no. 6, pp. 401–402, 2013.

[64] D. J. Geisler, R. Proietti, Y. Yin, R. P. Scott, X. Cai, N. Fontaine, L. Paraschis, O. Gerstel, and S. Yoo, "The first testbed demonstration of a flexible bandwidth network with a real-time adaptive control plane," in *European Conference and Exposition on Optical Communications*. Optical Society of America, 2011.

[65] D. J. Geisler, R. Proietti, Y. Yin, R. P. Scott, X. Cai, N. K. Fontaine, L. Paraschis, O. Gerstel, and S. Yoo, "Experimental demonstration of flexible bandwidth networking with real-time impairment awareness," *Opt. Express*, vol. 19, pp. B736–B745, 2011.

[66] O. Gerstel, M. Jinno, A. Lord, and S. B. Yoo, "Elastic optical networking: a new dawn for the optical layer?" *IEEE Commun. Mag.*, vol. 50, no. 2, pp. s12–s20, 2012.

[67] Ciena, "Ciena to demonstrate versatility of next-generation converged packet optical and packet networking solutions at OFC/NFOEC 2013," Tech. Rep., 2013.

[68] B. Szafraniec, T. S. Marshall, and B. Nebendahl, "Performance monitoring and measurement techniques for coherent optical systems," *IEEE/OSA J. Lightw. Technol.*, vol. 31, no. 4, pp. 648–663, 2013.

[69] M. Selmi, C. Gosset, M. Noelle, P. Ciblat, and Y. Jaouën, "Blockwise digital signal processing for polmux QAM/PSK optical coherent systems," *IEEE/OSA J. Lightw. Technol.*, vol. 29, no. 20, pp. 3070–3082, 2011.

[70] F. N. Hauske, M. Kuschnerov, B. Spinnler, and B. Lankl, "Optical performance monitoring in digital coherent receivers," *IEEE/OSA J. Lightw. Technol.*, vol. 27, no. 16, pp. 3623–3631, 2009.

[71] H. Wymeersch and P. Johannisson, "Maximum-likelihood-based blind dispersion estimation for coherent optical communication," *IEEE/OSA J. Lightw. Technol.*, vol. 30, no. 18, pp. 2976–2982, 2012.

[72] A. Bononi, N. Rossi, and P. Serena, "Transmission limitations due to fiber nonlinearity," in *Optical Fiber Communication Conference*. Optical Society of America, 2011.

[73] C. Xie, "Impact of nonlinear and polarization effects on coherent systems," in *European Conference and Exposition on Optical Communications*. Optical Society of America, 2011.

[74] E. Ip and J. Kahn, "Compensation of dispersion and nonlinear impairments using digital backpropagation," *IEEE/OSA J. Lightw. Technol.*, vol. 26, no. 20, pp. 3416 –3425, oct.15, 2008.

[75] E. F. Mateo, X. Zhou, and G. Li, "Improved digital backward propagation for the compensation of inter-channel nonlinear effects in polarization-multiplexed WDM systems," *Opt. Express*, vol. 19, no. 2, pp. 570–583, 2011.

[76] C. Behrens, S. Makovejs, R. I. Killey, S. J. Savory, M. Chen, and P. Bayvel, "Pulse-shaping versus digital backpropagation in 224Gbit/s PDM-16QAM transmission," *Opt. Express*, vol. 19, no. 14, pp. 12 879–12 884, 2011.

[77] D. Rafique and A. D. Ellis, "Various nonlinearity mitigation techniques employing optical and electronic approaches," *IEEE Photon. Technol. Lett.*, vol. 23, no. 23, pp. 1838–1840, 2011.

[78] *Reduced complexity back-propagation for optical communication systems*, 2012.

[79] A. P. T. Lau, J. M. Kahn *et al.*, "Signal design and detection in presence of nonlinear phase noise," *IEEE/OSA J. Lightw. Technol.*, vol. 25, no. 10, pp. 3008–3016, 2007.

[80] N. Stojanovic, Y. Huang, F. N. Hauske, Y. Fang, M. Chen, C. Xie, and Q. Xiong, "MLSE-based nonlinearity mitigation for wdm 112 Gbit/s PDM-QPSK transmissions with digital coherent receiver," in *Optical Fiber Communication Conference*. IEEE, 2011, pp. 1–3.

[81] Z. Tao, L. Dou, W. Yan, L. Li, T. Hoshida, and J. C. Rasmussen, "Multiplier-free intrachannel nonlinearity compensating algorithm operating at symbol rate," *IEEE/OSA J. Lightw. Technol.*, vol. 29, no. 17, pp. 2570–2576, 2011.

[82] D. Rafique, M. Forzati, and J. Martensson, "Impact of nonlinear fibre impairments in 112 Gb/s PM-QPSK transmission with 43 Gb/s and 10.7 Gb/s neighbours," in *Transparent Optical Networks (ICTON), 2010 12th International Conference on*. IEEE, 2010, pp. 1–4.

[83] T. Inoue, E. Mateo, F. Yaman, T. Wang, Y. Inada, T. Ogata, and Y. Aoki, "Low complexity nonlinearity compensation for 100G DP-QPSK transmission over legacy NZ-DSF link with OOK channels," in *European Conference and Exhibition on Optical Communication*. Optical Society of America, 2012.

[84] T. Mizuochi, T. Sugihara, Y. Miyata, K. Kubo, K. Onohara, S. Hirano, H. Yoshida, T. Yoshida, and T. Ichikawa, "Evolution and status of forward error correction," in *Optical Fiber Communication Conference*. Optical Society of America, 2012.

[85] T. Sugihara, T. Yoshida, and T. Mizuochi, "Collaborative signal processing with FEC in digital coherent systems," in *Optical Fiber Communication Conference*. Optical Society of America, 2013.

[86] L. Bahl, J. Cocke, F. Jelinek, and J. Raviv, "Optimal decoding of linear codes for minimizing symbol error rate (corresp.)," *Information Theory, IEEE Transactions on*, vol. 20, no. 2, pp. 284–287, 1974.

[87] S. Talakoub, L. Sabeti, B. Shahrrava, and M. Ahmadi, "A linear Log-MAP algorithm for turbo decoding and turbo equalization," in *Wireless And Mobile Computing, Networking And Communications, 2005.(WiMob'2005), IEEE International Conference on*, vol. 1. IEEE, 2005, pp. 182–186.

[88] D. Fertonani, A. Barbieri, and G. Colavolpe, "Reduced-complexity BCJR algorithm for turbo equalization," *IEEE Trans. Commun.*, vol. 55, no. 12, pp. 2279–2287, 2007.

[89] S. Song, A. C. Singer, and K.-M. Sung, "Soft input channel estimation for turbo equalization," *Signal Processing, IEEE Transactions on*, vol. 52, no. 10, pp. 2885–2894, 2004.

[90] M. Nissila and S. Pasupathy, "Soft-input soft-output equalizers for turbo receivers: A statistical physics perspective," *IEEE Trans. Commun.*, vol. 55, no. 7, pp. 1300–1307, 2007.

[91] M. Tuchler, R. Koetter, and A. C. Singer, "Turbo equalization: principles and new results," *IEEE Trans. Commun.*, vol. 50, no. 5, pp. 754–767, 2002.

[92] M. Tu chler and A. C. Singer, "Turbo equalization: An overview," *Information Theory, IEEE Transactions on*, vol. 57, no. 2, pp. 920–952, 2011.

[93] M. Jäger, T. Rankl, J. Speidel, H. Bülow, and F. Buchali, "Performance of turbo equalizers for optical PMD channels," *IEEE/OSA J. Lightw. Technol.*, vol. 24, no. 3, p. 1226, 2006.

[94] H. F. Haunstein, T. Schorr, A. Zottmann, W. Sauer-Greff, and R. Urbansky, "Performance comparison of MLSE and iterative equalization in FEC systems for PMD channels with respect to implementation complexity," *IEEE/OSA J. Lightw. Technol.*, vol. 24, no. 11, pp. 4047–4054, 2006.

[95] T. Schorr, W. Sauer-Greff, R. Urbansky, and H. Haunstein, "Design and performance of high-rate irregular LDPC codes for turbo equalization of PMD channels," in *Optical Fiber Communication Conference*, 2007, pp. 1–3.

[96] W. Sauer-Greff and R. Urbansky, "Iterative equalization and FEC decoding in optical communication systems: Concepts and performance," in *Optical Fiber Communication Conference*. Optical Society of America, 2008.

[97] I. B. Djordjevic, H. G. Batshon, M. Cvijetic, L. Xu, and T. Wang, "PMD compensation by LDPC-coded turbo equalization," *IEEE Photon. Technol. Lett.*, vol. 19, no. 15, pp. 1163–1165, 2007.

[98] I. B. Djordjevic, L. L. Minkov, L. Xu, and T. Wang, "Suppression of fiber nonlinearities and PMD in coded-modulation schemes with coherent detection by using turbo equalization," *IEEE/OSA J. Opt. Commun. Netw.*, vol. 1, no. 6, pp. 555–564, 2009.

[99] L. Xu, I. Djordjevic, and T. Wang, "Turbo equalization for mitigation of linear and nonlinear impairments in high-speed optical transmission systems," in *Photonics Conference (PHO), 2011 IEEE*, 2011, pp. 825–826.

[100] I. Djordjevic, L. Minkov, and H. Batshon, "Mitigation of linear and nonlinear impairments in high-speed optical networks by using LDPC-coded turbo equalization," *IEEE J. Sel. Areas Commun.*, vol. 26, no. 6, pp. 73–83, 2008.

[101] L. Minkov, I. Djordjevic, L. Xu, and T. Wang, "PMD compensation in polarization-multiplexed multilevel modulations by turbo equalization," *IEEE Photon. Technol. Lett.*, vol. 21, no. 23, pp. 1773–1775, 2009.

[102] M. P. C. Fossorier, "Quasicyclic low-density parity-check codes from circulant permutation matrices," *IEEE Trans. Inform. Theory*, vol. 50, no. 8, pp. 1788–1793, 2004.

[103] S. Zhang, Y. Zhang, M.-F. Huang, F. Yaman, E. Mateo, D. Qian, L. Xu, Y. Shao, and I. Djordjevic, "Transoceanic transmission of 40 117.6 gb/s pdm-ofdm-16qam over hybrid large-core/ultralow-loss fiber," *IEEE/OSA J. Lightw. Technol.*, vol. 31, no. 4, pp. 498–505, 2013.

[104] M. Sakib, V. Mahalingam, W. Gross, and O. Liboiron-Ladouceur, "Optical front-end for soft-decision LDPC codes in optical communication systems," *Optical Communications and Networking, IEEE/OSA Journal of*, vol. 3, no. 6, pp. 533–541, 2011.

[105] T. Wuth, E. Agrell, M. Karlsson, and M. Sköld, "Fiber communications using convolutional coding and bandwidth-efficient modulation," *Opt. Express*, vol. 14, no. 2, pp. 542–555, 2006.

[106] F. Tosato and P. Bisaglia, "Simplified soft-output demapper for binary interleaved cofdm with application to hiperlan/2," in *Communications, 2002. ICC 2002. IEEE International Conference on*, vol. 2. IEEE, 2002, pp. 664–668.

[107] B. Inan, B. Spinnler, F. Ferreira, D. van den Borne, A. Lobato, S. Adhikari, V. A. Sleiffer, M. Kuschnerov, N. Hanik, and S. L. Jansen, "Dsp complexity of mode-division multiplexed receivers," *Opt. Express*, vol. 20, no. 10, pp. 10 859–10 869, 2012.

[108] S. Ö. Arik, D. Askarov, and J. M. Kahn, "Effect of mode coupling on signal processing complexity in mode-division multiplexing," *IEEE/OSA J. Lightw. Technol.*, vol. 31, no. 3, pp. 423–431, 2013.

[109] H.-C. Chien, J. Yu, Z. Jia, Z. Dong, and X. Xiao, "Performance assessment of noise-suppressed nyquist-wdm for terabit superchannel transmission," *IEEE/OSA J. Lightw. Technol.*, vol. 30, no. 24, pp. 3965–3971, 2012.

[110] Y.-K. Huang, M.-F. Huang, E. Ip, E. Mateo, P. N. Ji, D. Qian, A. Tanaka, Y. Shao, T. Wang, Y. Aono *et al.*, "High-capacity fiber field trial using terabit/s all-optical ofdm superchannels with dp-qpsk and dp-8qam/dp-qpsk modulation," *IEEE/OSA J. Lightw. Technol.*, vol. 31, no. 4, pp. 546–553, 2013.

List of Acronyms

ASE	amplified spontaneous emission
FEC	forward error correction
ISI	inter-symbol interference
NRZ	non return-to-zero
OOK	On-Off Keying
QPSK	Quadrature Phase Shift Keying
WDM	Wavelength Division Multiplexing
RoF	Radio-over-Fiber
WDM	Wavelength Division Multiplexing
FEC	Forward Error Correction
DSP	Digital Signal Processing
QPSK	Quadrature Phase Shift Keying
QAM	Quadrature Amplitude Modulation
OFDM	Orthogonal Frequency-Division Multiplexing
CMA	Constant Modulus Algorithm
DFE	Decision Feedback Equalizer
PM-Coh	Phase Modulated RoF link assisted with Coherent Detection
VCSEL	Vertical-Cavity Surface-Emitting laser

UWB Ultra-Wide Band

IR Impulse Radio

DSP Digital Signal Processing

U-DWDM Ultra Dense Wavelength Division Multiplexing

TE Turbo Equalization

FEC Forward Error Correction

QAM Quadrature Amplitude Modulation

DFE Decision Feedback Equalizer

SISO Soft-Input Soft-Output

SOVA Soft Output Viterbi Algorithm

sbs-MAP Symbol-by-symbol Maximum a Posteriori

SOVE Soft Output Viterbi Equalizer

MLSE Maximum-Likelihood Sequence Estimation

CC Convolutional Code

LDPC Low-Density Parity-Check

DGD Differential Group Delay

PMD Polarization Mode Dispersion

CD Chromatic Dispersion

CMA Constant Modulus Algorithm

ICI Inter-Channel Interference

ISI Inter-Symbol Interference

PAPR Peak-to-Average Power Ratio

WDM Wavelength Division Multiplexing

OFDM Orthogonal Frequency Division Multiplexing

ROADM Reconfigurable Optical Add-Drop Multiplexers

MAP Maximum a Posteriori

DP Dual Polarization

WDM Wavelength Division Multiplexing

PDM Polarization Division Multiplexed

POF Polymer Optical Fiber

ASE Amplified Spontaneous Emission

RLS Recursive Least Squares

NLMS Normalized Least Mean Squared

NLPN Nonlinear Phase Noise

FPGA Field Programmable Gate Array